

In cooperation with the U.S. Army Corps of Engineers, Louisville District

Results of a Two-Dimensional Hydrodynamic and Sediment-Transport Model to Predict the Effects of the Phased Construction and Operation of the Olmsted Locks and Dam on the Ohio River near Olmsted, Illinois

Water-Resources Investigations Report 03-4336



1879–2004

**U.S. Department of the Interior
U.S. Geological Survey**

Results of a Two-Dimensional Hydrodynamic and Sediment-Transport Model to Predict the Effects of the Phased Construction and Operation of the Olmsted Locks and Dam on the Ohio River near Olmsted, Illinois

By **Chad R. Wagner**

Water-Resources Investigations Report 03-4336

In cooperation with the U.S. Army Corps of Engineers, Louisville District

**Louisville, Kentucky
2004**

U.S. DEPARTMENT OF THE INTERIOR
GALE A. NORTON, Secretary

U.S. GEOLOGICAL SURVEY
Charles G. Groat, Director

The use of trade, product, or firm names is for descriptive purposes only
and does not imply endorsement by the U.S. Government.

For additional information, write to:

District Chief, Kentucky District

U.S. Geological Survey

9818 Bluegrass Parkway

Louisville, KY 40299-1906

<http://ky.water.usgs.gov/>

Copies of this report can be purchased from:

U.S. Geological Survey

Information Services

Box 25286

Federal Center

Denver, CO 80225-0286

CONTENTS

Abstract.....	1
Introduction.....	2
Background.....	2
Purpose and scope	4
Study area	4
Construction-phase model	5
Modeling approach.....	5
Hydrograph development	5
Construction phases.....	5
Operational-phase model.....	8
Modeling approach.....	8
Hydrograph development	8
Hydrodynamic-model development	12
RMA-2 hydrodynamic model description.....	12
Field data collection and interpretation	12
Water-surface elevations.....	12
Velocity and discharge.....	14
Bathymetry	14
Computational-mesh configuration	14
Boundary conditions.....	16
Discussion of calibration and validation results	16
Sediment-transport model development	20
Sed2D sediment-transport model description.....	25
Model input parameters	25
Bed material.....	25
Selection of representative grain size	28
Time step	28
Particle-fall velocity	28
Concentration of sediment inflow	28
Calibration of sediment-transport model.....	28
Model results	29
Construction-phase model—hydrodynamics	29
Construction-phase model—sediment transport	29
Operational-phase model—hydrodynamics	40
Operational-phase model—sediment transport	40
Model comparison between Sed2D and previous TABS-1 simulation	48
Model development	48
Comparison of model results	48
Summary and conclusions	49
References cited.....	49
Appendix A: High-flow comparisons of baseline and phase-3 construction cross-sectional velocity profiles in the Olmsted Locks and Dam study reach	51
Appendix B: Low-flow comparisons of baseline and phase-3 construction cross-sectional velocity profiles in the Olmsted Locks and Dam study reach	57

FIGURES

1. Map showing location of study area on the Ohio River near Olmsted, Illinois	3
2-6. Hydrographs showing:	
2. 1997 stepped and daily unit values (years 2 and 5) for the Ohio River in the Olmsted Locks and Dam study reach	6
3. 1996 stepped and daily unit values (years 1, 3, 4 and 6) for the Ohio River in the Olmsted Locks and Dam study reach	7
4. 1985 stepped and daily unit values (year 7) for the Ohio River in the Olmsted Locks and Dam study reach	9
5. 1986 stepped and daily unit values (year 8) for the Ohio River in the Olmsted Locks and Dam study reach	10
6. 1973 stepped and daily unit values (year 9) for the Ohio River in the Olmsted Locks and Dam study reach	11
7. Map showing location of hydrographic-survey cross sections and gaging stations on the Ohio River in the Olmsted Locks and Dam study reach	13
8. Schematic showing mesh configuration around the simulated Olmsted Locks and Dam	15
9-13. Graphs showing:	
9. Measured and simulated velocity profiles for cross-section 4 in the Olmsted Locks and Dam simulation	17
10. Measured and simulated average cross-sectional velocities during low-flow conditions in the Olmsted Locks and Dam study reach	18
11. Measured and simulated average cross-sectional velocities during high-flow conditions in the Olmsted Locks and Dam study reach	19
12. ADCP-measured and simulated low-flow velocity vectors at cross-section 2 in the Olmsted Locks and Dam study reach	21
13. ADCP-measured and simulated low-flow velocity vectors at cross-section 4 in the Olmsted Locks and Dam study reach	22
14-16. Schematics showing:	
14. Velocity-magnitude contours and vectors of the flow field for a low-flow simulation with no flow-through gaps in the wicket gates of the Olmsted Locks and Dam model	23
15. Velocity-magnitude contours and vectors of the flow field for a low-flow simulation with flow-through gaps in the wicket gates of the Olmsted Locks and Dam model	24
16. Bed-material data collected by the U.S. Army Corps of Engineers, St. Louis, Mo., in the cross sections located on or near the mussel beds in the Olmsted Locks and Dam study reach	26
17. Graph showing the summary of the bed-material D_{50} for the samples collected by the U.S. Army Corps of Engineers, St. Louis, Mo., at four cross sections located around the mussel beds in the Olmsted Locks and Dam study reach	27
18-23. Schematics showing:	
18. Difference in bed change between baseline and phase 1-construction simulations after year 1 (1996 hydrograph) in the Olmsted Locks and Dam study reach	30
19. Difference in bed change between baseline and phase 2-construction simulations after year 2 (1997 hydrograph) in the Olmsted Locks and Dam study reach	31
20. Difference in bed change between baseline and phase 2-construction simulations after year 3 (1996 hydrograph) in the Olmsted Locks and Dam study reach	32
21. Difference in bed change between baseline and phase 3-construction simulations after year 4 (1996 hydrograph) in the Olmsted Locks and Dam study reach	33

22. Difference in bed change between baseline and phase 3-construction simulations after year 5 (1997 hydrograph) in the Olmsted Locks and Dam study reach	34
23. Difference in bed change between baseline and phase 3-construction simulations after year 6 (1996 hydrograph) in the Olmsted Locks and Dam study reach	35
24. Animation of bed change around the mussel beds for the 6-year Olmsted Locks and Dam construction simulation	36
25. Schematic showing difference in bed change between baseline and phase-3 construction after year 5 (1997 hydrograph), superimposed with hydrodynamics for a low-flow simulation (1997 hydrograph - step 7), for the Olmsted Locks and Dam model	37
26-28. Animations showing:	
26. Bed change during high-flow conditions (1997 hydrograph, step 3) for (A) baseline simulation and (B) phase 3 of the Olmsted construction in the study reach	38
27. Bed change during low-flow conditions (1997 hydrograph, step 7) for (A) baseline simulation and (B) phase 3 of the Olmsted construction in the study reach	39
28. Bed change around the mussel beds over the 1997 flood hydrograph in the Olmsted Locks and Dam study reach.....	41
29-32. Schematics showing:	
29. Cumulative bed change around the mussel beds during the 1997 flood (1997 hydrograph - step 5, minus step 2) for phase-2 construction in the Olmsted Locks and Dam study reach	42
30. Difference in bed change between baseline and fully operational locks and dam simulation after year 7 (1985 hydrograph) in the Olmsted Locks and Dam study reach	43
31. Difference in bed change between baseline and fully operational locks and dam simulation after year 8 (1986 hydrograph) in the Olmsted Locks and Dam study reach	44
32. Difference in bed change between baseline and fully operational locks and dam simulation after year 9 (1973 hydrograph) in the Olmsted Locks and Dam study reach	45
33. Animation showing bed change around the mussel beds over the 3-year operational simulation in the Olmsted Locks and Dam study reach	46
34. Animation showing bed change around the mussel beds over the entire 9-year construction and operational simulation in the Olmsted Locks and Dam study reach	47

TABLES

1. Hydrograph sequence for the construction-phase model	5
2. Construction scenarios and corresponding hydrographs.....	8
3. Hydrograph sequence for the operational-phase model.....	8
4. Summary of water-surface elevation calibration and validation for the Olmsted Locks and Dam study reach.....	16
5. Summary of continuity checks for the Olmsted Locks and Dam model	22
6. Sed2D model-input parameters.....	28

CONVERSION FACTORS, VERTICAL DATUM, AND HORIZONTAL DATUM

CONVERSION FACTORS

Multiply	By	To obtain
foot (ft)	0.3048	meter
foot per second (ft/s)	0.3048	meter per second
cubic foot per second (ft ³ /s)	0.02832	cubic meter per second
mile (mi)	5280.0	foot
mile (mi)	1.609	kilometer
millimeter (mm)	0.0033	foot

VERTICAL DATUM

Sea level: In this report "sea level" refers to the National Geodetic Datum of 1929 (NGVD of 1929)-a geodetic datum derived from a general adjustment of the first-order level nets of both the United States and Canada, formerly called Sea Level Datum of 1929.

Elevation, as used in this report, refers to the distance above or below sea level.

HORIZONTAL DATUM

The horizontal datum used in this report is state plane coordinates for the Kentucky-South. The units are in feet.

Results of a Two-Dimensional Hydrodynamic and Sediment-Transport Model to Predict the Effects of the Phased Construction and Operation of the Olmsted Locks and Dam on the Ohio River near Olmsted, Illinois

By Chad R. Wagner

Abstract

The Olmsted two-dimensional hydrodynamic and sediment-transport model was developed in cooperation with the U.S. Army Corps of Engineers, Louisville District. The model was used to estimate the effects that the phased-construction sequence and operation of the Olmsted Locks and Dam had on sediment-transport patterns in the 11.9-mile study reach (Ohio River miles 962.6 to 974.5), particularly over an area of endangered orange-footed pearly mussel (*Plethobasus cooperianus*) beds beginning approximately 2 miles downstream of the dam construction. A Resource Management Associates-2 (RMA-2) two-dimensional hydrodynamic model for the reach was calibrated to a middle-flow hydraulic survey (350,000 cubic feet per second) and verified with data collected during low- and high-flow hydraulic surveys (72,500 and 770,000 cubic feet per second, respectively). The calibration and validation process included matching water-surface elevations at the construction site and velocity profiles at 15 cross sections throughout the study reach.

The sediment-transport aspect of the project was simulated with the Waterways Experiment Station's Sed2D model for a 6-year planned-construction period (construction-phase modeling) and a subsequent 3-year operational period (operational-phase modeling). The sediment-transport results from the construction and operational models both

were compared to results of concurrent baseline simulations to determine the changes in erosional and depositional patterns induced by the dam construction and operation throughout the study reach and more importantly over the area of the endangered mussel beds.

Simulation of the phased-in-the-wet Olmsted Locks and Dam construction and subsequent operation period resulted in a maximum additional deposition of approximately 2 feet over a localized region of the mussel beds when compared to the bed change simulated with baseline conditions (river conditions that included only the completed locks section). Most areas on the mussel beds experienced less than 0.5 feet of cumulative bed change between the baseline and construction phases during the nine annual hydrographs. The bed change over the 9 year Olmsted Locks and Dam simulation reveals a continuous downstream progression and deepening of the main channel and deposition along the right bank with limited lateral migration toward the more densely populated mussel-bed areas. The sensitivity of the mussels to sediment deposition is difficult to quantify; therefore, the effect of simulated deposition on the welfare of the mussels is uncertain. The model also will provide the U.S. Army Corps of Engineers a tool to predict the locations of high deposition in navigable sections, which can save engineers time and resources when monitoring the need for dredging operations.

INTRODUCTION

The Olmsted Locks and Dam hydrodynamic and sediment-transport model was developed by the U.S. Geological Survey (USGS), in cooperation with the U.S. Army Corps of Engineers (USACE)–Louisville District, to evaluate the environmental effect of the construction and subsequent operation of the Olmsted Locks and Dam on the lower Ohio River. The Olmsted Locks and Dam will replace Locks and Dams 52 and 53 and be the final high-lift dam structure on the Ohio River. The modeling project was done in two phases; the first modeling phase focused on simulating the dam construction sequence and the second modeling phase focused on long-term effects of the fully operational locks and dam.

Background

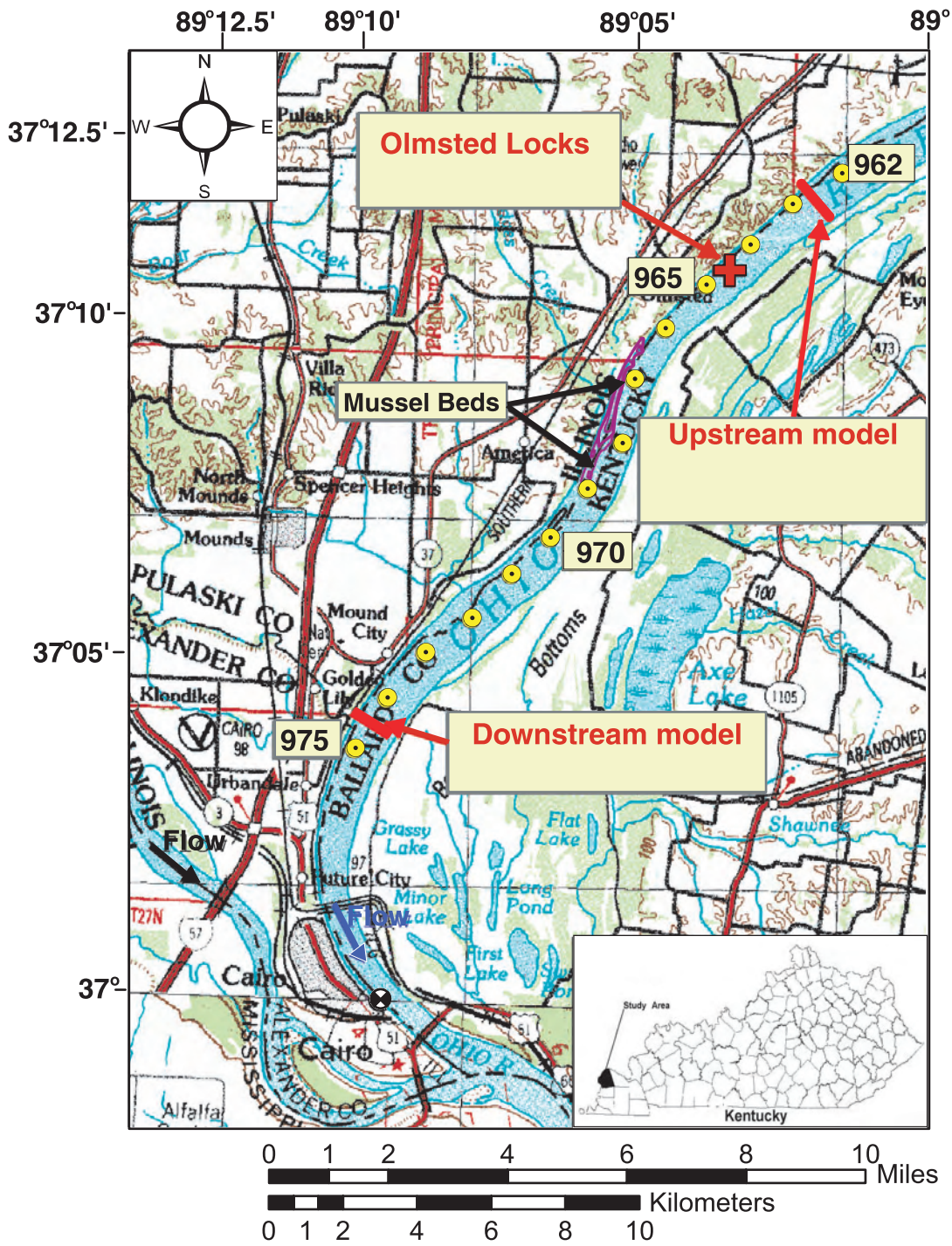
The Ohio River flows 981 mi from the confluence of the Alleghany and Monongahela Rivers at Pittsburgh, Penn., to the Mississippi River near Cairo, Ill. The entire river, aside from the last 19 mi (below Lock and Dam 53), has been altered and is now regulated by the operation of locks and dams to provide a stable navigational channel. During the past 50 years, all but two of the original wooden wicket dams and locks on the Ohio River have been replaced with high-lift dams. Current (2004) shipping traffic is growing rapidly and the antiquated design of the original wicket dams is making it impossible for the USACE to meet the shipping traffic demands. The lower Ohio River (from just upstream of Paducah, Ky., to the Mississippi River confluence) is of special importance because it provides the connection between the Cumberland, Mississippi, Ohio, and Tennessee Rivers.

The Ohio River and its tributaries have historically supported a multitude of aquatic species including a wide variety of fish and mussels. Construction of navigational facilities has appreciably altered the river's natural condition by slowing current velocities, which lead to the accumulation of sediment and subsequent reduction

in mussel fauna (Thorp and Covich, 1991). The lower 19 mi of the Ohio River (Locks and Dam 53 to the Mississippi River) is the only remaining free-flowing riverine habitat in the Ohio River and is home to the largest population of pre-impoundment fish and mussel species (U.S. Fish and Wildlife Service, 1993).

With the passage of the Water Resources Development Act of 1988, the USACE–Louisville District was authorized to replace Locks and Dams 52 and 53 with a single structure based on investigations to improve navigational conditions on the lower Ohio River. Construction of the new facility (Olmsted Locks and Dam) began in 1993 and is located at Ohio River Mile 964.4, near Olmsted, Ill., approximately 1.8 mi downstream from Locks and Dam 53 (fig. 1). The new structure will consist of wicket gates across the 1,400 ft navigable channel. The wicket gates will be raised at river elevations less than 295 ft, which will force barges to use the lock chambers to traverse the dam and direct the flow of the river through five tainter gates located adjacent to the locks on the Illinois bank. The historical flow data on the lower Ohio River, in conjunction with the proposed dam operational plan, indicate that the wicket gates will be down approximately 60 percent of the time allowing barges to bypass the locks.

A previous sediment-transport simulation was developed by the USACE for the study reach prior to the beginning of construction using the one-dimensional numerical model, TABS1. This model was used for various pre-dam-construction planning purposes including a variation of the USGS study described herein. Although the currently (2004) existing scour hole adjacent to the cofferdam/locks was not present at the time of the TABS-1 model, an estimated scour-hole geometry was modeled to predict the change in bed-material transport past a section located at the upstream end of the mussel beds because of a proposed Stage II cofferdam (comparable to the phase 2 geometry in the USGS model).



EXPLANATION

	Model boundaries		Ohio River mile
	Corps of Engineers Gaging Station		River mile marker

Figure 1. Location of study area on the Ohio River near Olmsted, Illinois.

The U.S. Fish and Wildlife Service (USFWS) is concerned that the construction and subsequent operation of the Olmsted Locks and Dam will alter the hydrodynamic and sediment-transport patterns on the lower Ohio River to a level that will eradicate the endangered species orange-footed pearly mussel (*Plethobasus cooperianus*). The orange-footed pearly mussel (*Plethobasus cooperianus*) is an Interior Basin species that reaches an average adult size of 2.5 in and is usually found in medium to large rivers at depths of 10 to 29 ft (U.S. Fish and Wildlife Service, 1993). The Ohio, Cumberland, and Tennessee River drainages contain the three known remaining population areas of this mussel in the historic range of the species (U.S. Fish and Wildlife Service, 1993). The mussel buries itself in the sand and gravel leaving only part of its shell and feeding siphon projecting above the riverbed thereby leaving itself very sensitive to sediment deposition and erosion. The mussel habitat begins approximately 2 mi downstream of the dam on the right descending bank. The center of the mussel beds is located near the inflection of two opposing bends in the river. Sediment-deposition and erosion patterns that were present prior to the construction and operation may change because of the following: loss of bed material during dredging for cofferdam construction, creation of temporary navigational channel, changes in flow-velocity magnitude and direction, associated river traffic, riverside development during construction, and operation of locks and dam. Physical biological monitoring has been ongoing since 1993 to evaluate the population and health of the endangered mussel species. The sediment-transport patterns over the mussel beds also were continuously monitored with a series of submerged altimeters from 1993 through February 2002 when one of the two deployment buoys was destroyed by a barge. In addition to the mussel-bed monitoring, the USFWS and USACE also wanted a method to predict how and to what extent the sediment-transport patterns would be affected by the various phases of dam construction and full operation. As a component of the biological impact statement requested by the USFWS, a two-dimensional numerical hydrodynamic and sediment-transport model was initiated by the USGS to predict the flow and sediment-transport patterns around the local orange-footed pearly mussel beds (*Plethobasus cooperianus*).

Purpose and Scope

The Olmsted Locks and Dam model was developed to predict the change in sediment-transport patterns around the endangered orange-footed pearly mussel beds (*Plethobasus cooperianus*) induced by the construction and subsequent operation of the Olmsted Locks and Dam. There is evidence (U.S. Fish and Wildlife Service, 1993) that indicates the orange-footed pearly mussels in the beds located in the lower Ohio River near the Olmsted Locks and Dam are reproducing, so any adverse effect on the population could threaten the survival of the species.

This report describes the development and results of the Olmsted Locks and Dam hydrodynamic and sediment-transport model developed on the lower Ohio River (Locks and Dam 53 to Ohio River Mile 974.5; fig.1). The field data and methodology used to develop and calibrate the models also are described herein. Floodplains were included in the model to accurately simulate high-flow conditions, which were of most concern at the onset of the project. The calibrated model was used to simulate sediment-transport patterns for hydraulic conditions ranging from 1,100,000 to 88,000 ft³/s under a wide range of backwater and free-flowing conditions.

Study Area

The Olmsted Locks and Dam study area begins at Locks and Dam 53 (Ohio River Mile 962.6) and extends downstream to Ohio River Mile 974.5, 6.5 river mi upstream from the confluence with the Mississippi River (fig. 1). The study reach also comprises most of the only remaining free-flowing riverine habitat in the entire 981-mi main stem of the Ohio River. Locks and Dam 53 is an old, wooden, wicket-dam structure with one 1,200-ft lock chamber and one 600-ft lock chamber on the Illinois bank, an approximately 1,000-ft wide navigable channel, followed by a chanoine weir (approximately 530-ft wide). The channel generally has a trapezoidal shape with moderately steep banks rising at slopes from 3 percent (.03 ft/ft) to 15percent (.15 ft/ft). The banks extend to an approximate elevation of 310 ft.

The following river characteristics were determined from the data collected during the hydrographic surveys of the study reach. At a low-flow discharge of 72,500 ft³/s (with no dominant backwater effects from the Mississippi River), the average depth of the river thalweg is approximately 22 ft. The average width of the river at a discharge of 72,500 ft³/s is approximately 3,100 ft. A discharge of 770,000 ft³/s (no backwater conditions) produces an average depth in the thalweg of approximately 54 ft and an average width (including floodplains) of 3.5 mi. The bank and floodplain vegetation consists predominately of small shrubbery and thick low-level vegetation. The Kentucky floodplain is expansive (ranging from 1.5 to 5-mi wide) and is comprised mostly of the Ballard County State Wildlife Refuge. The Illinois floodplain is narrow and bounded by steep bluffs adjacent to the river.

CONSTRUCTION-PHASE MODEL

The purpose of the construction-modeling phase of the Olmsted sediment-transport simulation was to estimate the effects that the phased in-the-wet construction sequence of the Olmsted Locks and Dam would have on sediment-transport patterns in the study reach and more specifically over the mussel beds beginning approximately 2-mi downstream of the dam.

Modeling Approach

A Resource Management Associates–2 (RMA-2, version 4.53) two-dimensional hydrodynamic model for the reach was calibrated to a middle-flow hydraulic survey (350,000ft³/s) and verified with data collected during a low- and high-flow hydraulic survey (72,500 and 770,000 ft³/s, respectively). The calibration and validation process included matching water-surface elevations at the construction site and velocity profiles at 15 cross sections throughout the study reach. The sediment-transport aspect of the project was simulated with the Waterways Experiment Station’s (WES) Sed2D model (version 4.52).

Hydrograph Development

The phased-construction process was estimated for completion in 6 years; therefore, the steady-state sediment-transport model simulated six annual stepped hydrographs. The hydrographs used were representative of 1996 (a more typical annual hydrograph for the reach) and 1997 (a year of extreme high- and low-flow periods); table 1 outlines the sequence in which these hydrographs were applied.

Table 1. Hydrograph sequence for the construction-phase model

Year	Stepped hydrograph
1	1996
2	1997
3	1996
4	1996
5	1997
6	1996

The 1996 and 1997 stepped hydrographs are shown in figures 2 and 3 along with the flow-numbering scheme used to denote the various hydrograph steps.

Construction Phases

The final Olmsted Locks and Dam structure will consist of five tainter gates near the Illinois bank, a 1,400-ft navigable channel equipped with wicket gates, and a fixed weir on the Kentucky bank. The phased-construction process was simulated by use of the following three construction scenarios:

1. Locks + 2-1/2 Tainter Gates + Fixed Weir (interim elevation = 315 ft)
2. Locks + 5 Tainter Gates + Fixed Weir (interim elevation)
3. Locks + 5 Tainter Gates + 1,400-ft Navigable Pass + Fixed Weir (final elevation = 303.5 ft)

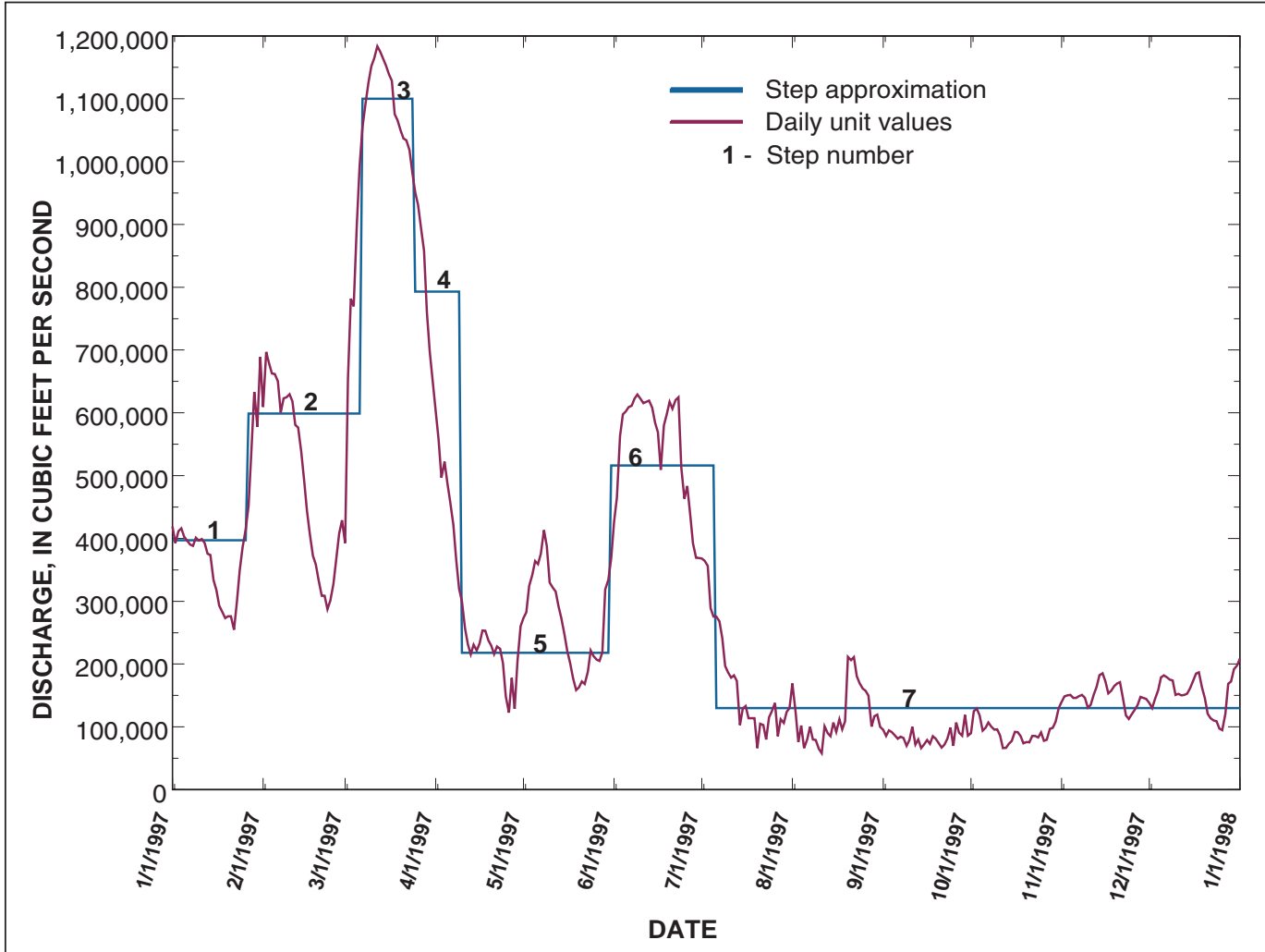


Figure 2. 1997 stepped and daily unit values (years 2 and 5) for the Ohio River in the Olmsted Locks and Dam study reach near Olmsted, Illinois.

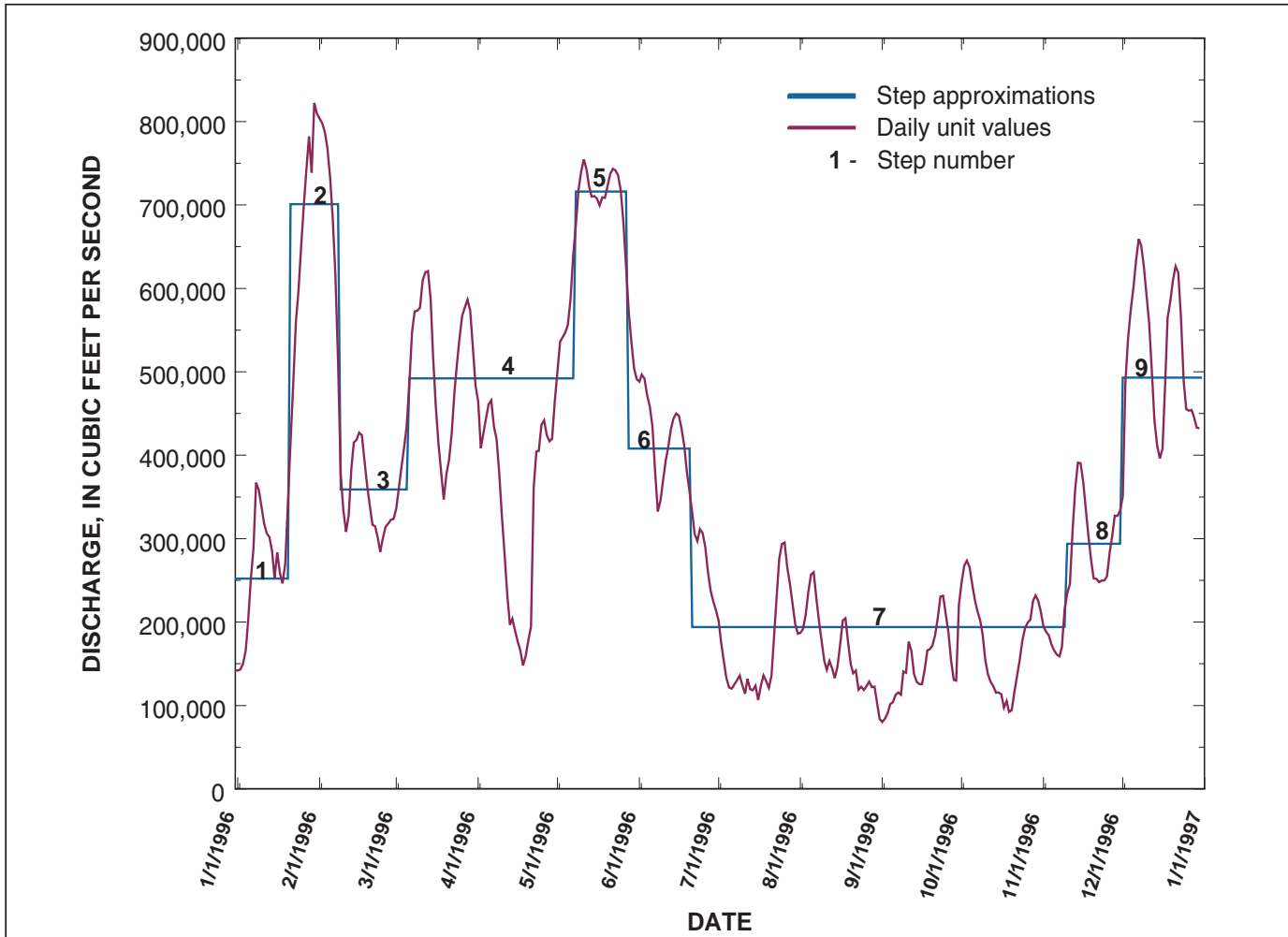


Figure 3. 1996 stepped and daily unit values (years 1, 3, 4, and 6) for the Ohio River in the Olmsted Locks and Dam study reach near Olmsted, Illinois.

The construction phases and the corresponding stepped hydrograph that was applied to each scenario are outlined in table 2.

A baseline scenario that included only the completed lock section was run concurrently with the phased-construction scenarios for the 6-year construction period to determine the sediment-transport patterns induced by the dam construction.

Table 2. Construction scenarios and corresponding hydrographs

Construction scenario	Stepped hydrograph
1	1996
2	1997
2	1996
3	1996
3	1997
3	1996

OPERATIONAL-PHASE MODEL

The purpose of the operational-modeling phase of the Olmsted sediment-transport modeling project was to evaluate the long-term effects that the fully operational Olmsted Locks and Dam would have on sediment-transport patterns in the reach and more specifically over the mussel beds.

Modeling Approach

The RMA-2 two-dimensional hydrodynamic model developed in the construction phase was used to simulate the hydraulics in the study reach for the operational phase. The sediment-transport aspect of the project also was simulated with the WES Sed2D model. A baseline scenario that included only the completed lock section was run concurrently with the fully operational locks and dam scenarios for the

3 year simulation in phase 2 to determine the sediment-transport patterns caused by the dam operation.

Hydrograph Development

The fully operational locks and dam were simulated for 3 years beginning at the end of the 6-year construction sequence modeled in the construction phase. The sediment-transport model in modeling phase 2 simulated three annual stepped hydrographs. In contrast to the hydrographs in the construction-phase model, the hydrographs in the operational-modeling phase were representative of the hydrograph patterns that occur on a regular basis. The development of the representative set of hydrographs included the compilation of all annual hydrographs for the period of record at the Olmsted Locks and Dam construction site (1966-2001). An average annual hydrograph was derived from all the data, and individual annual data sets were inspected to find hydrographs that represented the average year. The hydrographs used to model the 3 years in phase 2 were representative of the data collected in 1985, 1986, and 1973 on the lower Ohio River. Representations of the actual hydrographs were used instead of synthetic hydrographs in order to include the Mississippi River backwater conditions, which are common on the lower Ohio River. The sequence in which these hydrographs were applied is outlined in table 3. The 1985, 1986, and 1973 stepped hydrographs are shown in figures 4-6 along with the flow-numbering scheme used to denote the various hydrograph steps.

Table 3. Hydrograph sequence for the operational-phase model

Year	Stepped hydrograph
7	1985
8	1986
9	1973

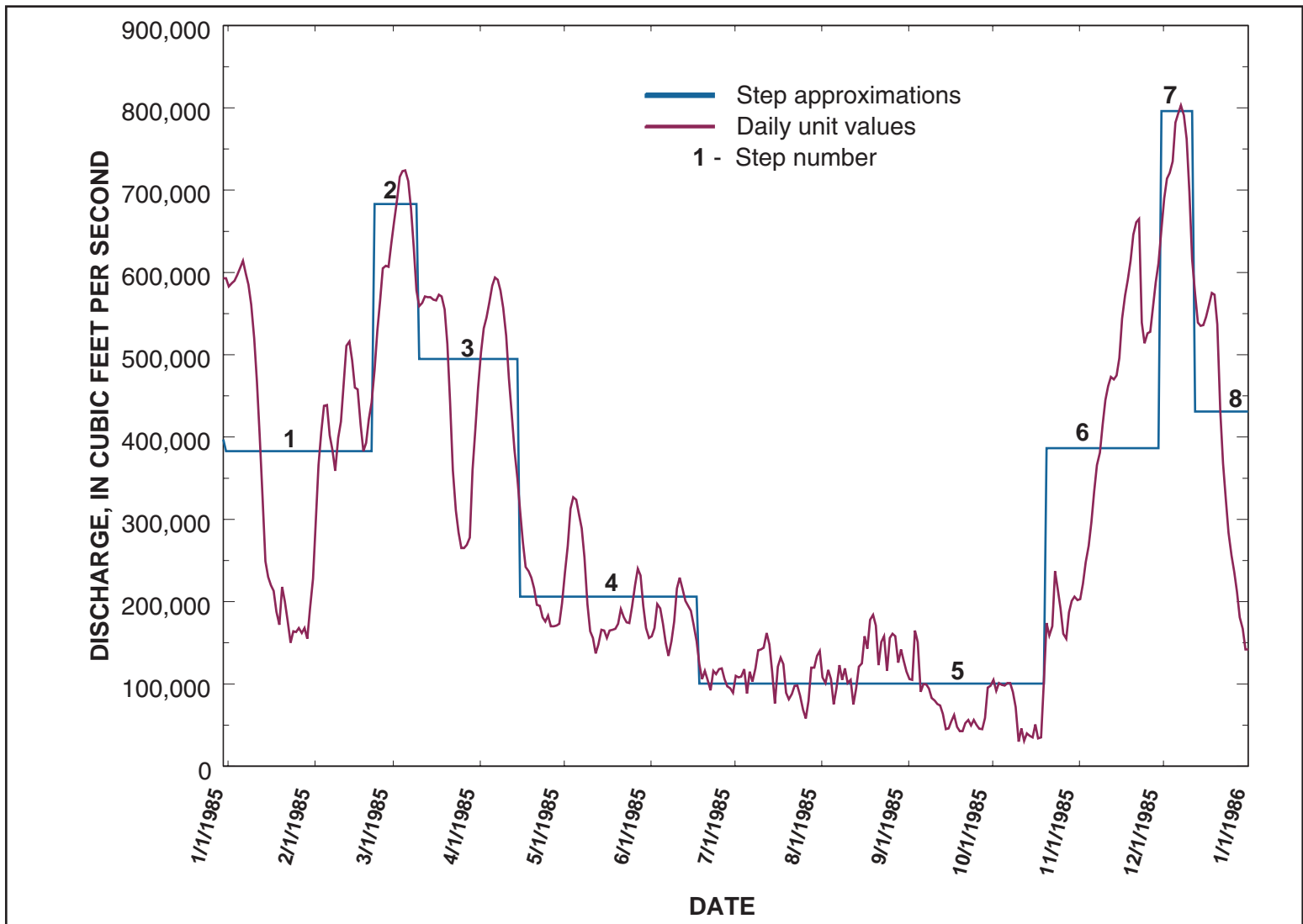


Figure 4. 1985 stepped and daily unit values (year 7) for the Ohio River in the Olmsted Locks and Dam study reach near Olmsted, Illinois.

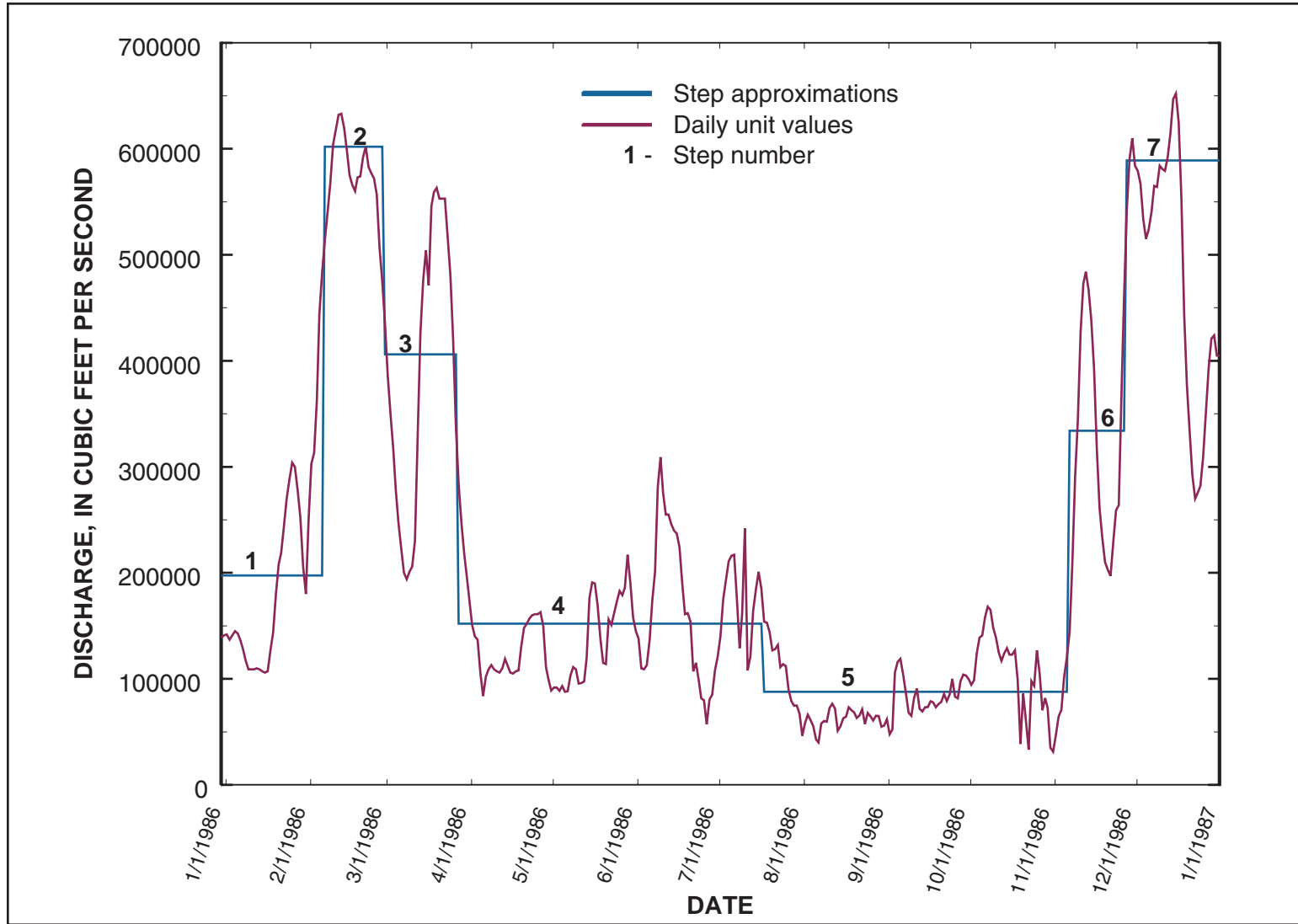


Figure 5. 1986 stepped and daily unit values (year 8) for the Ohio River in the Olmsted Locks and Dam study reach near Olmsted, Illinois.

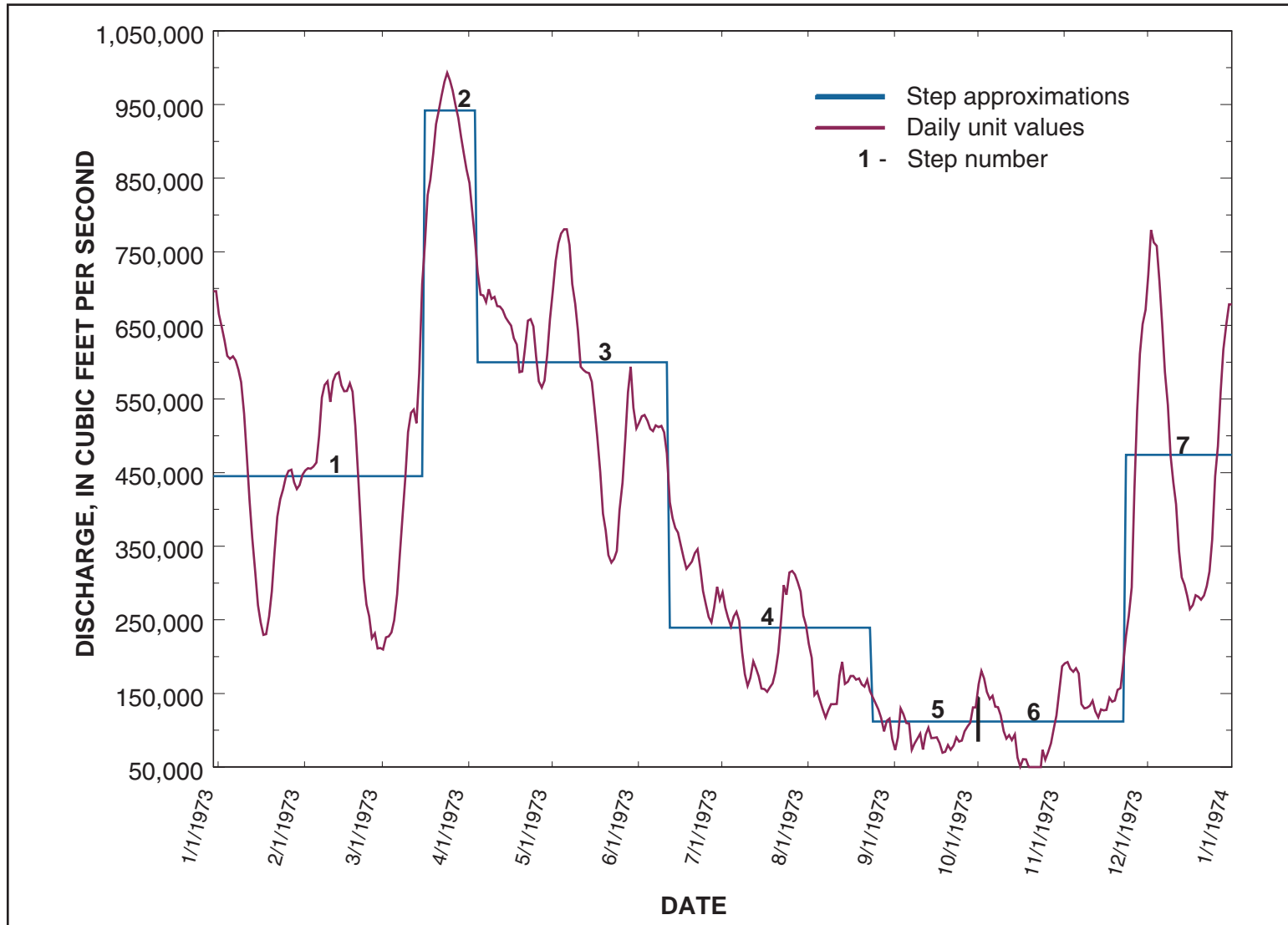


Figure 6. 1973 stepped and daily unit values (year 9) for the Ohio River in the Olmsted Locks and Dam study reach near Olmsted, Illinois.

HYDRODYNAMIC-MODEL DEVELOPMENT

At least two data sets are required to calibrate and validate a numerical model. The general procedure used to calibrate and validate the RMA-2 hydrodynamic model was to develop field data (bathymetry, roughness, etc.), which allowed the development of the computational mesh. Next, the model was calibrated to the water-surface elevations and velocities observed in the field for the initial mid-flow condition (350,000 ft³/s). Finally, both a low- and high-flow condition (72,500 and 770,000 ft³/s, respectively) were simulated without changing the computational mesh or model parameters, and the simulated water-surface elevations and velocities were compared with those observed in the field for these additional flow conditions.

RMA-2 Hydrodynamic Model Description

RMA-2 is a two-dimensional depth-averaged finite-element hydrodynamic numerical model capable of computing water-surface elevations and horizontal-velocity components for sub-critical, free-surface flow in two-dimensional flow fields (Donnell, Letter, McAnally and others, 2001). The model is designed for situations where vertical accelerations are negligible and velocity vectors generally point in the same direction over the entire depth of the water column at any discrete moment in time. The model is not intended for applications in which vortexes, vibrations, or vertical accelerations are the primary interests; therefore, the modeling of vertically stratified flow fields is beyond the capabilities of RMA-2 (Donnell, Letter, McAnally and others, 2001).

Typical applications of the RMA-2 numerical model include calculating water-surface elevations and flow distribution around islands; flow patterns at bridges having one or more relief openings, in contracting and expanding reaches, into and out of off-channel hydropower plants, and at river

junctions; circulation and transport in water bodies with wetlands; and general water levels and flow patterns in rivers, reservoirs, and estuaries.

The modeling interface used in the study was the Surface Water Modeling System (SMS) (version 8.0) developed by the Environmental Modeling Research Laboratories (EMRL) at Brigham Young University in Provo, Utah (Brigham Young University, 1999).

Field Data Collection and Interpretation

Water-surface elevations, channel bathymetry, and detailed water-velocity measurements were collected at three different flow conditions (72,500, 350,000, and 770,000 ft³/s). The low-, mid-, and high-flow surveys were collected September 16-17, 1997, June 30-July 1, 1997, and April 29-30, 1998, respectively. Water-surface elevations were measured at the Olmsted construction site and tailwater of Locks and Dam 53 concurrent with all three hydraulic surveys. Detailed water-velocity measurements and channel-bathymetry data were collected at 15 cross sections spaced from 2,000 to 5,000-ft apart during each of the hydraulic surveys (fig. 7).

Water-Surface Elevations

Water-surface elevations at the three locations in the study reach were determined from USGS and USACE gaging stations (fig. 7). The USACE collects stage data by use of a staff plate at the Olmsted construction site and shares a gaging station with the USGS in the tailwater of Locks and Dam 53. Water-surface elevations at the model boundary were determined by translating the stage upstream from the USACE–St. Louis District gaging station at Cairo, Ill., by use of the water-surface slope measured between the gages at Locks and Dam 53 and Cairo, Ill.

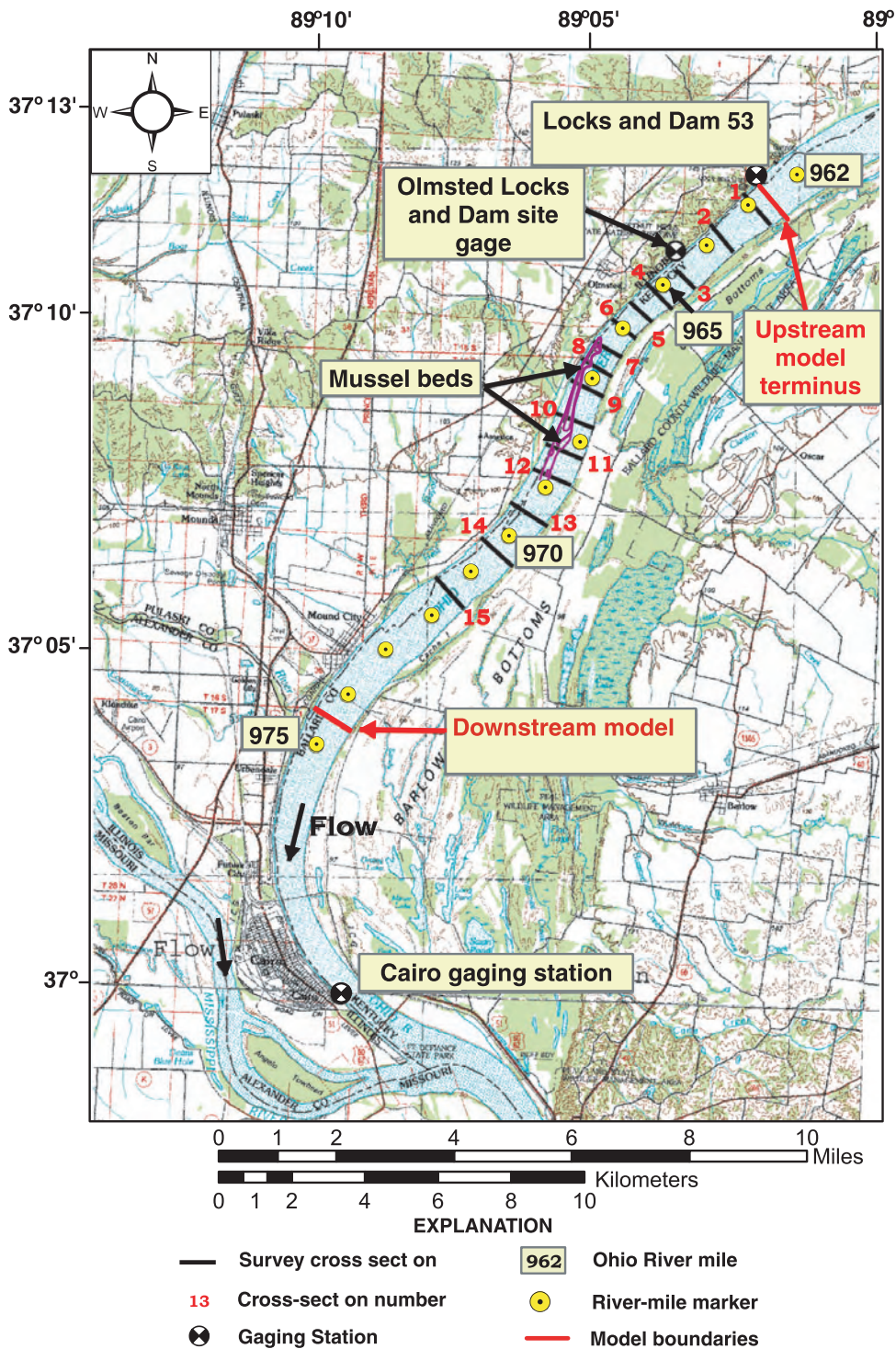


Figure 7. Location of hydrographic-survey cross sections and gaging stations on the Ohio River in the Olmsted Locks and Dam study reach near Olmsted, Illinois.

Velocity and Discharge

Water-velocity and discharge data were collected from a moving boat. The horizontal position of the boat was measured by use of a differentially corrected global positioning system (DGPS) receiver. The DGPS system used receives its differential corrections from a commercial service's communications satellite. The unit is specified by the manufacturer to be accurate to 3.3 ft at two standard deviations; tests and prior use of this unit indicate that typically about 80 percent of the data are within 3.3 ft of the true location.

Advances in velocity-measurement technology allow three-dimensional velocities to be collected from a moving boat using an acoustic Doppler current profiler (ADCP) (Oberg and Mueller, 1994; Mueller, 1996). All velocities were measured with an ADCP. At the time of the survey, the ADCP allowed three-dimensional velocities to be measured from approximately 4 ft beneath the water surface to within 6 percent of the depth to the bottom. Established methods were used to estimate the discharge in the unmeasured top and bottom portions of the profile (Simpson and Oltmann, 1992). Cross-sectional average velocities were computed by dividing the measured discharge by the measured cross-sectional area. In addition, depth-averaged velocities were computed for subsections of the flow in each cross section; however, these discrete depth-averaged velocities were computed as an average of the measured velocity and did not account for the velocity in the unmeasured portions of the water column.

All of the discharge measurements collected were averaged to produce a flow rate that was representative of the entire survey period to compensate for the slight changes in discharge of the river during the survey.

Bathymetry

Bathymetry data also were collected from a moving boat. The horizontal position of the boat was measured by use of a DGPS receiver. Starting in 1993, bathymetric surveys were done annually by the USACE–St. Louis District by use of a phased-array echo sounder. The phased-array system

produced an extremely dense data set for a majority of the study reach. The raw bathymetry data was processed onto a grid with 40 by 40 ft spacing to make the file size more manageable. The most recent survey at the time of the model development (2000) was used to create the main-channel bathymetry; however, the survey in 2000 was done during a low-flow period and did not include much of the banks. The 2000 survey data were supplemented with the bank bathymetry data from the 1996 survey, which was done during a high-flow period. The floodplains were digitized from USGS 7.5-minute quadrangle topographic maps with 5-ft contour intervals.

Computational-Mesh Configuration

The number of active elements that comprise the finite-element mesh for the baseline model ranged from 13,850 to 22,790, depending upon the simulated-flow conditions. The model with the fully constructed Olmsted Locks and Dam had a finite-element mesh of 14,700 to 24,475 active elements. The resolution of the grid is increased in the area surrounding the Olmsted Locks and Dam to improve simulation of hydraulic complexities caused by these structures (fig.8). The lock chambers were not modeled individually but rather as a single prismatic structure with an elevation set to the top of the lock walls (310 ft). The piers at the upstream end of the locks and those supporting the tainter gates were modeled as gaps in the mesh corresponding to their planned dimensions. Baffle blocks at the end of the tainter-gate spillways were modeled by increasing the Manning's roughness value ($n=.06$) of the elements representing the baffles; this value allowed flow through the elements under an increased resistance. An increased Manning's roughness value ($n=.09$) also was assigned to the elements representing the lock walls to simulate the passage of flow under the four floating guide walls leading into and out of the lock chambers.

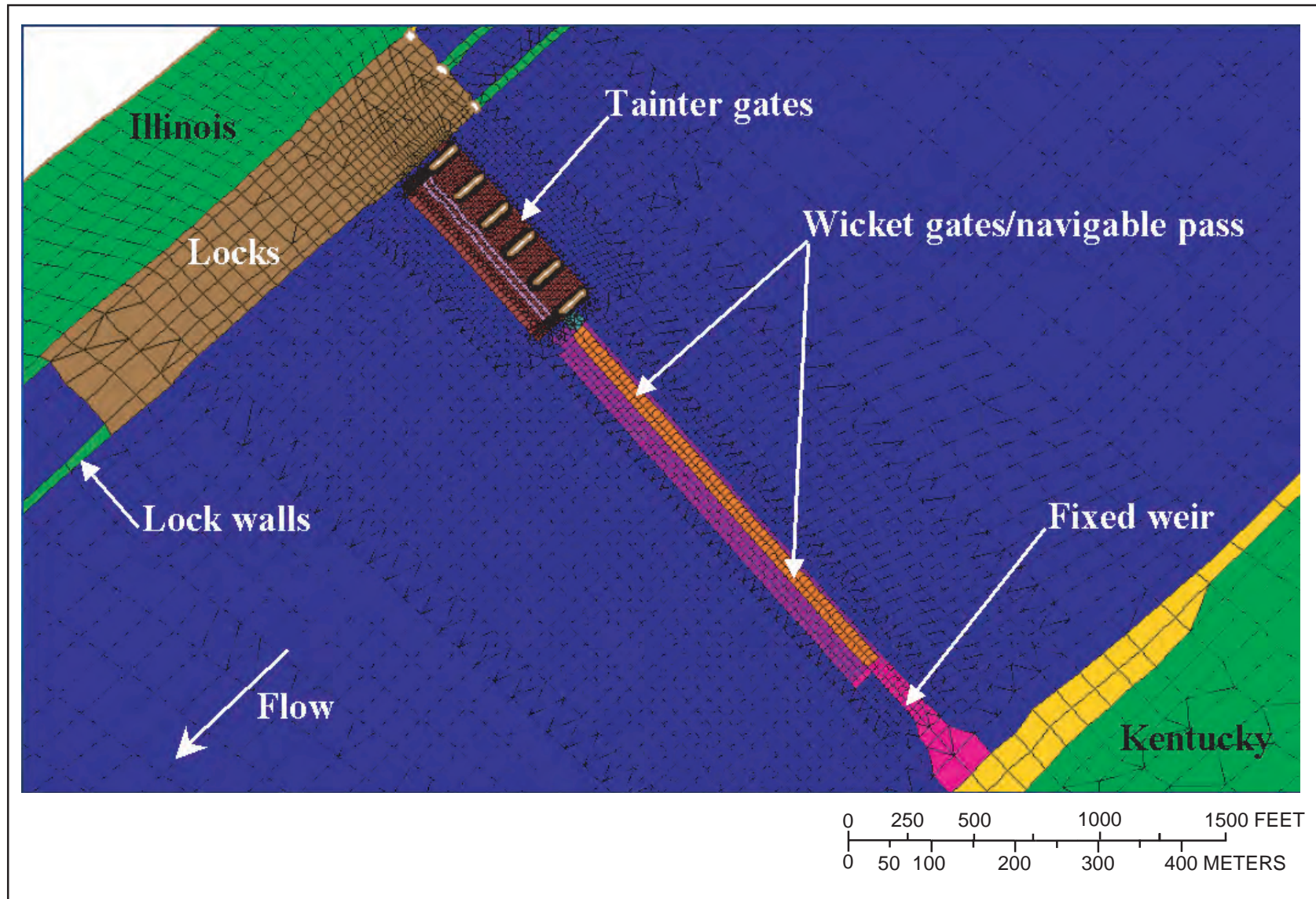


Figure 8. Mesh configuration around the simulated Olmsted Locks and Dam near Olmsted, Illinois.

Boundary Conditions

A steady-state discharge of 350,000 ft³/s was used to calibrate the model and steady-state discharges of 72,500 and 770,000 ft³/s were used to validate the model. These discharges were used as the upstream-boundary condition for the model, and the lateral inflow was based on depth across the inflow boundary for the middle- and high-flow conditions. The low-flow discharge was distributed uniformly across the inflow boundary. The justification for the specified lateral distribution of inflow is a comparison of the velocity data collected just downstream of Locks and Dam 53 (inflow boundary). The inflow distribution was adjusted until the velocity distribution of the model matched the distribution collected with the ADCP.

The downstream head-boundary conditions for all discharges were determined by translating the stage upstream approximately 5 mi from the USACE–St. Louis District gaging station at Cairo, Ill., to the model boundary using the water-surface slope measured between the gages at Locks and Dam 53 and Cairo, Ill.

Discussion of Calibration and Validation Results

Data from the mid-flow (350,000 ft³/s) hydraulic survey were used to calibrate the model and data from the low- and high-flow (72,500 and 770,000 ft³/s, respectively) surveys were used to validate the model.

The calibration and validation process consisted of comparing the simulated water-surface elevations at the water-surface-elevation stations and cross-sectional velocity profiles with those surveyed in the field. A Manning’s roughness coefficient (*n*) was assigned to each element and iteratively adjusted until the model most accurately simulated both the surveyed water-surface elevations and velocity profiles.

Inspection of the velocity profiles collected in the field revealed no-slip conditions along the riverbanks, which means the shear stress along the banks is great enough to cause the tangential velocity to approach zero. To simulate this characteristic with RMA-2, the Manning’s *n* value was increased to .036 for one row of elements along

the edges of the channel. The calibrated Manning’s *n* in the remainder of the channel was .020. This combination produced the best simulation of water-surface elevation (table 1), velocity magnitudes, and lateral-velocity distribution for the mid-flow condition. The low- and high-flow conditions were then run through the calibrated model and the results were verified with surveyed water-surface elevation (table 4) and velocity data.

Table 4. Summary of water-surface elevation calibration and validation for the Olmsted Locks and Dam study reach near Olmsted, Illinois

Olmsted Locks and Dam site			
Discharge (cubic feet per second)	Field water-surface elevation (feet above sea level)	Model water-surface elevation (feet above sea level)	Difference ¹ (feet)
75,000	286.84	287.06	-0.22
350,000	305.94	306.00	-.06
750,000	322.34	322.10	.24

¹Difference is determined by subtracting modeled from field water-surface elevation.

The simulated-velocity magnitudes and distributions compared well with the field measurements. A comparison of the simulated- and measured-velocity profiles for cross-section number 4, which is directly downstream of the cofferdam that was in place during the construction of the Olmsted locks, is shown in figure 9. The shape of the field- and model-velocity distributions compared very well, while on average, the velocity magnitudes were within 0.25 ft/s. The average cross-sectional velocities for the 15 cross sections also were compared, and the model adequately reproduced the average field velocities (figs. 10 and 11), although a bias was observed. From the experience of other two-dimensional hydrodynamic models on the Ohio River, the bias in the velocity distributions is likely to be a function of the model bathymetry. The date of the bathymetric survey used in the model development (2000) and the hydrographic surveys used in the calibration (1997 and 1998) differ by 2 to 3 years. During that time, bathymetry data in the study reach showed riverbed aggradation and degradation in response to variation in flow patterns.

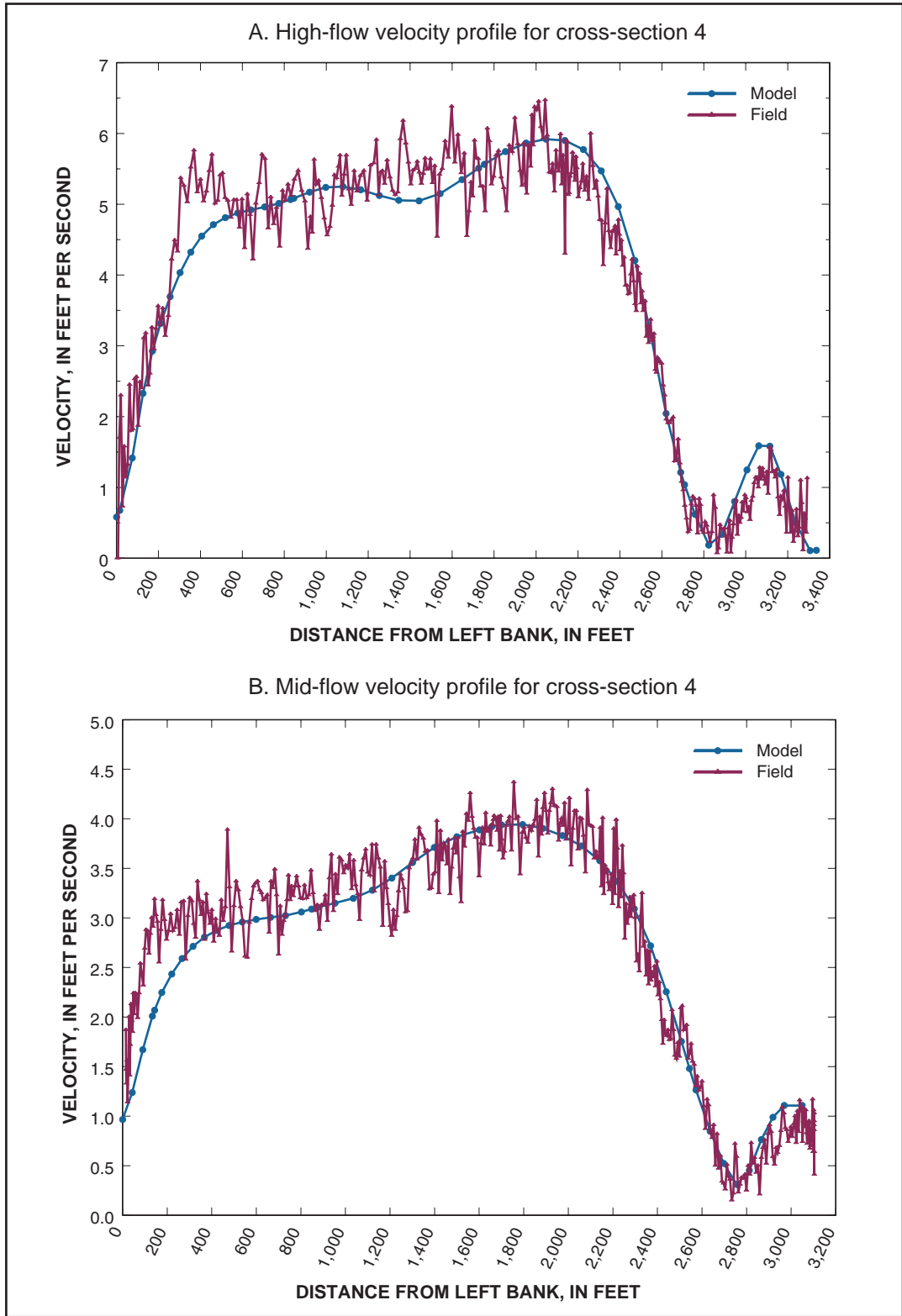


Figure 9. Measured and simulated velocity profiles for cross-section 4 in the Olmsted Locks and Dam simulation near Olmsted, Illinois.

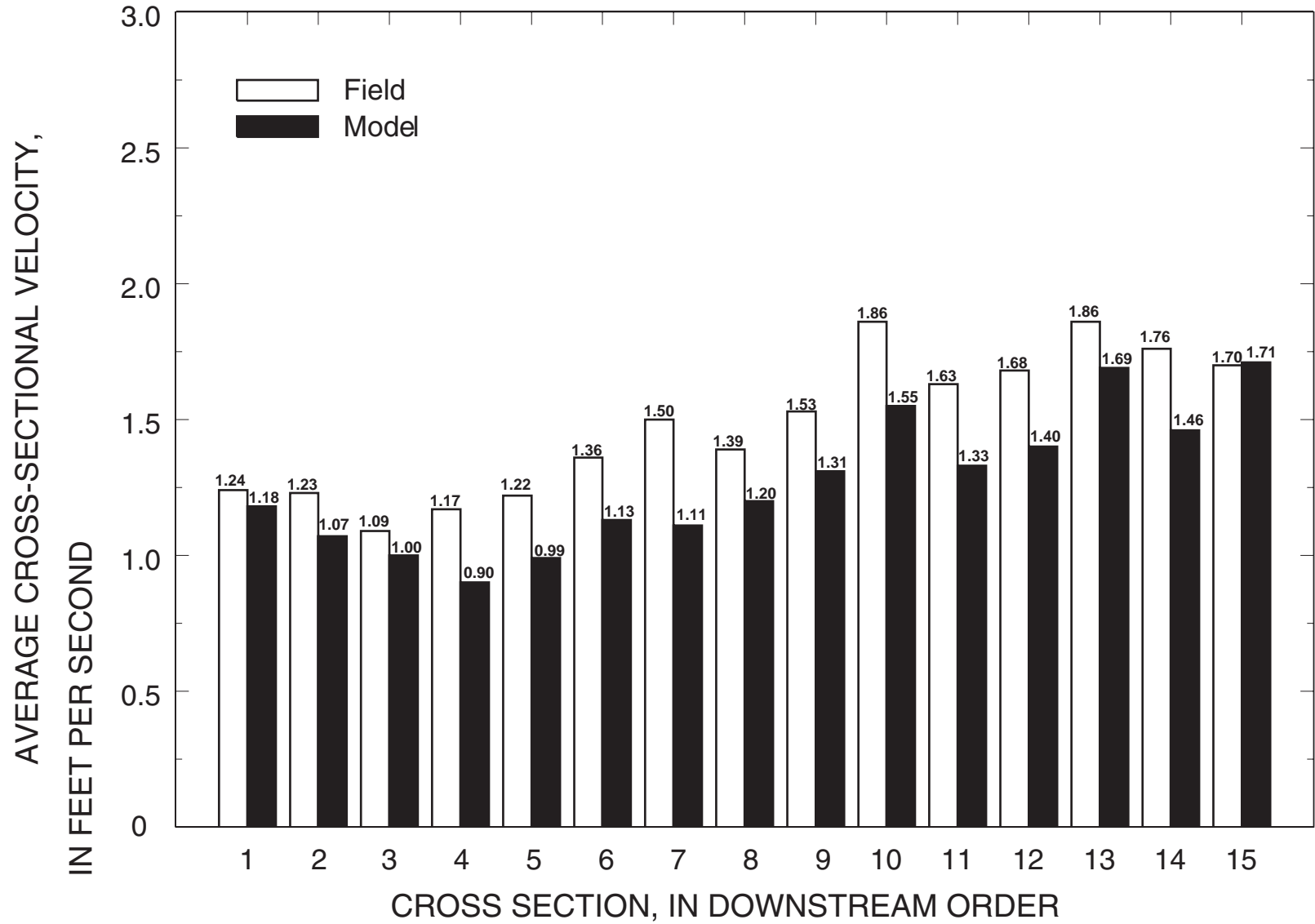


Figure 10. Measured and simulated average cross-sectional velocities during low-flow conditions in the Olmsted Locks and Dam study reach near Olmsted, Illinois.

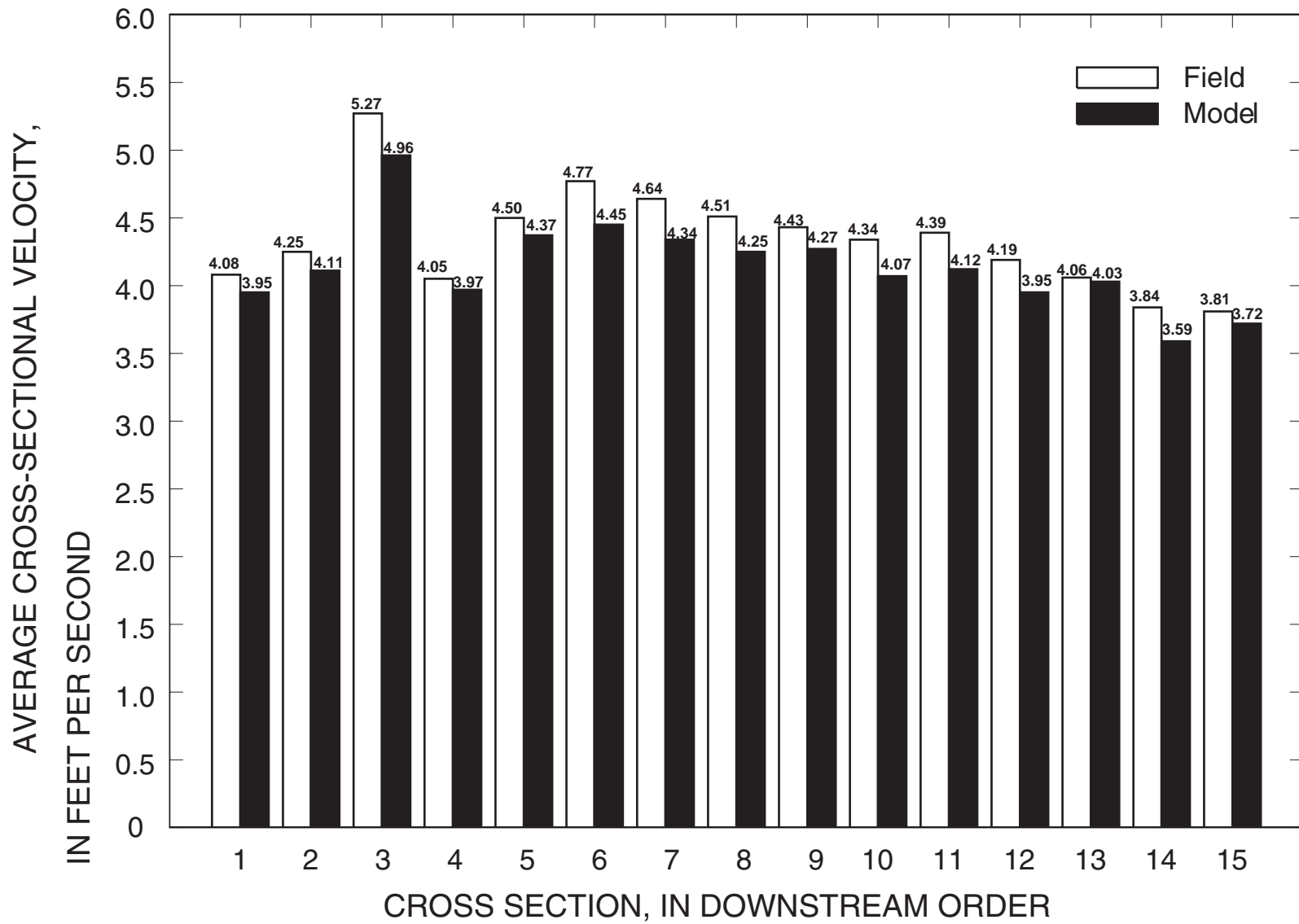


Figure 11. Measured and simulated average cross-sectional velocities during high-flow conditions in the Olmsted Locks and Dam study reach near Olmsted, Illinois.

The USGS has shown that on the Ohio River the difference in channel depths (and corresponding cross-sectional area) between the model and calibration data contributes to the bias experienced in the average cross-sectional velocities (Wagner and Mueller, 2001).

The model accurately reproduced the velocity directions, especially in areas of reverse flow experienced along the Kentucky bank just downstream of Locks and Dam 53 (fig. 12) and in the shadow of the Olmsted cofferdam (fig. 13).

Continuity was checked throughout the model to assure that mass was being conserved. Table 5 shows that the model conserved mass throughout the reach under the low-, mid-, and high-flow conditions. A tolerance of +/- 3 percent in mass conservation discrepancy is typically acceptable for most models (Donnell, Letter, McAnally and others, 2001).

Upon completion of the calibration and validation process, the proposed Olmsted Locks and Dam structures were added to the model without the ability to compare the model results with field data. The alternative to field data was to compare the numerical model to results from a physical model developed by the USACE Waterways Experiment Station in Vicksburg, Miss. The flow fields for the numerical and physical models were consistent for flow conditions that did not require the use of the wicket gates across the navigable pass (stages at the dam greater than 295 ft). Differences between the numerical and physical model-flow fields were observed for low-flow conditions requiring the wicket gates to be raised, which forced the entire flow of the river (aside from the leakage through 6-in gaps between each wicket gate) to be diverted through the five-tainter gates.

The numerical model of the Olmsted Dam can simulate flow across the wicket gates with or without leakage through the 6-in gaps between the wickets. Simulation without leakage produces results that are consistent with results obtained by

use of the physical model. In particular, simulation results without leakages show the velocity thalweg markedly bending toward the left bank (Kentucky shoreline) (fig. 14). In contrast, results with leakage show the velocity thalweg remains in line with the tainter gates along the Illinois shoreline (fig. 15) in a way that is consistent with the physical model. Therefore, simulation with leakage across the wicket gates is considered the appropriate representation in the numerical model.

USACE leakage calculations for the proposed Olmsted Locks and Dam wicket gates as well as other wicket-gate structures on the Ohio River revealed an average leakage of approximately 15,000 ft³/s over the wide range of tailwater/headwater stage combinations expected once the dam is fully operational. The estimated leakage is an appreciable percentage (14 to 17 percent) of the total discharge modeled during the low-flow periods. The low-flow numerical simulations were adjusted to allow the leakage through the wicket gates and resulted in a more reasonable flow field (fig. 15), which matched the WES physical-model output.

SEDIMENT-TRANSPORT MODEL DEVELOPMENT

Simulated velocities and water levels from the hydrodynamic simulations were used with the WES Sed2D model and information on bed-material characteristics to simulate the effects of the Olmsted Locks and Dam on sediment deposition and erosion in the study reach. The following sections describe the application and results of the sediment-transport modeling on the lower Ohio River.

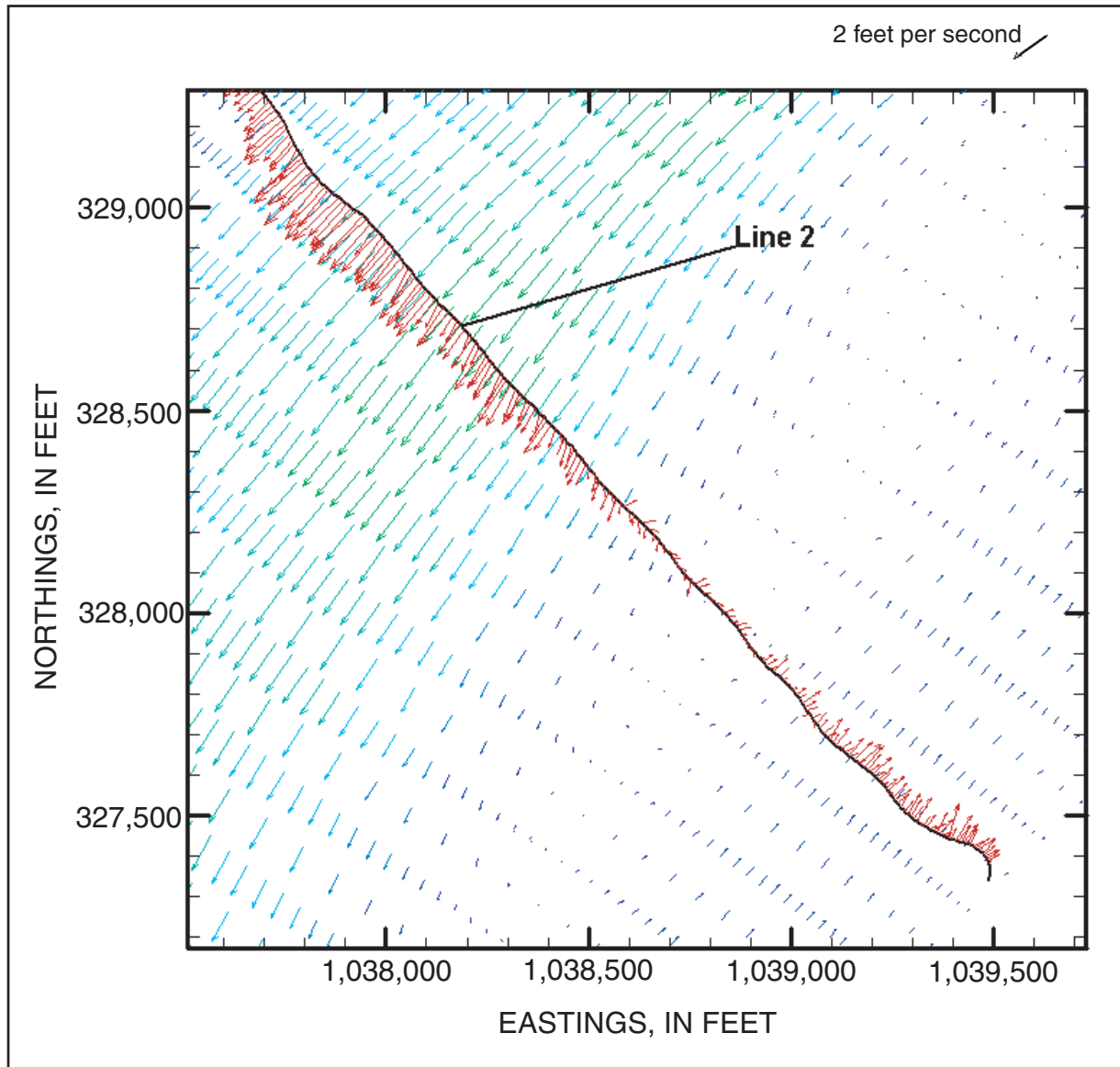


Figure 12. ADCP-measured and simulated low-flow velocity vectors at cross-section 2 in the Olmsted Locks and Dam study reach near Olmsted, Illinois (red arrows - field data, multi-colored arrows - model data) (horizontal datum - state plane coordinates, Ky. South).

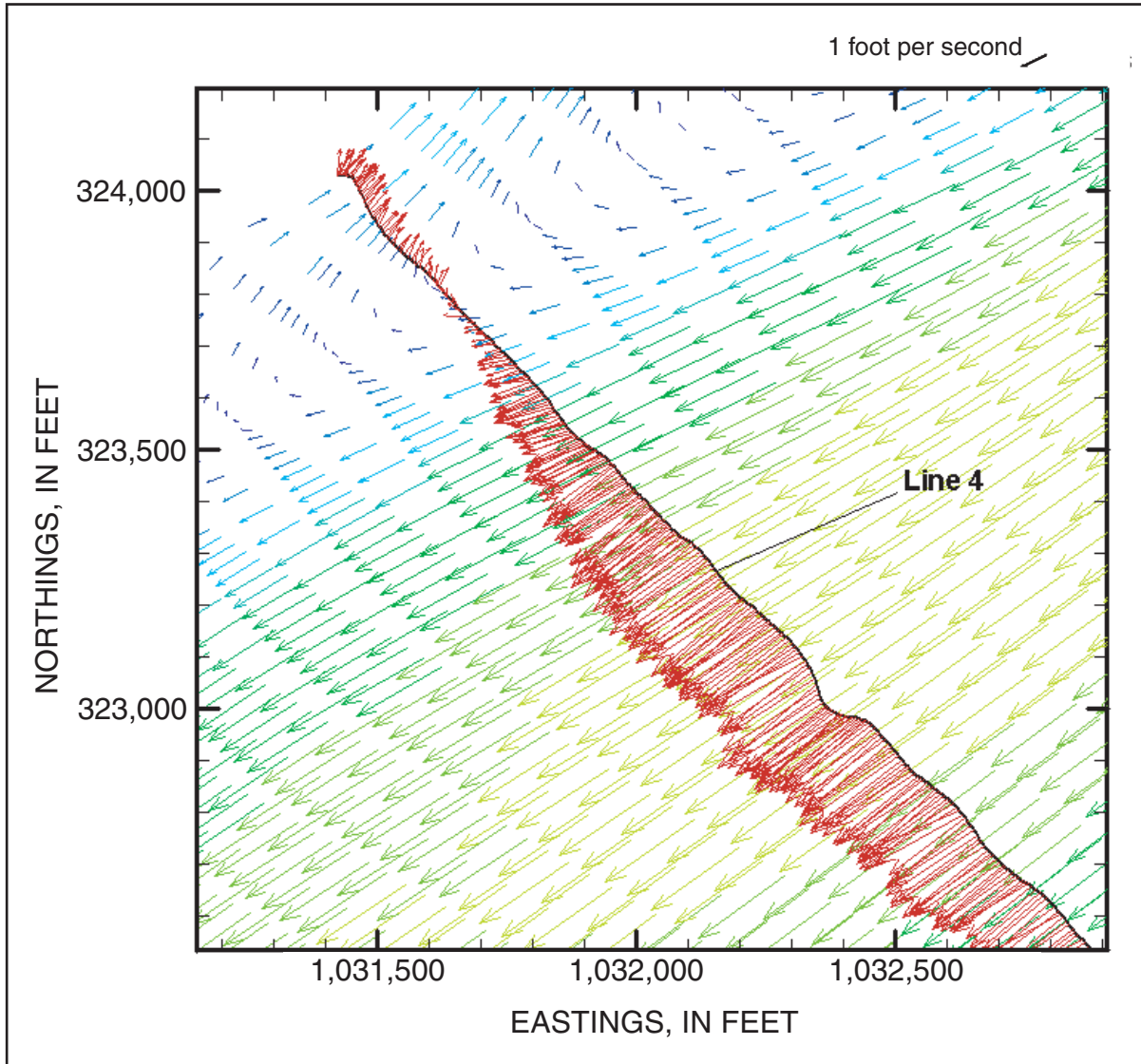


Figure 13. ADCP-measured and simulated low-flow velocity vectors at cross-section 4 in the Olmsted Locks and Dam study reach near Olmsted, Illinois (red arrows - field data, multi-colored arrows - model data) (horizontal datum - state plane coordinates, Ky. South).

Table 5. Summary of continuity checks for the Olmsted Locks and Dam model

Continuity check line description	Percent of total discharge		
	Low flow	Mid flow	High flow
Inflow	100.0	100.0	100.0
Cross-section 4	99.3	100.2	100.5
Cross-section 10	99.9	100.4	100.7
Cross-section 14	100.1	100.4	100.6
Total outflow	100.0	100.5	100.4

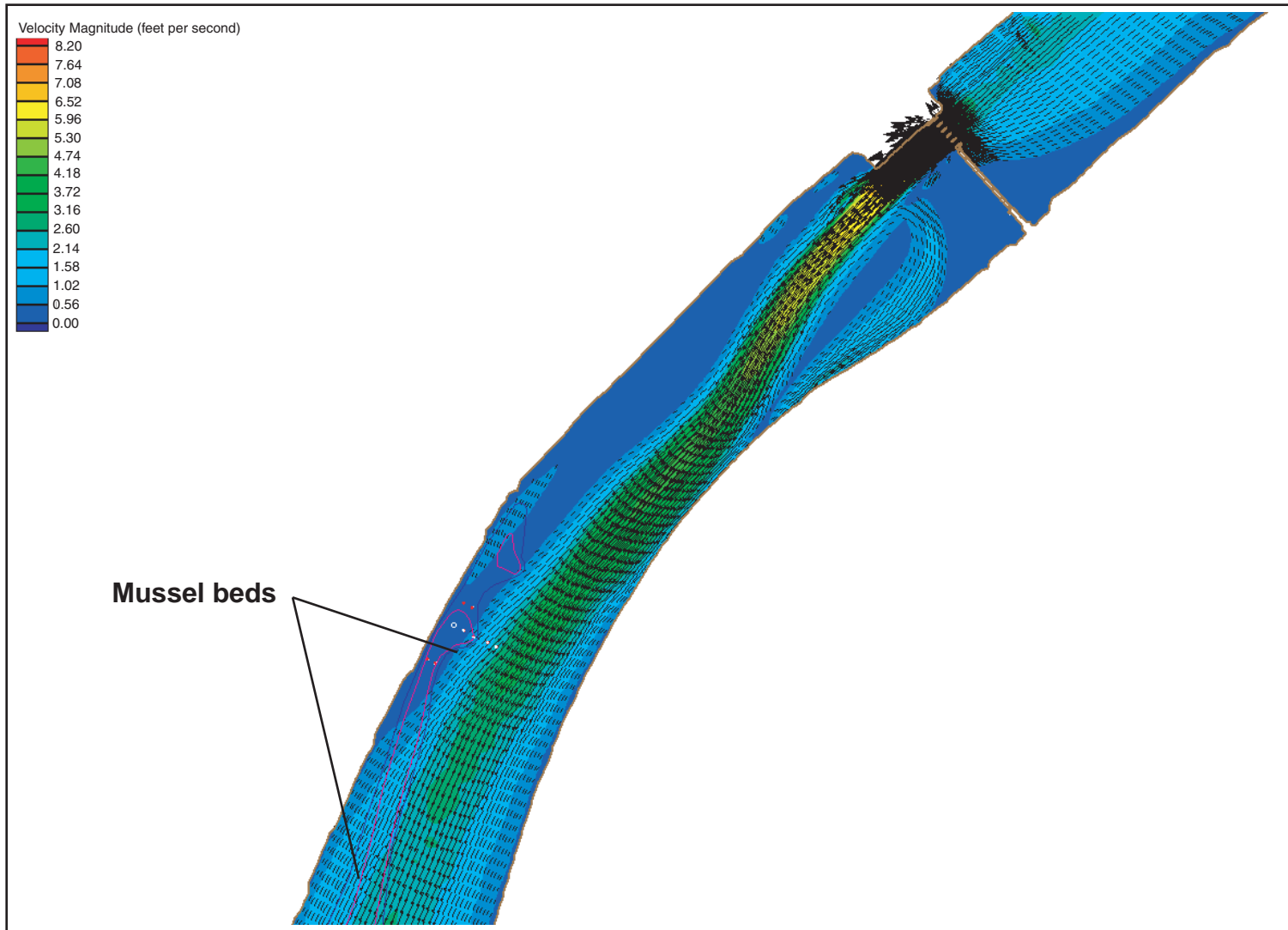


Figure 14. Velocity-magnitude contours and vectors of the flow field for a low-flow simulation with no flow-through gaps in the wicket gates of the Olmsted Locks and Dam model near Olmsted, Illinois.

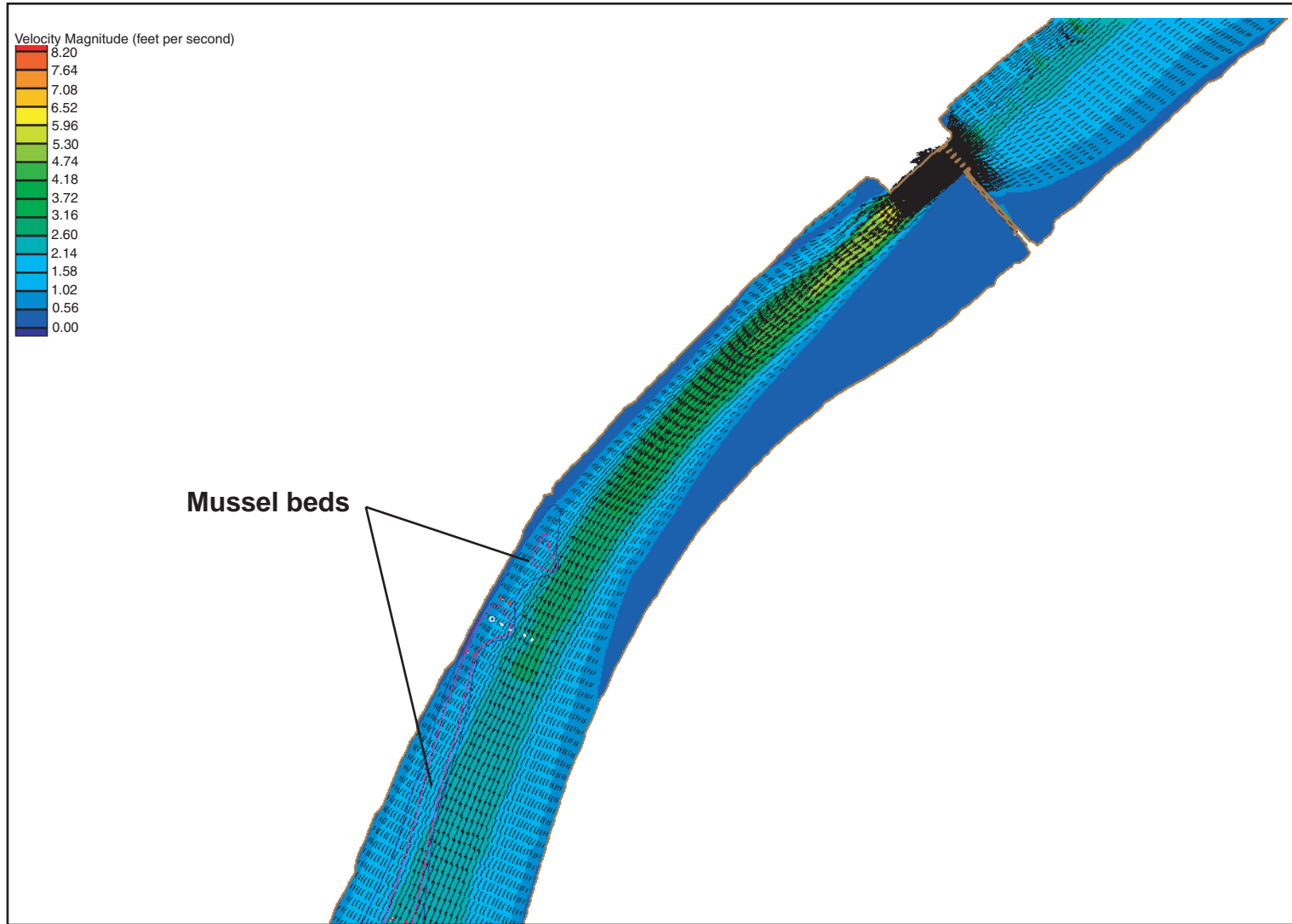


Figure 15. Velocity-magnitude contours and vectors of the flow field for a low-flow simulation with flow-through gaps in the wicket gates of the Olmsted Locks and Dam model near Olmsted, Illinois.

Sed2D Sediment-Transport Model Description

Sed2D (version 4.52) (U.S. Army Corps of Engineers, 2000) is a two-dimensional, vertically averaged finite element, numerical sediment-transport model for open-channel flows capable of computing deposition, erosion, and transport patterns for bed-load sediments (those sediments comprising the river bed throughout the model domain). It is the sediment-transport companion for the RMA-2 hydrodynamic model and can be applied to clay- or sand-bed sediments where flow velocities can adequately be represented by a two-dimensional, depth-averaged solution. The Sed2D code handles two categories of sediment:

(1) noncohesive, which is referred to as sand; and (2) cohesive, which referred to as clay. For the study discussed herein, noncohesive sediment was modeled in Sed2D using the Ackers and White (1973) formula as the governing sediment-transport equation. The exchange of the material in suspension with the bed can be calculated by the model or suppressed (U.S. Army Corps of Engineers, 2000).

Both steady-state and transient-flow problems can be analyzed. The user can prescribe input data on sediment characteristics or default values may be used for most of the input parameters. Bed-shear stresses caused by flow currents can be calculated by either a smooth-wall velocity profile or the Manning's equation.

One of the predominant limitations to the model is that although both clay and sand material can be analyzed, only a single, effective grain size is considered during each simulation. Therefore, a separate model run is required for each effective grain size in the bed load. Fall velocity, water-surface elevations, and x- and y-velocity components are parameters that must be specified, while diffusion coefficients, bed density, critical-shear stress for erosion, erosion rate constants, and critical-shear stress for deposition are input data for which default or prescribed values may be applied (U.S. Army Corps of Engineers, 2000).

An implicit assumption of the Sed2D model is that changes in the bathymetry caused by erosion and (or) deposition do not appreciably affect the computed flow field. When the bed change

calculated by the model does become appreciable (based on a user-defined bed-change tolerance), the externally calculated flow field is no longer valid. The Sed2D model run should then be stopped, a new flow field should be calculated using the new deformed bed, and the Sed2D run restarted with the new flow field as input. Another assumption by the Sed2D model is that the input geometric mesh and resulting hydrodynamic solution are of adequate resolution and quality to allow for an accurate and reasonable solution to the governing sediment-transport equation being solved (U.S. Army Corps of Engineers, 2000).

Model-Input Parameters

The following sections will provide a discussion of the input data required to solve the governing equations of the Sed2D model as well as a brief explanation of the methods used to develop the input parameters.

Bed Material

The USACE–St. Louis District collected bed-material data in the study reach on June 30, 1993, and February 13, 1994. These data were processed into a percent-finer format and geographically positioned to evaluate the composition of the bed material throughout the study reach. The bed-material sampling locations around the mussel beds are spatially referenced in figure 16 along with the D_{16} , D_{50} , and D_{95} data collected for the cross sections. The percent-finer-than values D_{16} , D_{50} , and D_{95} correspond to a grain size diameter that a given percentage of the material in a sample is less than (i.e., D_{50} is the grain size diameter for which 50 percent of the sample is less than). A summary of the D_{50} for all of the bed-material data collected in the four cross sections is shown in figure 16 and is plotted in figure 17 along with each sample's position in the cross section. The data reveal that the mussel bed primarily is composed of gravel (average grain size around 10 mm), and the main channel primarily is composed of sand.

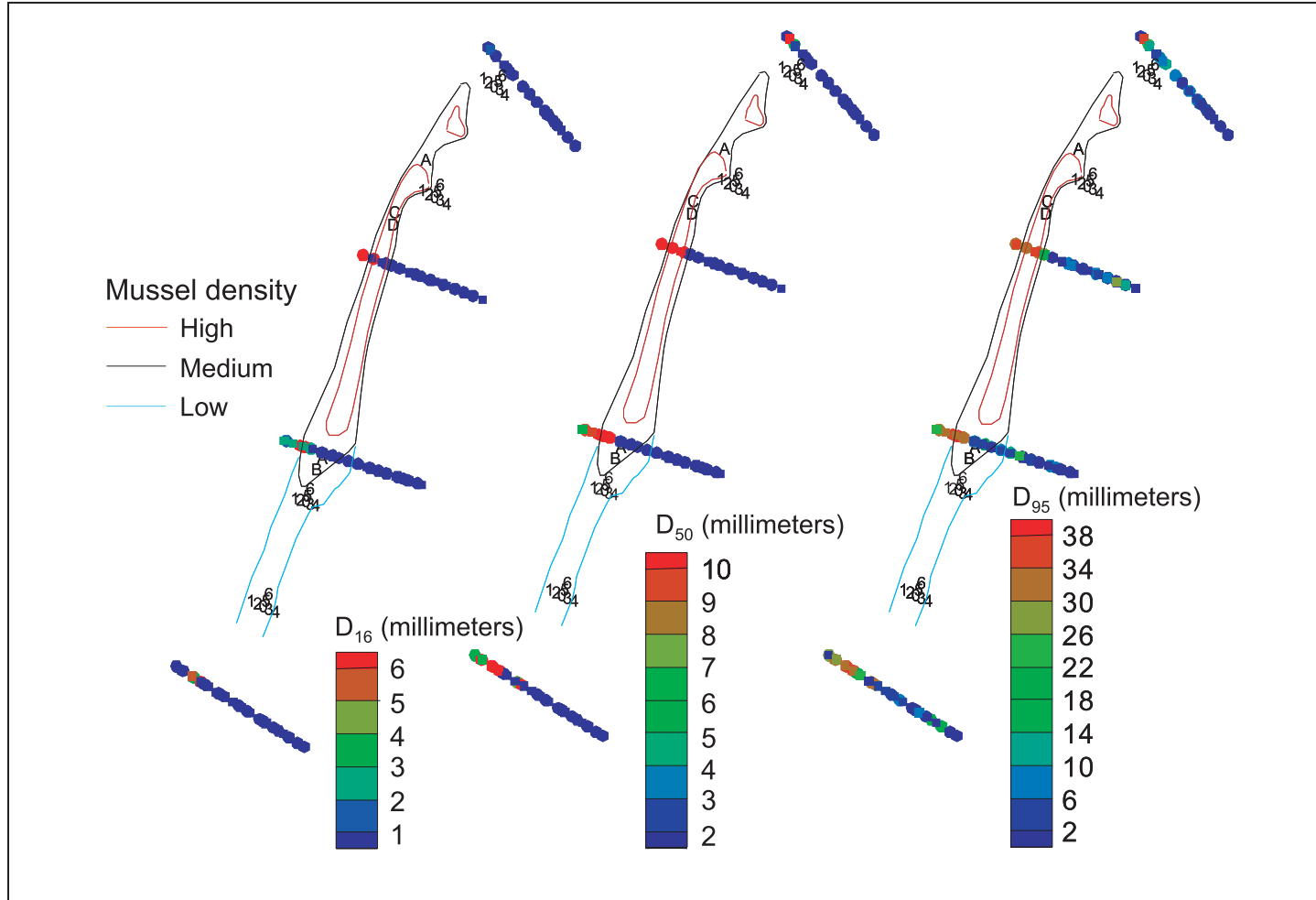


Figure 16. Bed-material data collected by the U.S. Army Corps of Engineers, St. Louis, Mo., in the cross sections located on or near the mussel beds in the Olmsted Locks and Dam study reach near Olmsted, Illinois.

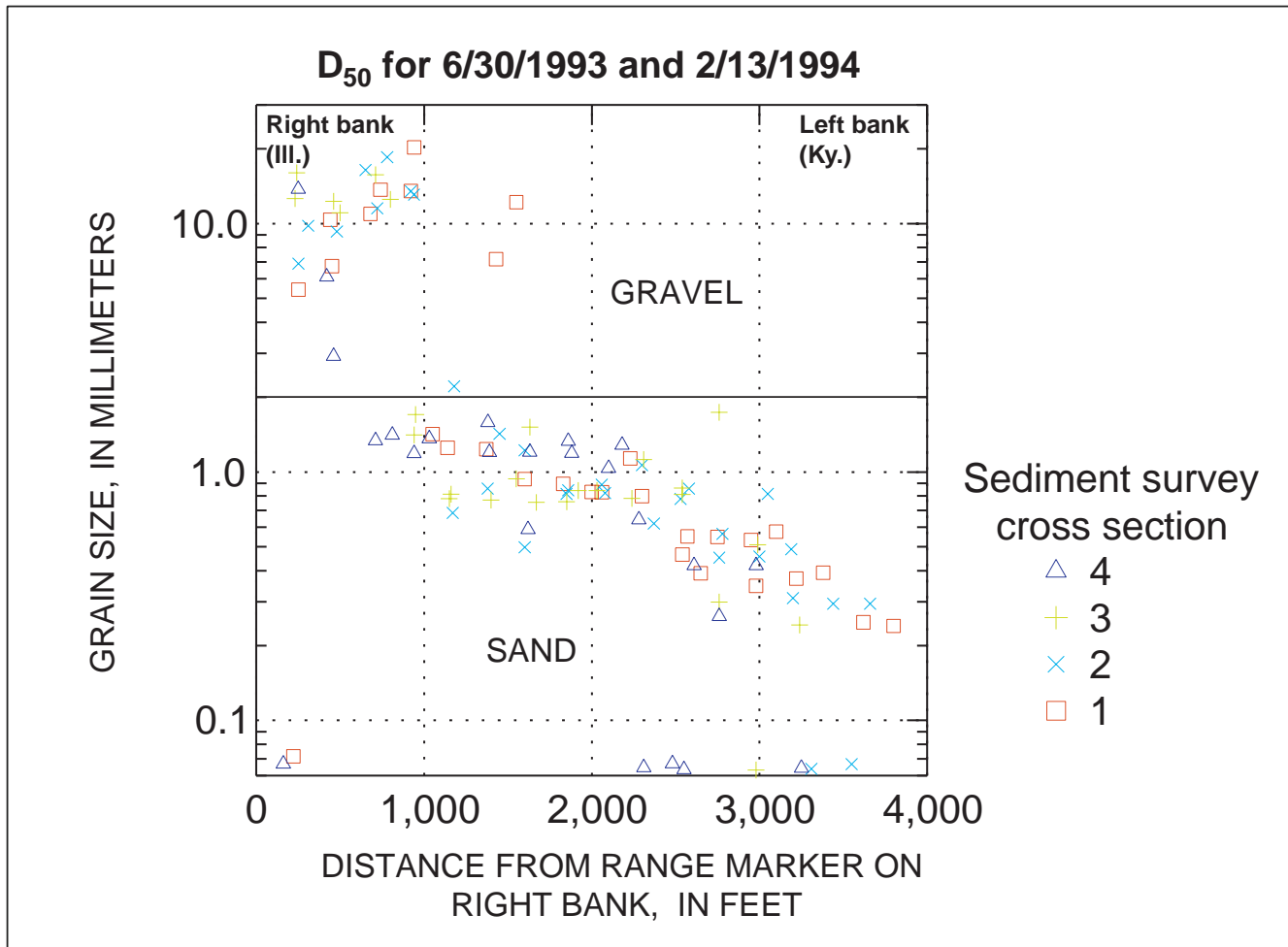


Figure 17. Summary of the bed-material D_{50} for the samples collected by the U.S. Army Corps of Engineers, St. Louis, Mo., at four cross sections located around the mussel beds in the Olmsted Locks and Dam study reach near Olmsted, Illinois.

Selection of Representative Grain Size

Currently (2004), Sed2D (version 4.52) only considers a single, effective grain size during each simulation. From substitution of the mussel-bed grain size (10 mm) into the Hydraulic Engineering Circular-18 (HEC-18) (Richardson and Davis, 2001) equation for critical velocity, it was estimated that the mussel bed would not scour at any of the hydraulic conditions being modeled; therefore, the representative grain size for the reach was determined by inspection of the D_{50} in the other areas of the reach. The field data shown in figures 16 and 17 indicate that aside from the mussel beds the average grain size of the material comprising the channel bed is around 0.6 mm. A grain size of 0.6 mm was thought to be the most representative of the reach assuming no scour of the mussel beds would occur for the hydraulic conditions to be modeled.

Time Step

The time step of 2 hours was selected for the sediment-transport simulation after doing a sensitivity analysis with time steps ranging from 0.25 to 8 hours. The results of the sensitivity analysis, engineering judgment, and the project's time constraints were the governing factors in the selection of the 2-hour time step.

Particle-Fall Velocity

The fall velocity of the representative particle size was determined using the graphical relation developed for quartz spheres with specific gravity of 2.65 in fresh water by Rouse (1937). From Rouse's graphical relation, the corresponding fall velocity for a 0.6-mm sand particle is 0.000295 ft/s.

Concentration of Sediment Inflow

The sediment-inflow boundary conditions for the annual hydrographs were established by a rating curve developed by use of Sed2D. The various hydrograph steps were modeled with no sediment supply to the study reach to allow the river to reach equilibrium conditions. The equilibrium-sediment concentration for each step was used to build the bed-material inflow-rating curve. The absence of

grain-size distributions for the suspended-sediment concentrations collected in the field and the inability for Sed2D to model multiple grain sizes prevented the use of empirical bed-load equations.

Other model parameters such as dispersion coefficients, bed thickness, and characteristic erosional and depositional lengths were estimated by sensitivity analysis, model documentation, and engineering judgment of the output from numerous preliminary Sed2D runs on the reach and use of default values specified by WES (table 6).

Table 6. Sed2D model-input parameters

[ft, foot; mm, millimeter; ft/s, foot per second; ft²/s, square foot per second]

Input parameter	Value
Bed material	Sand
Grain size	0.0002 ft (0.6 mm)
Specific gravity	2.65
Time step	2 hours
Particle-fall velocity	0.00030 ft/s
Dispersion coefficient (xx)	161.5 ft ² /s
Dispersion coefficient (yy)	161.5 ft ² /s
Grain-shape factor	*.67
Deposition-length factor	*1.0
Erosion-length factor	*10
Bed thickness	13 ft
Grain roughness	0.002 ft

*Sed2D default values.

Calibration of Sediment-Transport Model

The sediment-transport model was not calibrated because of time constraints placed on the project requiring the results to be included in the Environment Impact Assessment requested by the USFWS. Although the bathymetric surveys of the study reach could have been used to calibrate the model, the length of time between available survey data sets and the size of the model domain were limiting factors in the calibration process. For example, using the bathymetry from the 1996

survey as the initial bed and simulating a hydrograph representative of the time between the 1996 and 1997 bathymetric survey, the deformed bed at the end of the simulation could be compared to the bathymetry collected in 1997. The input parameters then could be adjusted until the modeled and surveyed beds match. The average computer run time for an annual hydrograph was 1.5 to 2 weeks, which precluded using the available data for calibration because of the time constraints.

It is important in this section to reiterate that the overall objective of the simulation was to determine the sediment-transport changes caused by the Olmsted Locks and Dam construction and operation. Therefore, as long as the input parameters and hydrographs were identical for both the baseline- and dam-model configurations the calibration process was not as important as if absolute deposition and scour estimates were required.

MODEL RESULTS

The results of the Olmsted modeling project are summarized according to the two modeling phases. The construction-phase modeling will focus on results of the 6-year dam-construction simulation and the operational-phase modeling will focus on the long-term results of the 3-year fully operational locks and dam simulation.

Construction-Phase Model—Hydrodynamics

Comparison of the baseline and construction-phase velocity magnitudes and distributions provides valuable insight into the changes in sediment-transport patterns caused by the Olmsted Locks and Dam project. Velocity profiles at cross-sections 4-11, shown in figure 7, were extracted from the baseline and the construction phase-3 scenarios for a comparison at low-, mid-, and high-flow conditions. Examples of the general agreement between the baseline and construction phase-3 velocity profiles are shown in appendix A, and

velocity-profile differences between the baseline and construction-phase 3 are shown in appendix B. The effects of construction-scenario 3 on the hydrodynamics are minimal downstream of cross-section 5 for the high-flow condition and cross-section 7 for the mid- and low-flow conditions. Phase 3 has little effect on the hydrodynamics beyond cross-section 7 for the mid-flow condition and cross-section 5 for the high-flow condition. The effects of phase 3 on the hydrodynamics during low-flow conditions (stages less than elevation 295 ft) are appreciable because of the closure of the navigable pass and the use of the tainter gates to pass the entire flow of the river. The hydrodynamic changes caused by the dam configuration in phase 3 during low-flow are still evident in the velocity profiles at cross-section 10, which is located near the middle of the mussel-bed region.

Construction-Phase Model—Sediment Transport

The difference in bed change between the baseline and construction phases for each of the six annual hydrographs in modeling-phase 1 are shown in figures 18-23 and in an animation of the bed change over the 6-year simulation (fig. 24). The interaction between the hydrodynamics (1997 hydrograph, step 7) and corresponding bed change in the section of river located between the dam and mussel beds at the end of year 5 is shown in figure 25. The amount and downstream extent of deposition caused by the dam construction progressively increases from year 1 through year 6. The initial concerns by USFWS and USACE were that high-flow conditions would have the most effect on sediment-transport patterns in the study reach (fig. 26); however, the most significant bed change occurred during the low-flow period at the end of year 5 in which the wicket gates were closed and the flow of the river passed through the tainter gates (fig. 27).

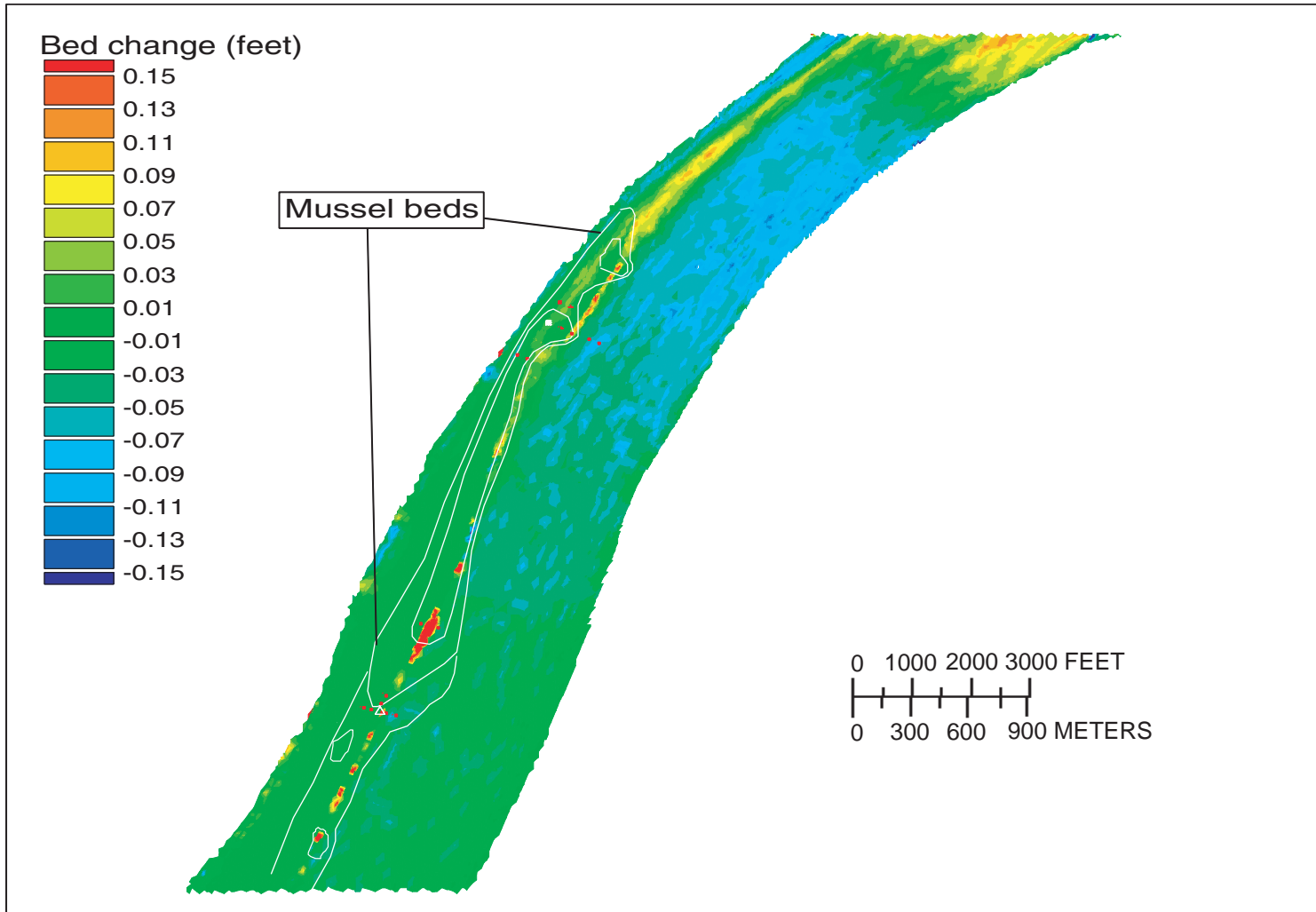


Figure 18. Difference in bed change between baseline and phase 1-construction simulations after year 1 (1996 hydrograph) in the Olmsted Locks and Dam study reach near Olmsted, Illinois.

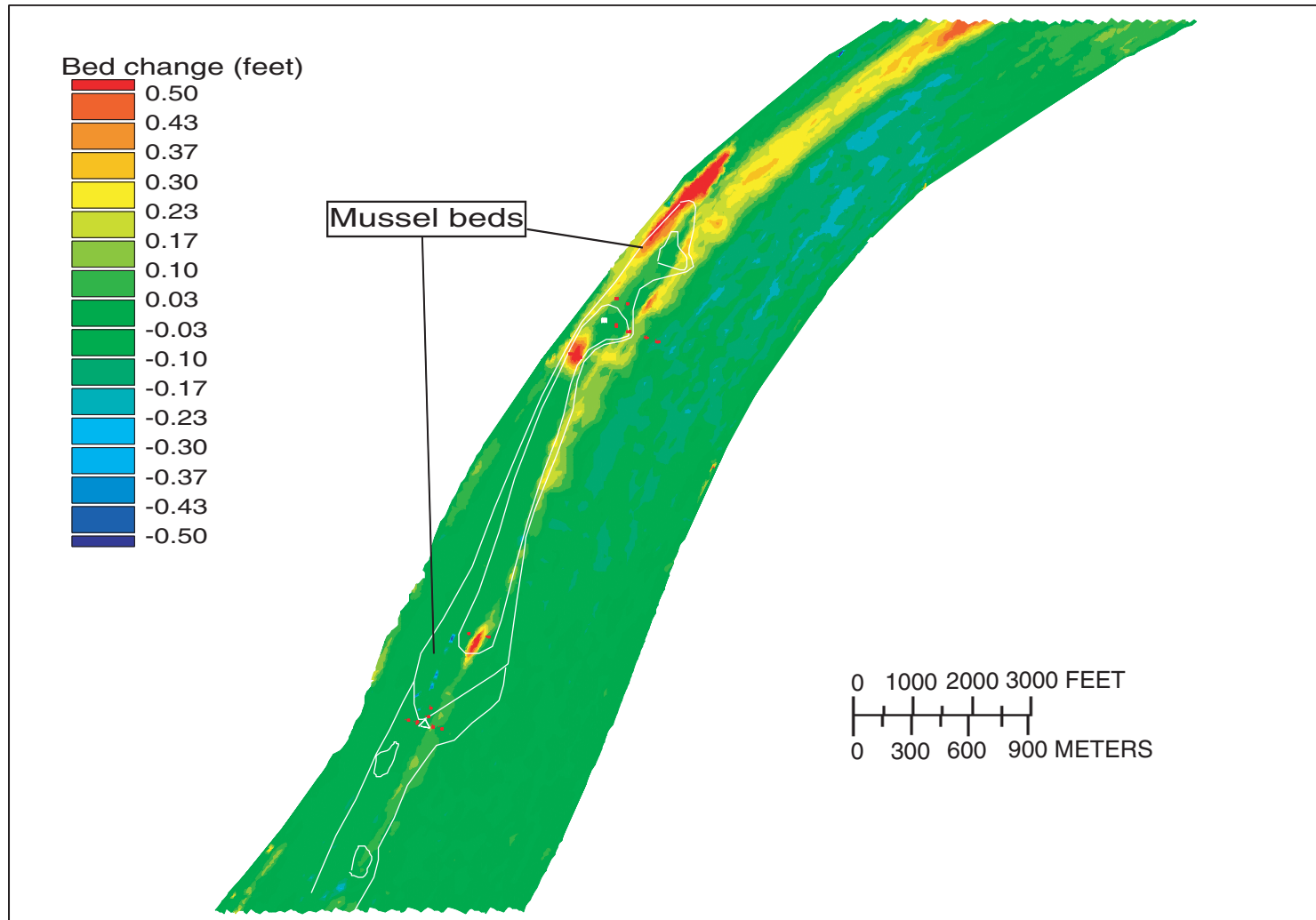


Figure 19. Difference in bed change between baseline and phase 2-construction simulations after year 2 (1997 hydrograph) in the Olmsted Locks and Dam study reach near Olmsted, Illinois.

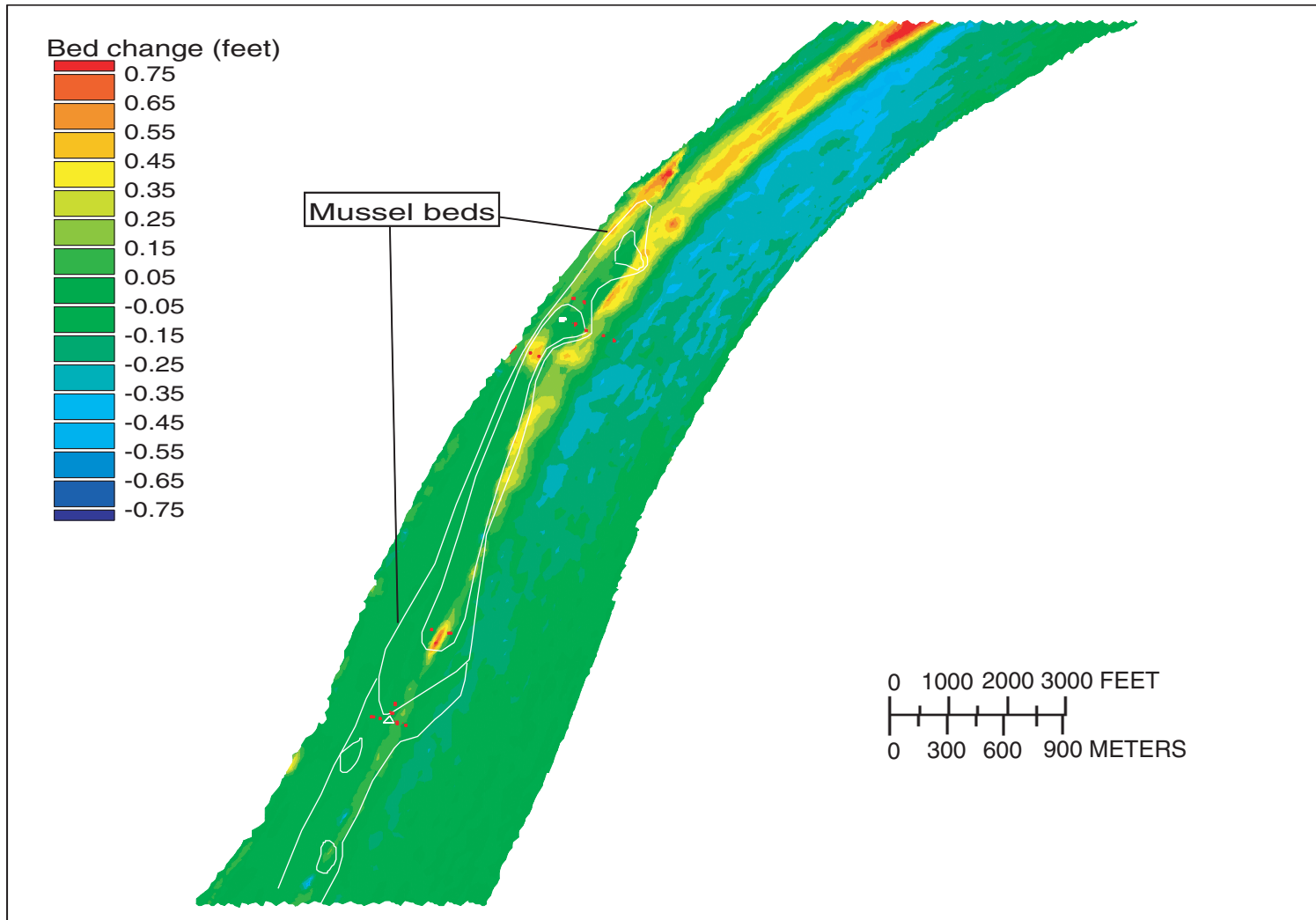


Figure 20. Difference in bed change between baseline and phase 2-construction simulations after year 3 (1996 hydrograph) in the Olmsted Locks and Dam study reach near Olmsted, Illinois.

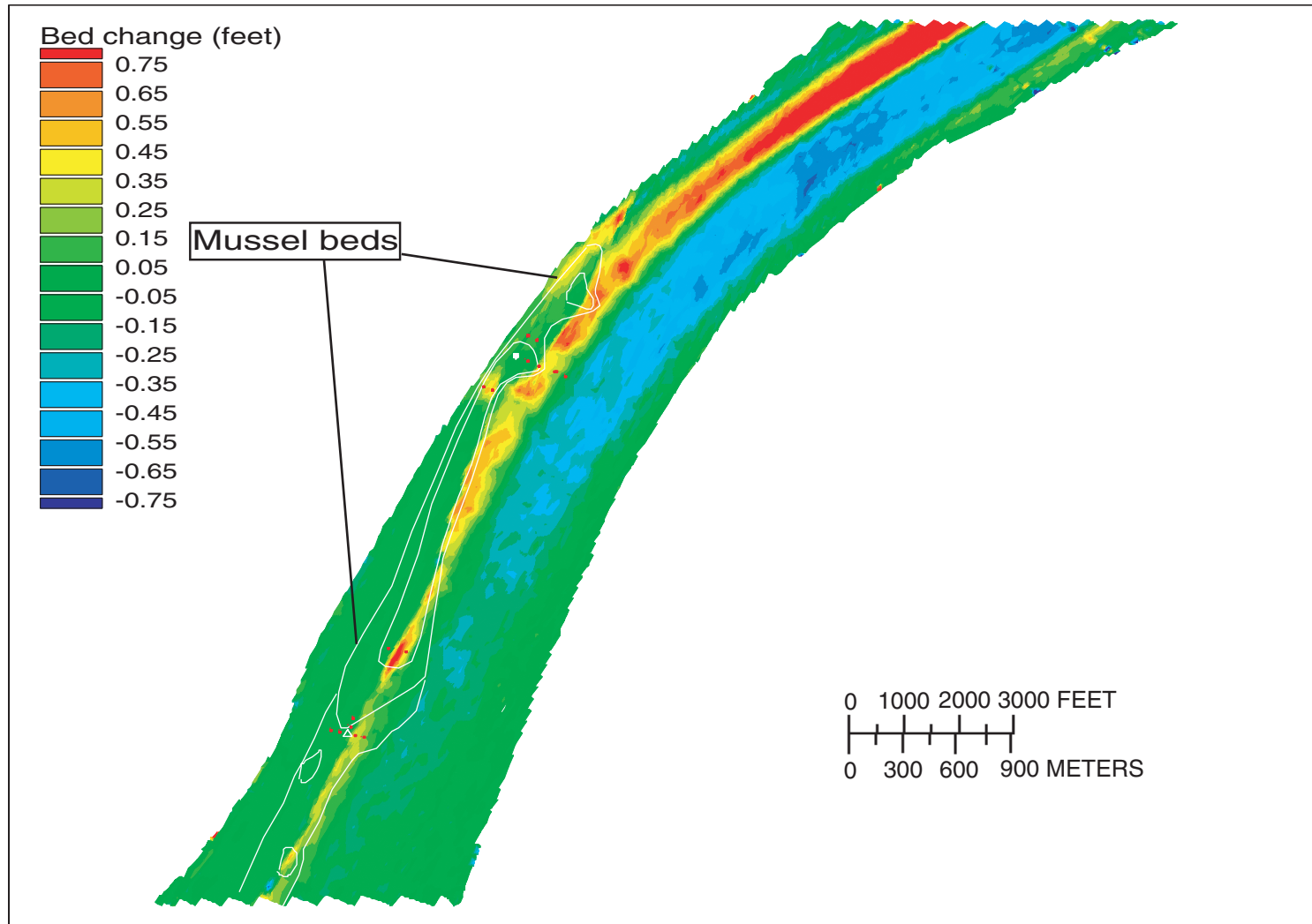


Figure 21. Difference in bed change between baseline and phase 3-construction simulations after year 4 (1996 hydrograph) in the Olmsted Locks and Dam study reach near Olmsted, Illinois.

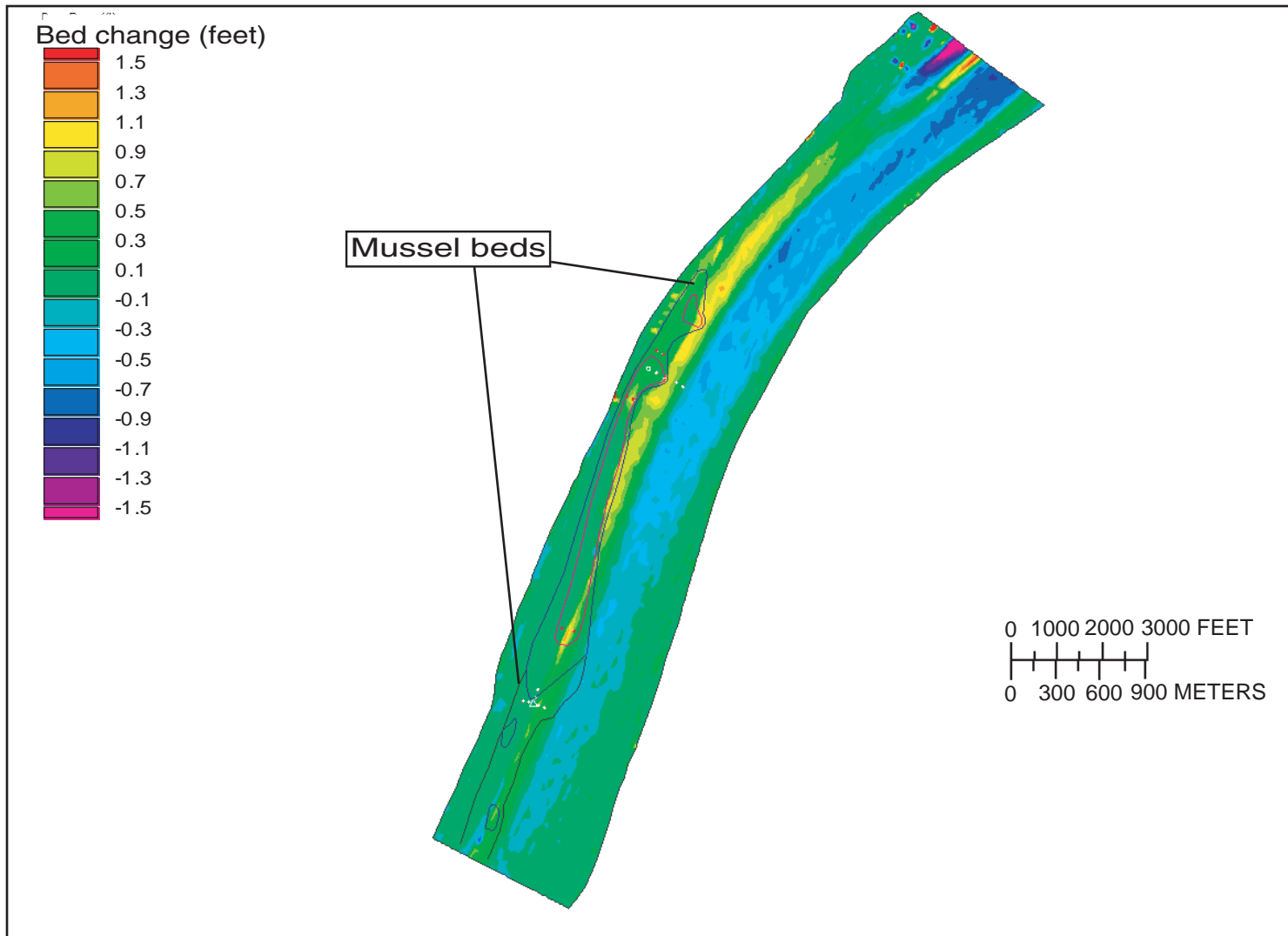


Figure 22. Difference in bed change between baseline and phase 3-construction simulations after year 5 (1997 hydrograph) in the Olmsted Locks and Dam study reach near Olmsted, Illinois.

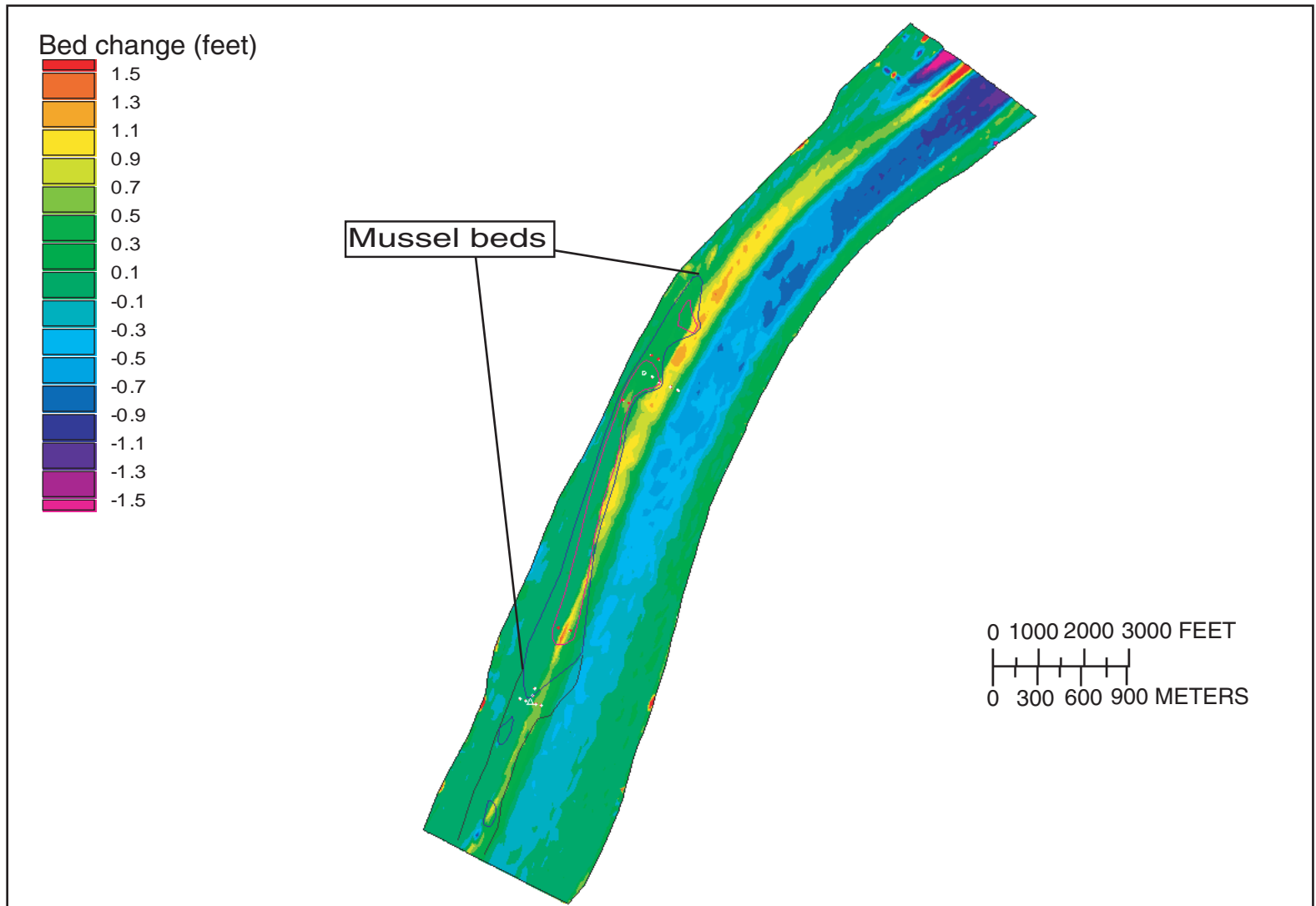


Figure 23. Difference in bed change between baseline and phase 3-construction simulations after year 6 (1996 hydrograph) in the Olmsted Locks and Dam study reach near Olmsted, Illinois.

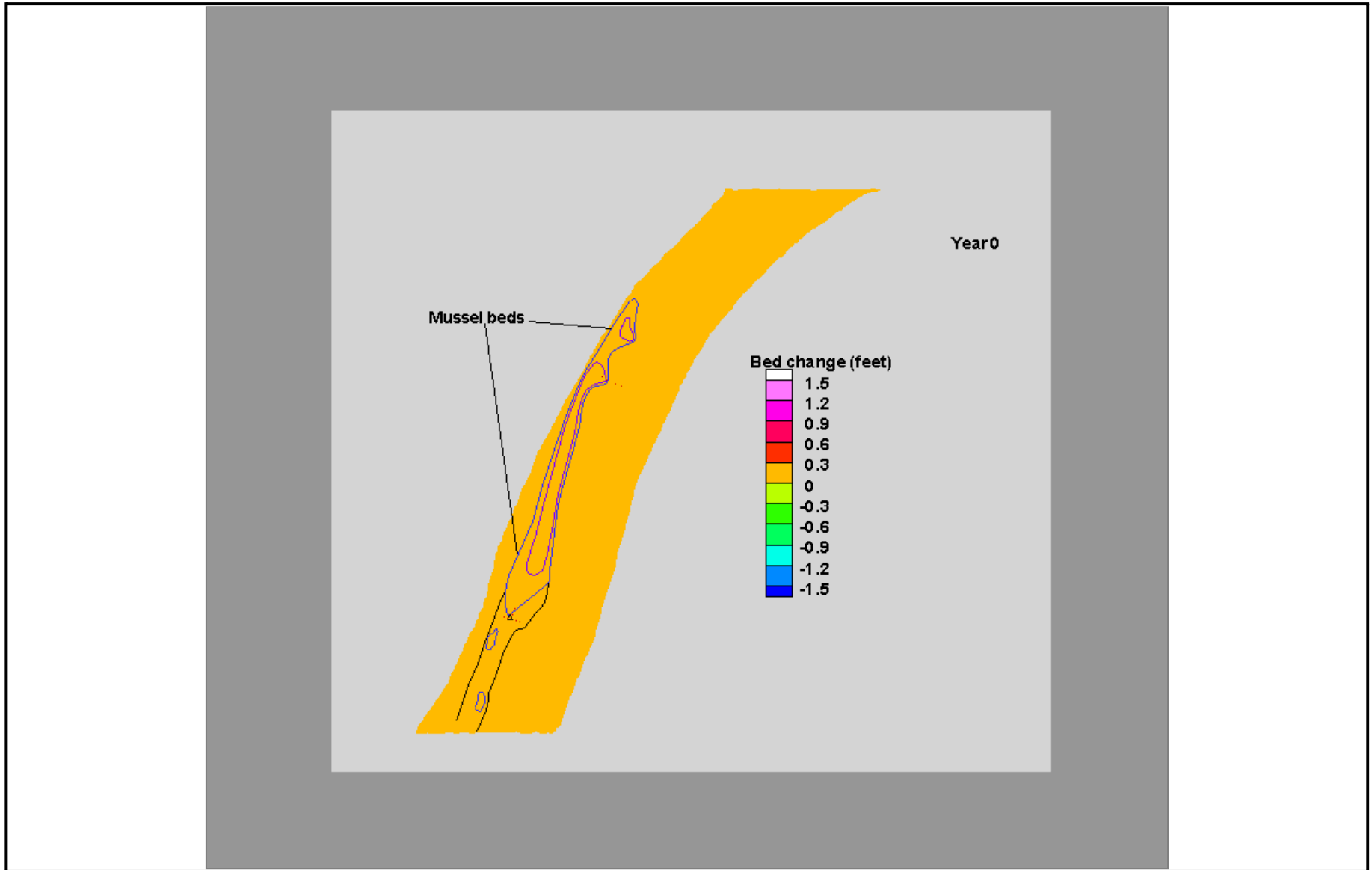


Figure 24. Bed change around the mussel beds for the 6-year Olmsted Locks and Dam construction simulation near Olmsted, Illinois.

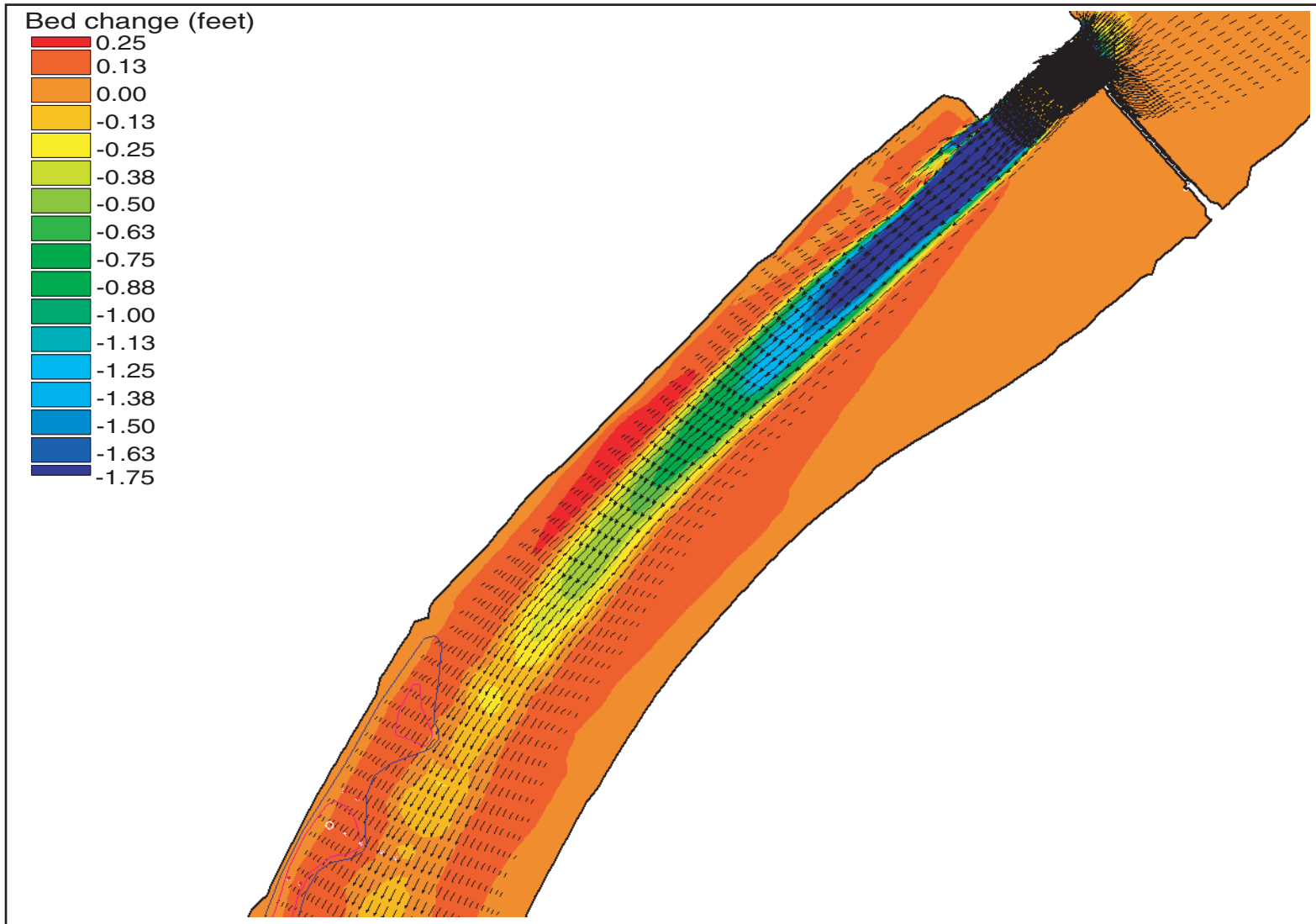


Figure 25. Difference in bed change between baseline and phase 3-construction after year 5 (1997 hydrograph), superimposed with hydrodynamics for a low-flow simulation (1997 hydrograph - step 7), for the Olmsted Locks and Dam model near Olmsted, Illinois.

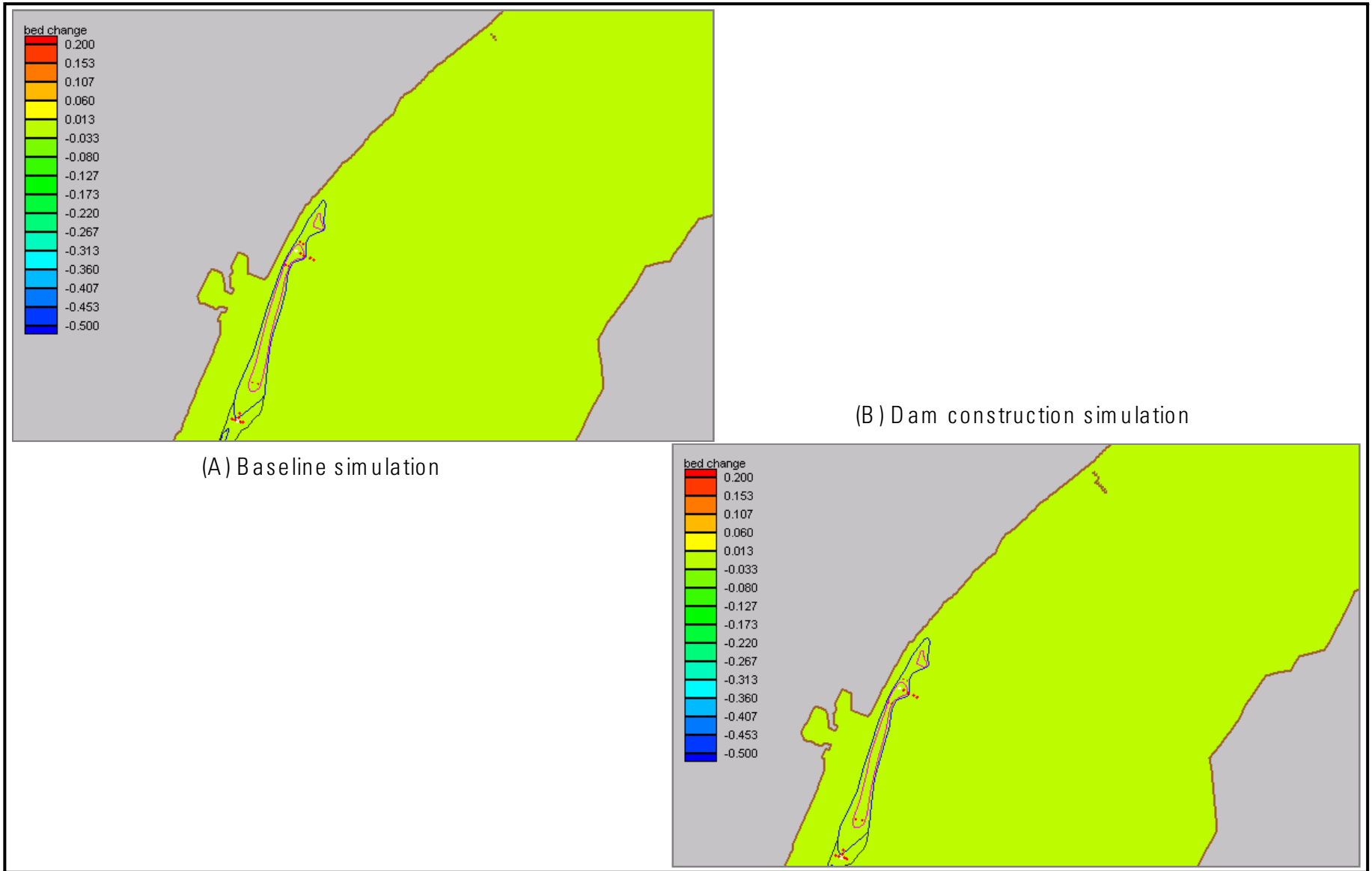


Figure 26. Bed change during high-flow conditions (1997 hydrograph, step 3) for (A) baseline simulation and (B) phase 3 of the Olmsted construction in the study reach near Olmsted, Illinois.

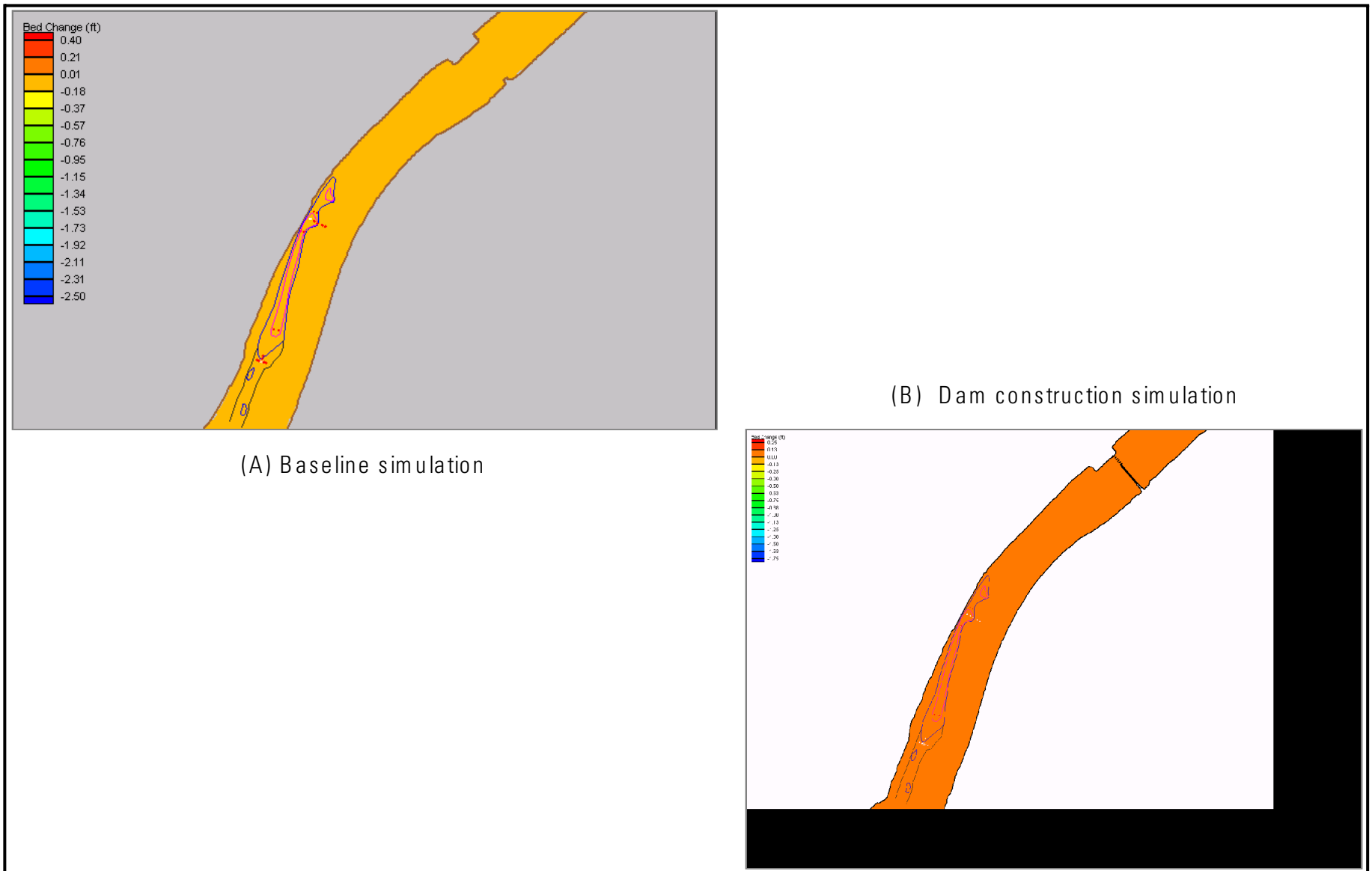


Figure 27. Bed change during low-flow conditions (1997 hydrograph, step 7) for (A) baseline simulation and (B) phase 3 of the Olmsted construction in the study reach near Olmsted, Illinois.

The maximum cumulative deposition on the mussel beds is approximately 1.5 ft occurring at the end of year 6. The greatest areas of deposition are shown to develop at the upstream section of the mussel beds as well as near the downstream end of the mussel beds, along the edge of the area where scour was prevented. The reason for the isolated downstream area of deposition is not fully understood and should be further investigated to determine if the deposition is real or a product of numerical anomalies between adjacent elements with distinctly different transport characteristics.

Aside from these two sections, a majority of the mussel-bed area is expected to have little or no bed change over the 6-year simulation that can be associated with the dam construction process. Most areas on the mussel beds indicated less than 0.5 ft of bed change between the baseline and construction phases during the six annual hydrographs. Inspection of the scour and deposition patterns caused by the dam construction reveals a large scoured area in the channel downstream of the navigable pass and will deposit a large amount of sediment in a section located along the right bank. The location of maximum deposition can be attributed to the hydrodynamic changes in the reach or more specifically the zone of slack and reverse flow formed along the right descending (Illinois) bank and overall shifting of the thalweg toward the left descending (Kentucky) bank caused by the various phases of dam construction.

In order to focus on the sedimentation processes over the mussel beds caused by the dam construction during extreme high-flow events, the bed change between the hydrograph steps just prior to, during, and following the 1997 flood is shown in figure 28 (animation). The animation in figure 28 shows scouring near the downstream end of the mussel beds associated with the removal of previously deposited material and minimal deposition on the mussel beds during the recession period of the 1997 flood. The simulated occurrence of the 1997 flood during construction-phase 2 resulted predominately in the scouring of material previously deposited on the mussel beds and an

overall maximum deposition of less than 0.3 ft located at the upstream end of the mussel beds (fig. 29).

Operational-Phase Model—Hydrodynamics

The general behavior of the velocity distributions in the operational-phase model is representative of those described in construction-phase 3 of the construction-phase model.

Operational-Phase Model—Sediment Transport

The difference in bed change between the baseline and construction phases for each of the three annual hydrographs in the operational-phase model is shown in figures 30-32 and an animation of the bed change over the 3-year operational period (fig. 33). The depth and downstream extent of scour and deposition caused by the dam operation progressively increases from year 7 through year 9. Although the depth of deposition continued to increase around the mussel beds in the operational-phase model, the lateral migration of the deposition toward the mussel beds is limited. The spatial distribution of the depositional areas at the end of year 9 (fig. 34) is nearly identical to what was simulated through year 6 in the construction-phase model (fig. 23). As in the construction-phase model, the most appreciable bed change during the operational-phase model occurred during the low-flow periods in which the wicket gates were closed and the flow of the river passed through the tainter gates. The maximum cumulative deposition on the mussel beds is approximately 2 ft occurring at the end of year 9. The greatest area of deposition continued to be the upstream section of the mussel beds with a small, localized area near the downstream end of the mussel beds.

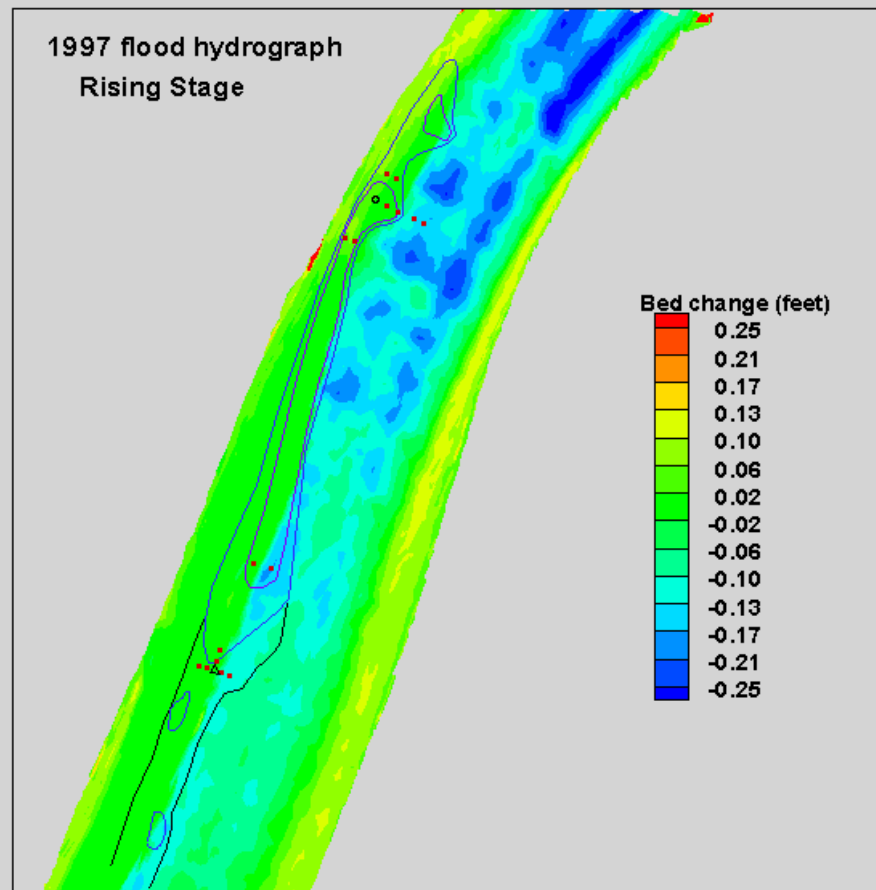


Figure 28. Bed change around the mussel beds over the 1997 flood hydrograph in the Olmsted Locks and Dam study reach near Olmsted, Illinois.

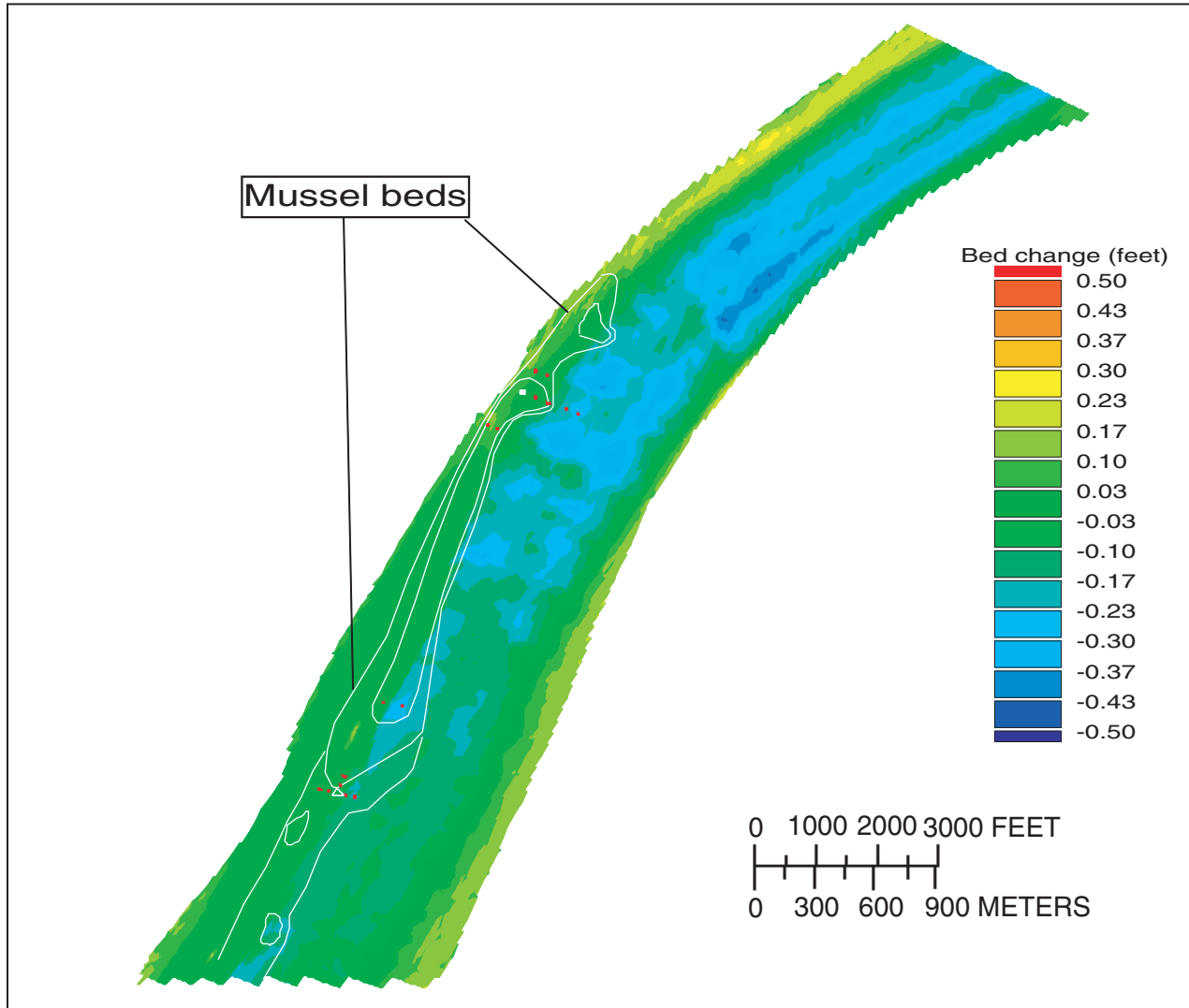


Figure 29. Cumulative bed change around the mussel beds during the 1997 flood (1997 hydrograph - step 5, minus step 2) for phase-2 construction in the Olmsted Locks and Dam study reach near Olmsted, Illinois.

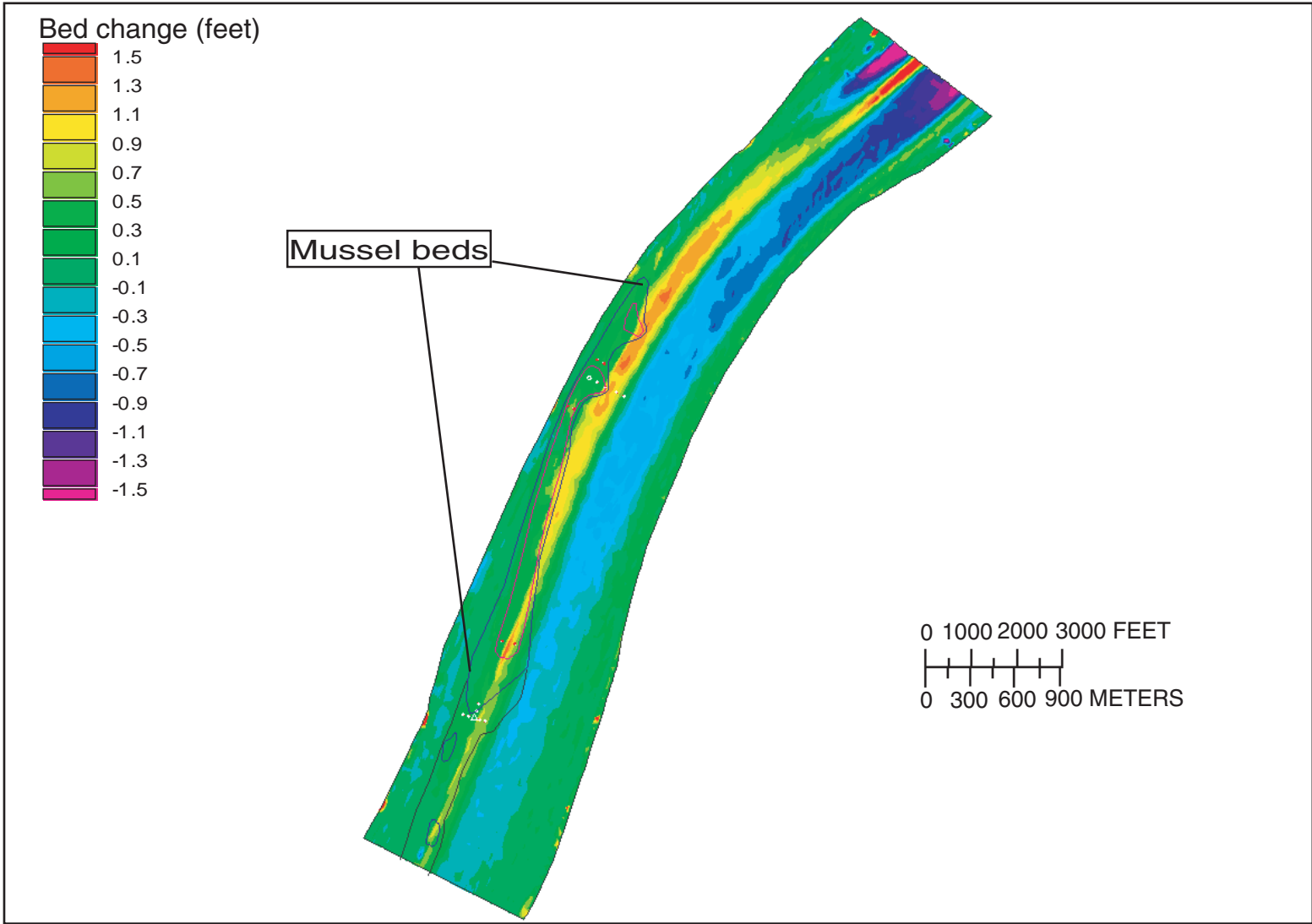


Figure 30. Difference in bed change between baseline and fully operational locks and dam simulation after year 7 (1985 hydrograph) in the Olmsted Locks and Dam study reach near Olmsted, Illinois.

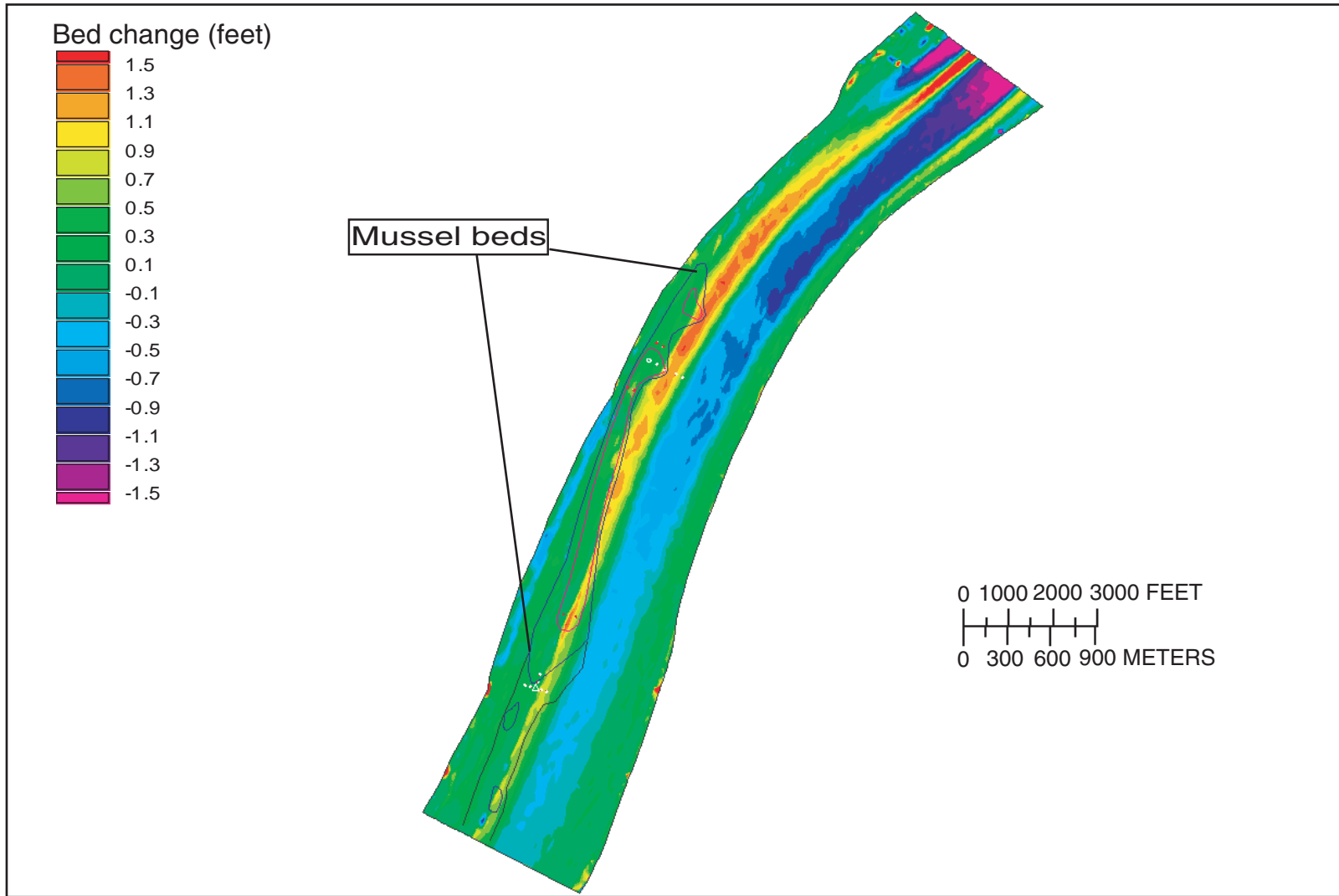


Figure 31. Difference in bed change between baseline and fully operational locks and dam simulation after year 8 (1986 hydrograph) in the Olmsted Locks and Dam study reach near Olmsted, Illinois.

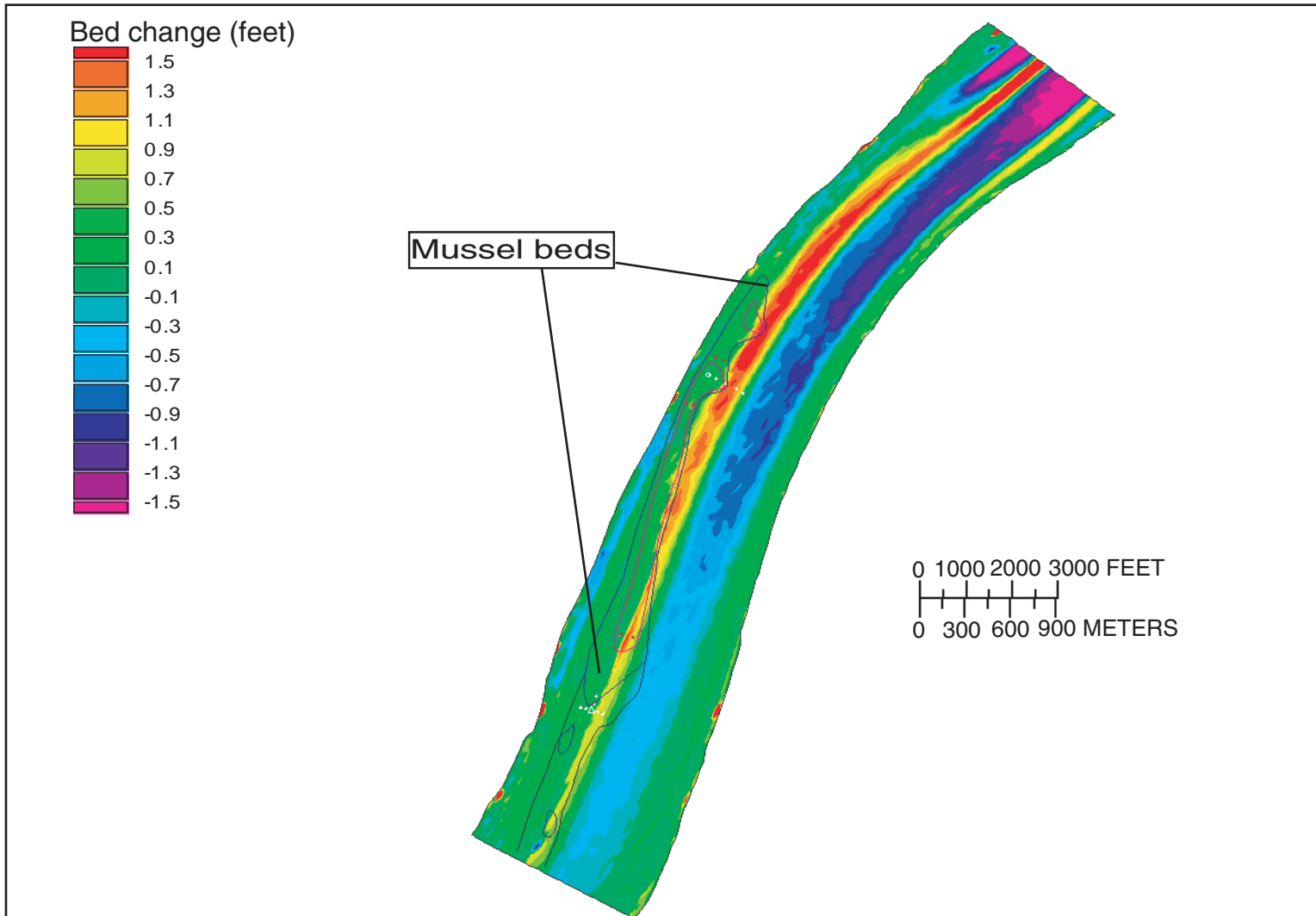


Figure 32. Difference in bed change between baseline and fully operational locks and dam simulation after year 9 (1973 hydrograph) in the Olmsted Locks and Dam study reach near Olmsted, Illinois.

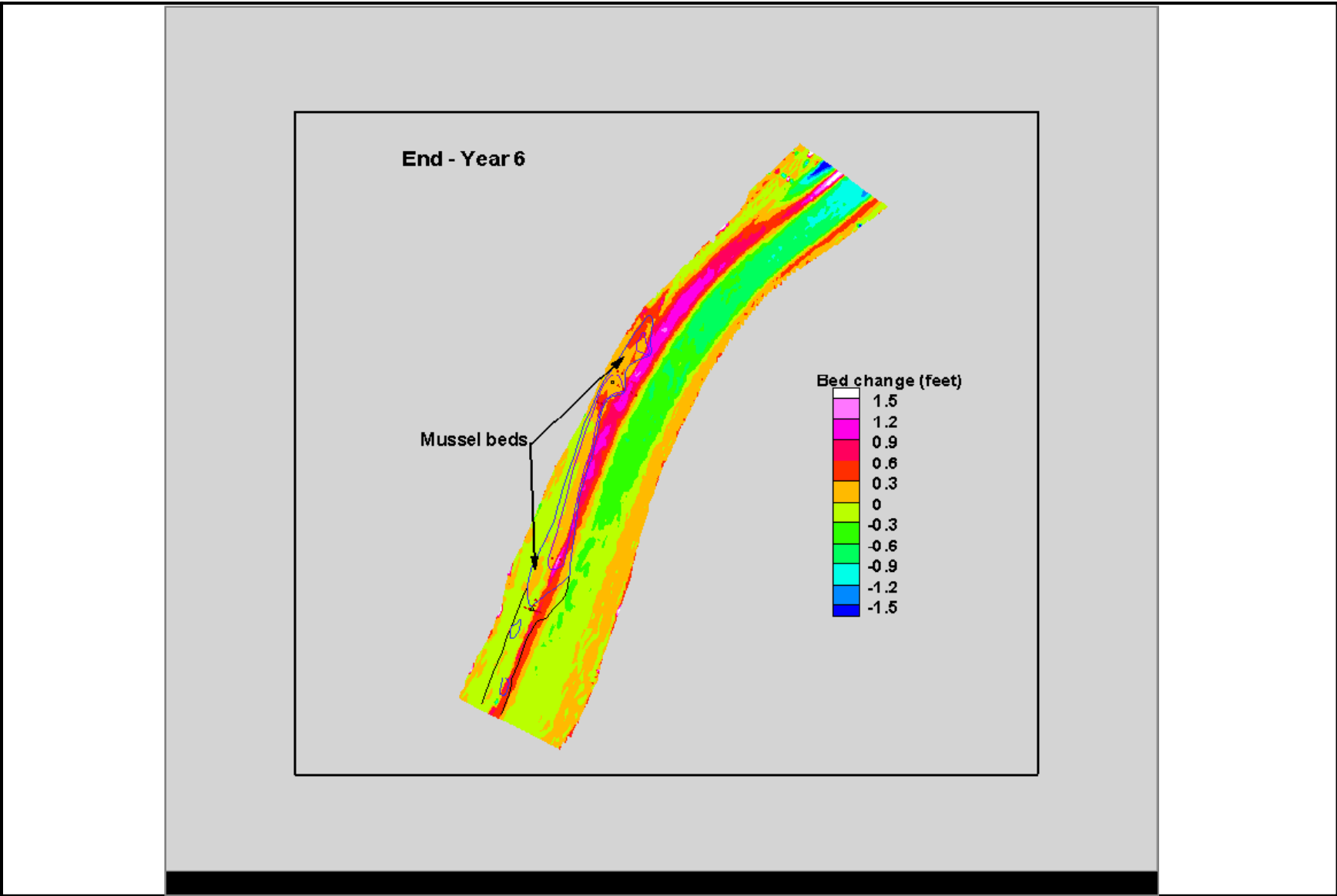


Figure 33. Bed change around the mussel beds over the 3-year operational simulation in the Olmsted Locks and Dam study reach near Olmsted, Illinois.

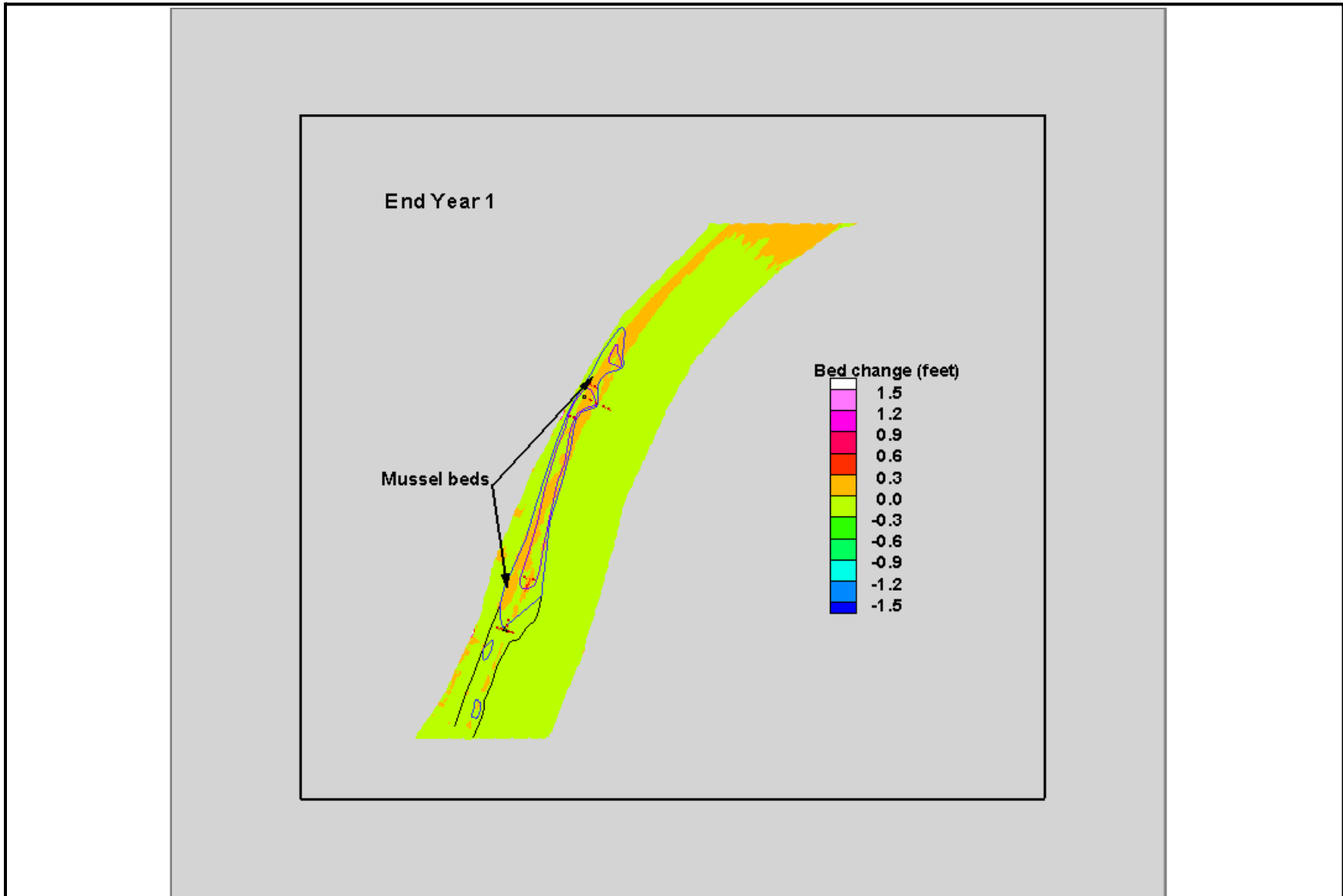


Figure 34. Bed change around the mussel beds over the entire 9-year construction and operational simulation in the Olmsted Locks and Dam study reach near Olmsted, Illinois.

MODEL COMPARISON BETWEEN SED2D AND PREVIOUS TABS-1 SIMULATION

The initial sediment-transport simulation developed for the Olmsted Locks and Dam study reach used the one-dimensional numerical model, TABS-1. The one-dimensional TABS-1 model only was able to deposit and erode uniformly over a particular cross section (the general scour in a contacted reach). The Sed2D model was capable of simulating the variations in deposition and erosion throughout the reach and thereby able to estimate local scour and deposition. One particular area sensitive to lateral variations is the separation zone immediately downstream of the locks. Unlike TABS-1, Sed2D is capable of predicting the sediment deposition that is likely in this ineffective flow region, which is a critical factor in the determination of the bed-material transport to the mussel beds. Additionally, the TABS-1 model did not account for the overtopping of the locks as the USGS model did; therefore, would tend to overpredict the potential for scour downstream of the construction area.

Model Development

The TABS-1 model only extends from Locks and Dam 53 downstream to Ohio River mile 966.7, just downstream of the upstream end of the mussel beds. Differences in maximum depth and geometry exist between the scour-hole configurations estimated for the TABS-1 model and measured for the USGS Sed2D simulation. The minimum elevation and extent of the measured scour hole was approximately at elevation 235 ft and mile 965.3, respectively, compared to elevation 240 ft and mile 965 in the TABS-1 model. The TABS-1 model was run for a 3-year construction period with a representative annual hydrograph developed from a historical-flow duration curve for Metropolis, Ill. Separate low- and high-tailwater (low or high stages on the Mississippi River) rating curves were developed to bracket the range of tailwater conditions experienced at the site from 1966 to 1988. The Sed2D construction simulation used representative stepped annual hydrographs for 1996 and 1997. Both low- and high-tailwater conditions

existed in the 1996 and 1997 hydrographs making it more difficult to develop a direct comparison between the hydrodynamic conditions of the TABS-1 and Sed2D simulations.

The bed-material inflow-concentration rating curve for the TABS-1 model was developed from suspended-sediment samples collected near Locks and Dam 53 and adjusted for the contribution of the unmeasured (bed) load. In contrast, the inflow-rating curve for the Sed2D simulation was developed by modeling equilibrium conditions for the various hydrographs steps, as previously discussed.

Comparison of Model Results

The location of the reattachment point for the flow separation caused by the construction is a critical factor in the amount of bed material being transported over the mussel beds. The reattachment point for the TABS-1 and Sed2D models were Ohio River miles 965.9 and 965.4, respectively. The following is a summary of the transport results for both simulations.

1. USACE TABS-1 Model
 - Low-Tailwater Condition
 - Additional expansion of scour hole from mile 965 to 965.25, most of which occurred between years 1 and 2
 - Maximum deposition of approximately 1.5 to 2.5 ft at upstream portion of mussel beds after 3-year construction period
 - High-Tailwater Condition
 - No additional expansion of scour hole
 - Maximum deposition of less than 1 ft shown at upstream portion of mussel beds after 3-year construction period
2. USGS Sed2D Model
 - Year 1 (geometric scenario 1)
 - 0.4-ft maximum deposition at upstream edge of mussel beds
 - Year 2 (geometric scenario 2)
 - 0.35-ft maximum deposition at upstream edge of mussel beds
 - Year 3 (geometric scenario 3)
 - 0.35-ft maximum deposition at upstream edge of mussel beds

- Cumulative Results
 - 1.10-ft maximum deposition at upstream edge of mussel beds
 - Minimal expansion of scour hole from mile 965.3 to approximately mile 965.38

SUMMARY AND CONCLUSIONS

The Olmsted Locks and Dam hydrodynamic and sediment-transport model was developed by the U.S. Geological Survey (USGS), in cooperation with the U.S. Army Corps of Engineers (USACE)—Louisville District, to evaluate the environmental effect of the construction and subsequent operation of the Olmsted Locks and Dam on the lower Ohio River. Simulation of the phased Olmsted Locks and Dam construction and subsequent 3-year operation period resulted in a maximum additional deposition of approximately 2 feet when compared to the bed change simulated with baseline conditions. The areas of highest deposition are located at the upstream section of the mussel beds as well as the small area located near the downstream extent of the beds. Aside from these two sections, a majority of the mussel bed area experienced minimal bed change over the 9-year simulation that can be associated with the dam construction and (or) operation. Most areas on the mussel beds experienced less than 0.5 feet of cumulative bed change between the baseline and construction phases during the nine annual hydrographs. Inspection of the scour and deposition patterns caused by the dam construction reveals a large scoured area in the channel downstream of the navigable pass and tainter gates (as a result of the flow contraction in those regions) and a section of high deposition located along the right descending (Illinois) bank, downstream of the tainter gates. The location of maximum deposition can be attributed to the hydrodynamic changes in the reach or more specifically the zone of reverse and slack flow along the right (Illinois) bank created by the shift in the river's thalweg toward the left (Kentucky) bank caused by the Olmsted Locks and Dam. The hydrodynamic changes are most prominent during low-flow conditions when the river is entirely passed through the tainter gates. The most

appreciable increase in bed change between the baseline- and construction-phase conditions occurred during year-5 of the simulation because of an extended low-flow period (1997 hydrograph, step 7) in which the tainter gates passed the entire flow for nearly 6 months, which greatly altered the hydrodynamics of the river.

The bed change over the 9-year Olmsted Locks and Dam simulation reveals a continuous downstream progression and deepening of the regions of scour in the main channel and deposition along the right bank with limited lateral migration toward the more densely populated mussel-bed areas.

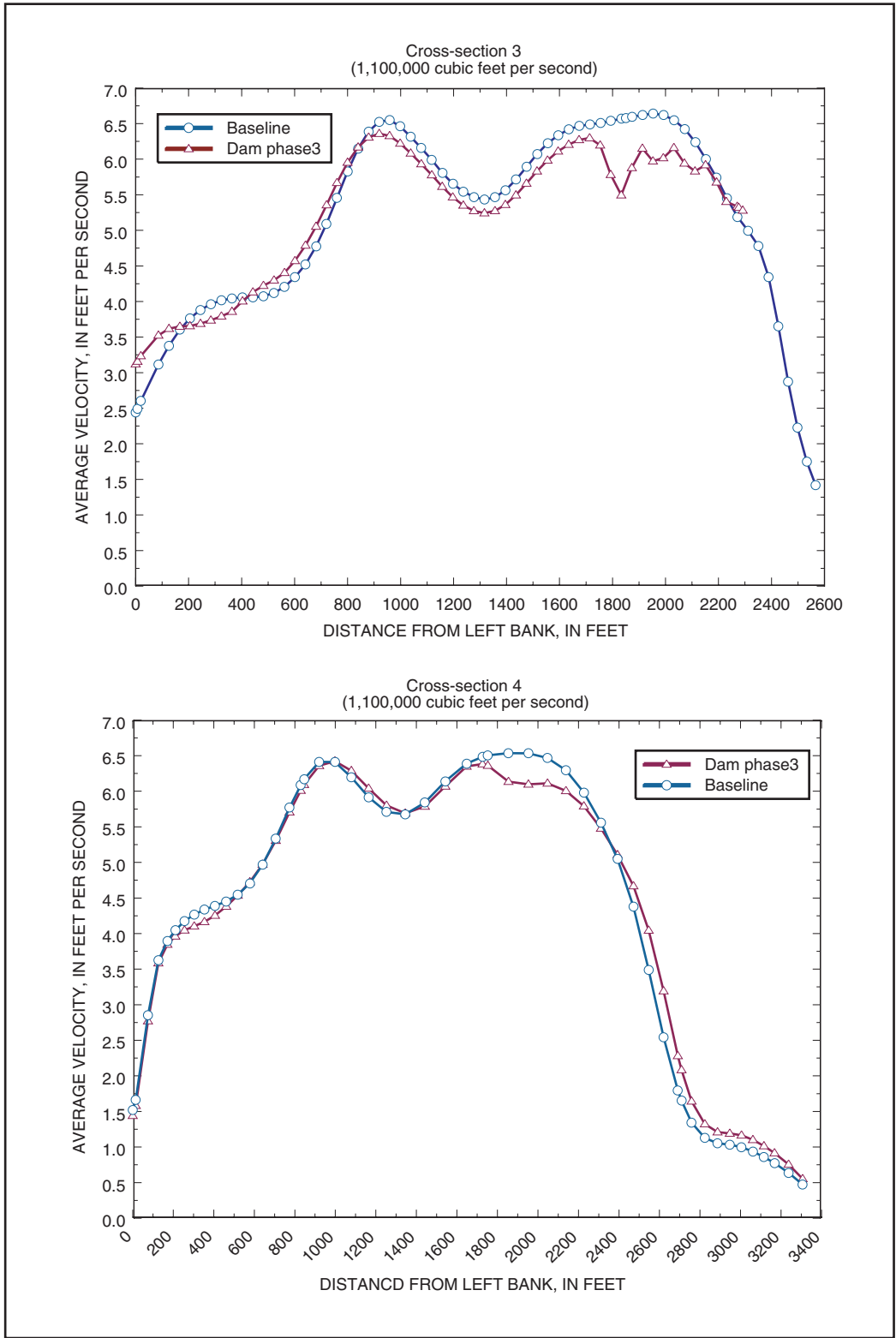
REFERENCES CITED

- Ackers, Peter, and White, W.R., 1973, Sediment transport—new approach and analysis: American Society of Civil Engineers, Journal of the Hydraulics Division, v. 99, no. HY11, Proceedings Paper 10167, p. 2,041-2,060.
- Brigham Young University, 1999, Surface-Water Modeling System (SMS) Reference Manual (ver. 8.0): Provo, Utah, Environmental Modeling Research Laboratory [variously paged].
- Donnell, B.P., Letter, J.V., McAnally, W.H., and others, 2001, User's Guide for RMA2 Version 4.5: Vicksburg, Miss., U.S. Army, Engineer Research and Development Center, Waterways Experiment Station, Coastal and Hydraulics Laboratory, on line at <URL: <http://chl.wes.army.mil/software/tabs/docs.htm>>, accessed March 10, 2004.
- Mueller, D.S., 1996, Scour at bridges—detailed data collection during floods, *in* Federal Interagency Sedimentation Conference, 6th, Las Vegas, Nev., 1996, Proceedings: Subcommittee on Sedimentation Interagency Advisory Committee on Water Data, p. IV 41-48.
- Oberg, K.A., and Mueller, D.S., 1994, Recent applications of Acoustic Doppler Current Profilers, *in* Fundamentals and Advancements in Hydraulic Measurements and Experimentation, Buffalo, New York, 1994, Proceedings: Hydraulics Division/American Society of Civil Engineers (ASCE), p. 341-350.
- Richardson, E.V., and Davis, S.R., 2001, Evaluating Scour at Bridges: Washington, D.C., Federal Highway Administration, Hydraulic Engineering Circular No. 18, FHWA-NHI-01-001, 378 p.

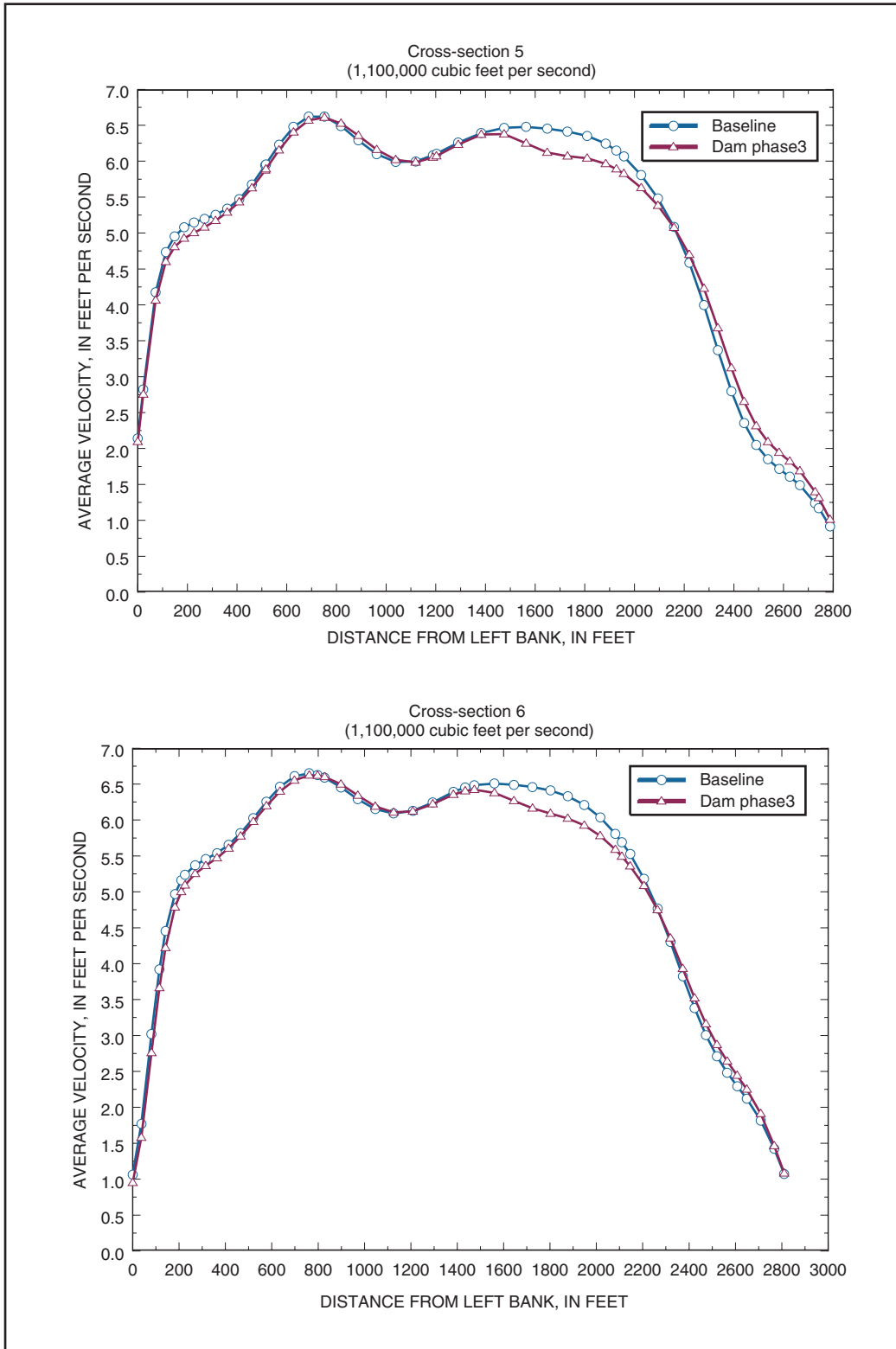
- Rouse, H., 1937, Nomogram for the Settling Velocity of Spheres, *in* Exhibit D of the Report of the Commission on Sedimentation, 1936-37: Washington, D.C., National Research Council, Division of Geology and Geography, p. 57-64.
- Simpson, M.R., and Oltmann, R.N., 1992, Discharge-measurement system using an acoustic Doppler current profiler with applications to large rivers and estuaries: U.S. Geological Survey Open-File Report 91-487, 49 p.
- Thorp, J.H., and Covich, A.P., eds., 1991, Ecology and classification of North American freshwater invertebrates: New York, Academic Press, Inc., 911 p.
- U.S. Army Corps of Engineers, 2000, Users Guide to Sed2D WES (ver. 4.5): Vicksburg, Miss., Waterways Experiment Station, 162 p.
- U.S. Fish and Wildlife Service, 1993, Supplemental biological opinion for the proposed Olmsted Locks and Dam, Ballard County, Kentucky: Cookeville, Tenn., 15 p.
- Wagner, C.R., and Mueller, D.S., 2001, Calibration and validation of a two-dimensional hydrodynamic model of the Ohio River, Jefferson County, Kentucky: U.S. Geological Survey Water-Resources Investigations Report 01-4091, 33 p.

APPENDIX A:

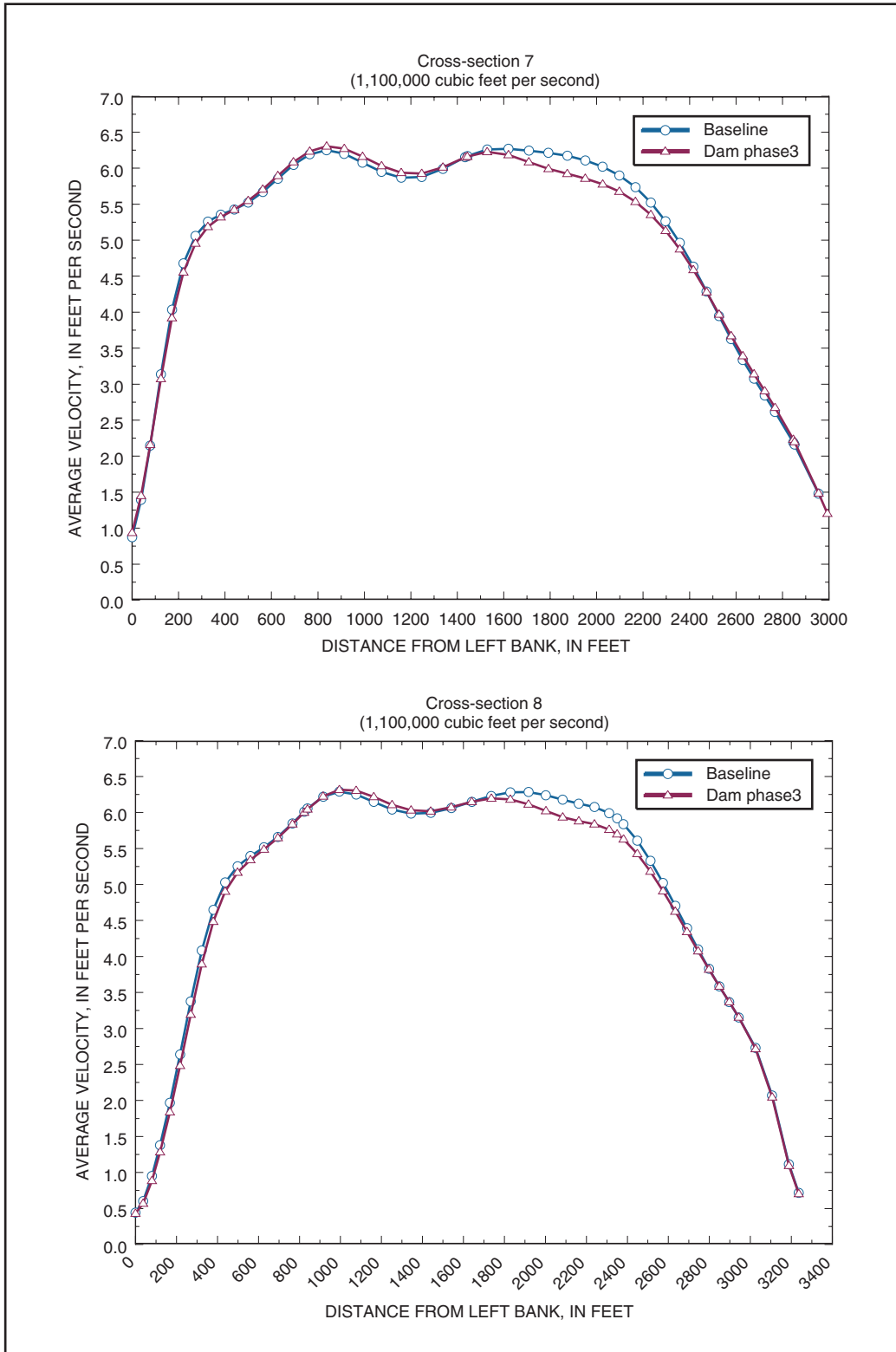
High-flow comparisons of baseline and phase-3 construction cross-sectional velocity profiles in the Olmsted Locks and Dam study reach near Olmsted, Illinois



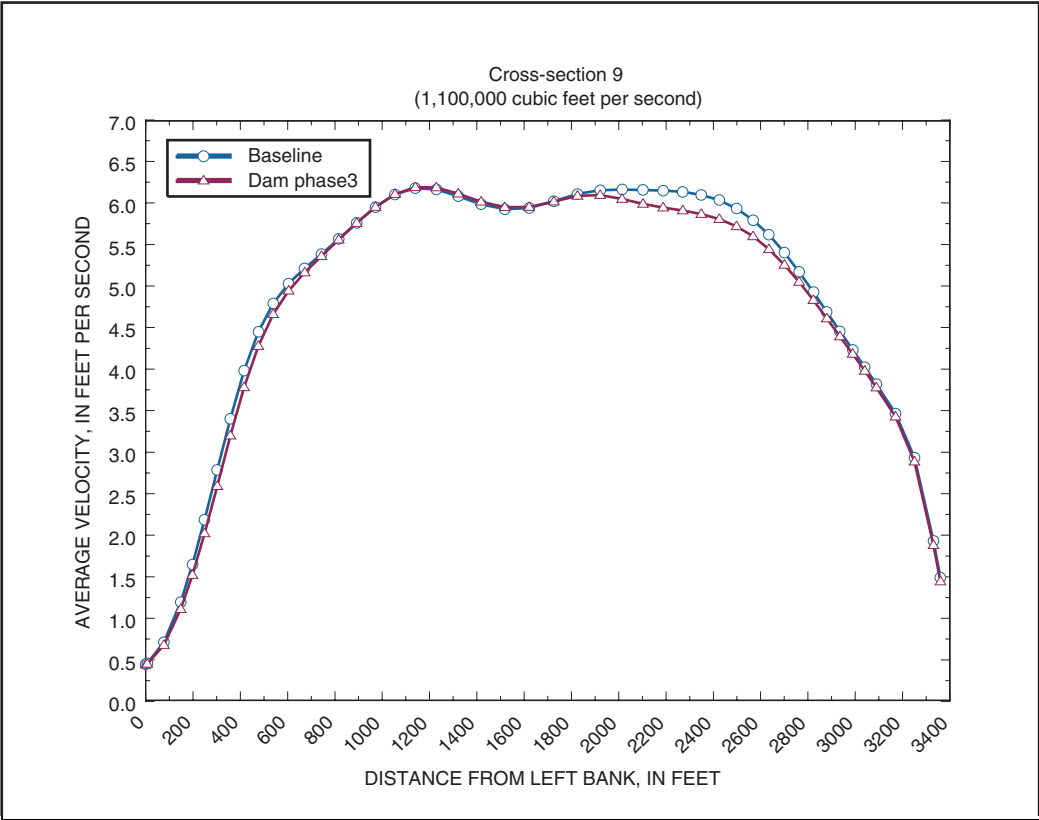
Comparisons of baseline and construction-phase 3 velocity profiles at cross-sections 3 and 4 for the year-5, high-flow simulation (1997 hydrograph, step 3) in the Olmsted Locks and Dam study reach near Olmsted, Illinois.



Comparisons of baseline and construction-phase 3 velocity profiles at cross-sections 5 and 6 for the year-5, high-flow simulation (1997 hydrograph, step 3) in the Olmsted Locks and Dam study reach near Olmsted, Illinois.



Comparisons of baseline and construction-phase 3 velocity profiles at cross-sections 7 and 8 for the year-5, high-flow simulation (1997 hydrograph, step 3) in the Olmsted Locks and Dam study reach near Olmsted, Illinois.

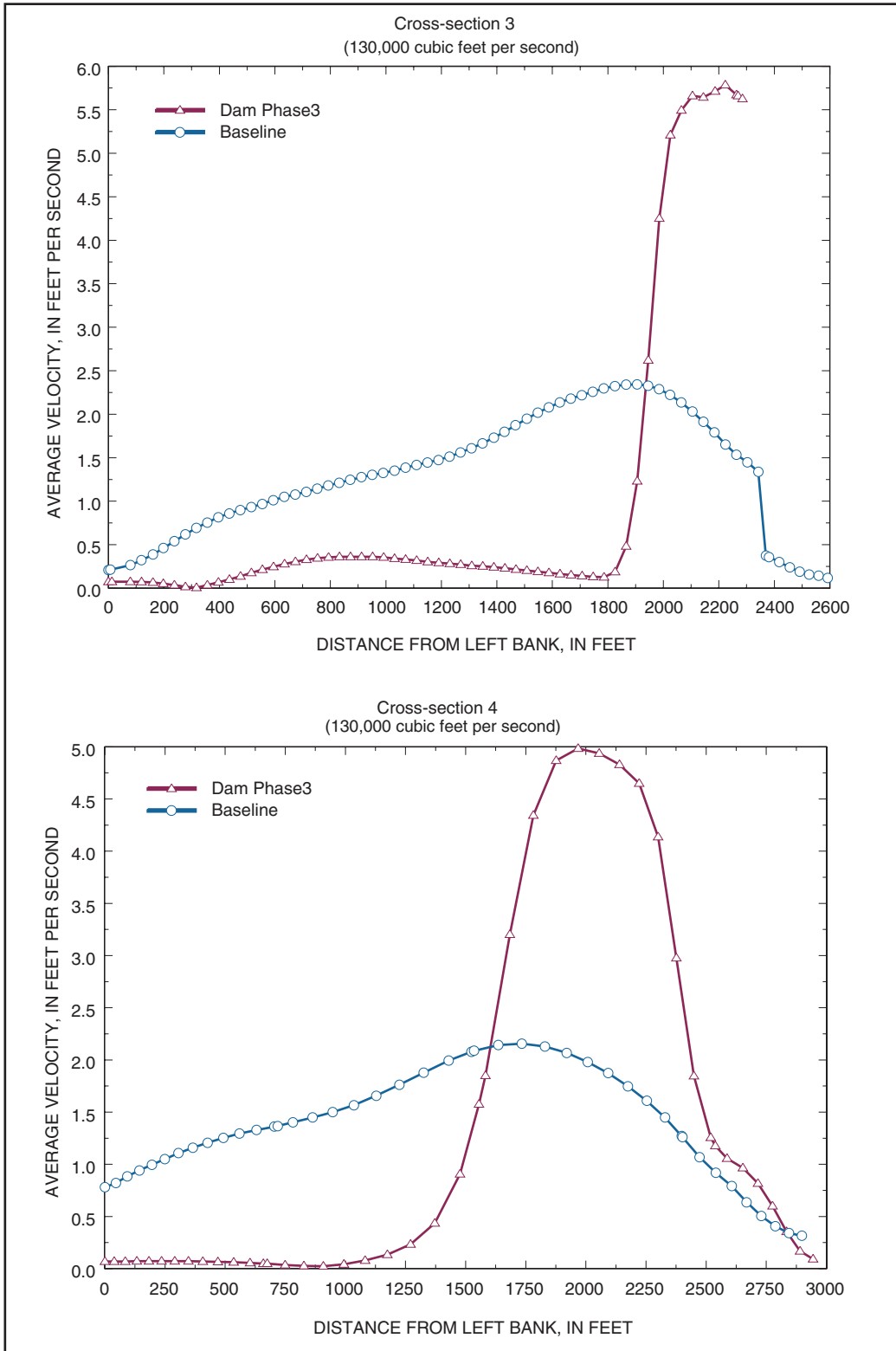


Comparisons of baseline and construction-phase 3 velocity profiles at cross-section 9 for the year-5, high-flow simulation (1997 hydrograph, step 3) in the Olmsted Locks and Dam study reach near Olmsted, Illinois.

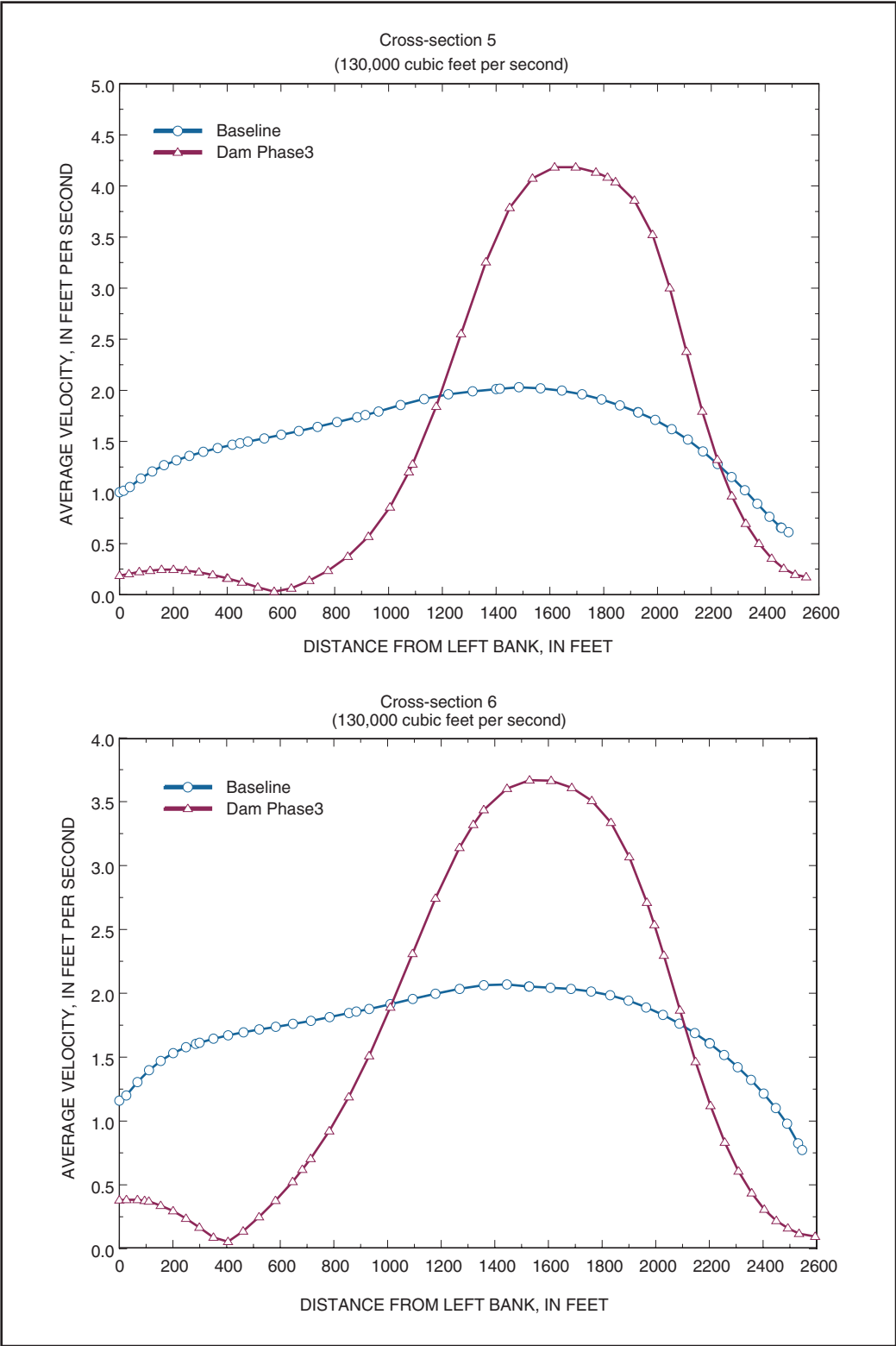
[This page intentionally blank.]

APPENDIX B:

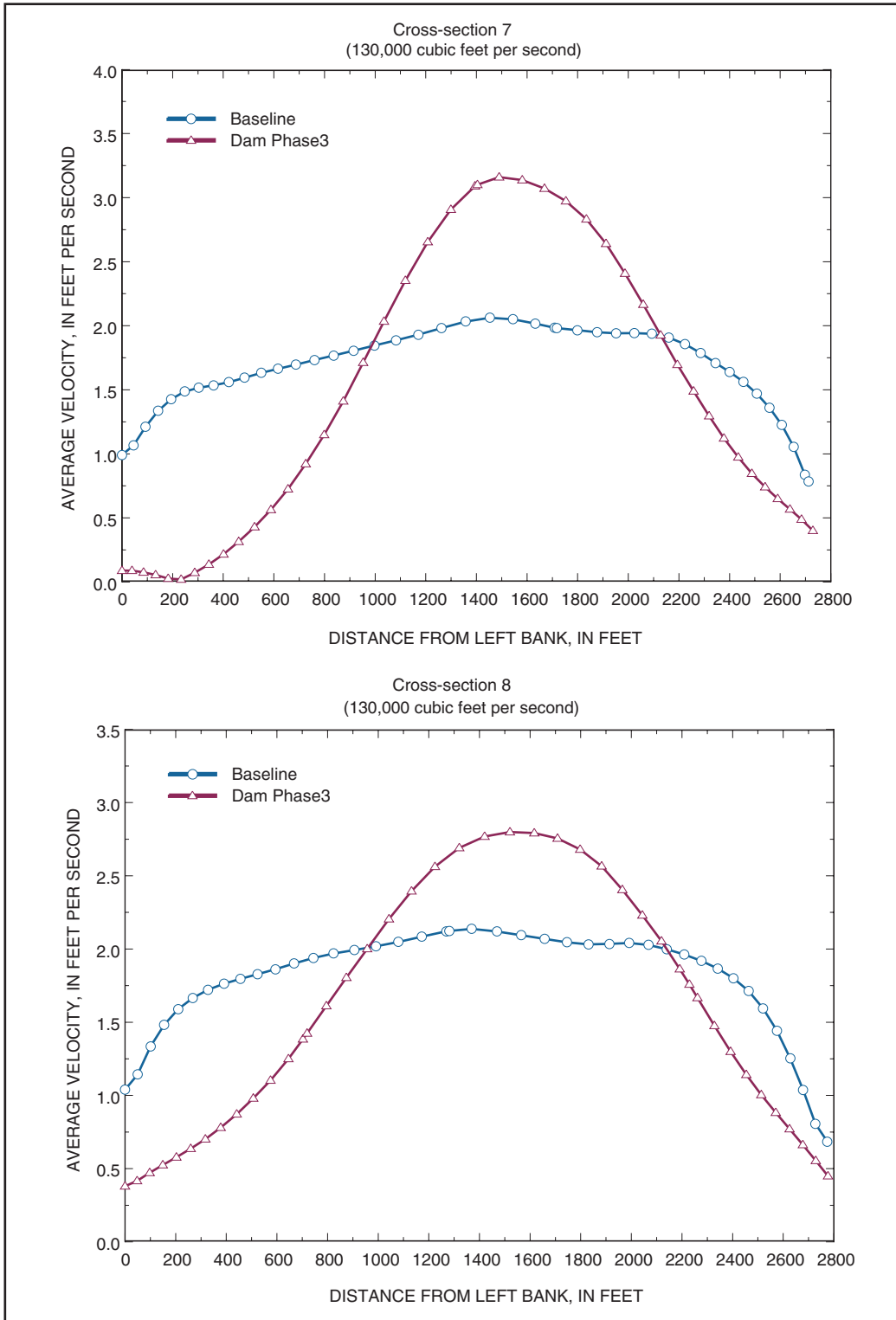
Low-flow comparisons of baseline and phase-3 construction cross-sectional velocity profiles in the Olmsted Locks and Dam study reach near Olmsted, Illinois



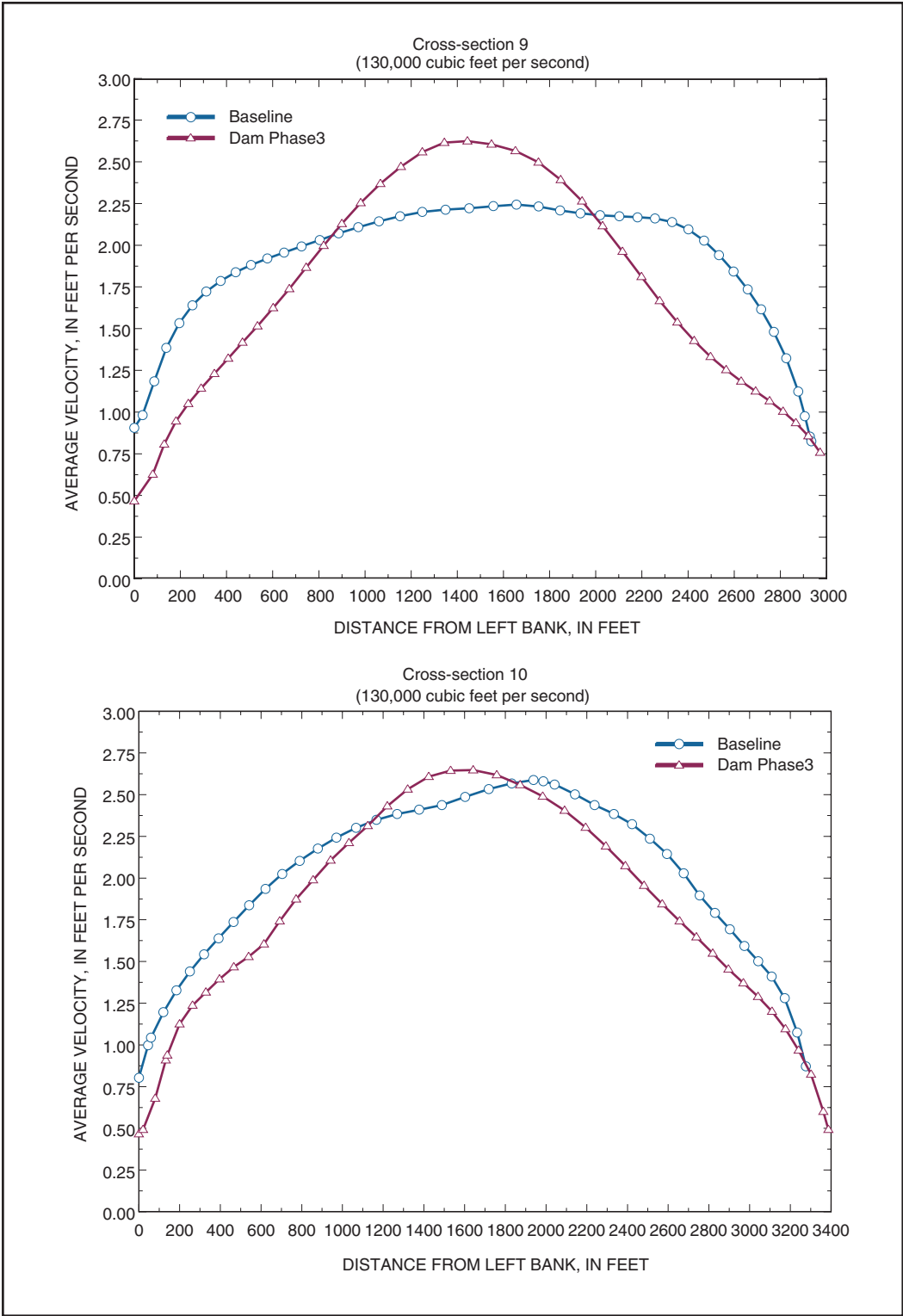
Comparisons of baseline and construction-phase 3 velocity profiles at cross-sections 3 and 4 for the year-5, low-flow simulation (1997 hydrograph, step 7) in the Olmsted Locks and Dam study reach near Olmsted, Illinois.



Comparisons of baseline and construction-phase 3 velocity profiles at cross-sections 5 and 6 for the year-5, low-flow simulation (1997 hydrograph, step 7) in the Olmsted Locks and Dam study reach near Olmsted, Illinois.



Comparisons of baseline and construction-phase 3 velocity profiles at cross-sections 7 and 8 for the year-5, low-flow simulation (1997 hydrograph, step 7) in the Olmsted Locks and Dam study reach near Olmsted, Illinois.



Comparisons of baseline and construction-phase 3 velocity profiles at cross-sections 9 and 10 for the year-5, low-flow simulation (1997 hydrograph, step 7) in the Olmsted Locks and Dam study reach near Olmsted, Illinois.